The Effects of Load on Cardiac Function

A thesis submitted for the Degree of Doctor of Medicine

by

Dr Eveline S P Lee

MB ChB (Liverpool), MRCP (London)

Department of Cardiology

Wales Heart Research Institute

Cardiff University

UK

December 2018

DECLARATIONS

STATEMENT 1

This thesis is being submitted in partial fulfilment of the requirements for the degree of MD.

Signed ___Eveline Lee_____ Date ____31/12/2018__

STATEMENT 2

This work has not been submitted in substance for any other degree or award at this or any other university or place of learning, nor is it being submitted concurrently for any other degree or award (outside of any formal collaboration agreement between the University and a partner organisation)

Signed ___Eveline Lee_____ Date ____31/12/2018_____

STATEMENT 3

I hereby give consent for my thesis, if accepted, to be available in the University's Open Access repository (or, where approved, to be available in the University's library and for inter-library loan), and for the title and summary to be made available to outside organisations, subject to the expiry of a University-approved bar on access if applicable.

Signed ___Eveline Lee_____ Date ____31/12/2018_____

DECLARATION

This thesis is the result of my own independent work, except where otherwise stated, and the views expressed are my own. Other sources are acknowledged by explicit references. The thesis has not been edited by a third party beyond what is permitted by Cardiff University's Use of Third Party Editors by Research Degree Students Procedure.

Signed ___Eveline Lee_____ Date ____31/12/2018_____

WORD COUNT ____25,077_____

(Excluding summary, acknowledgements, declarations, contents pages, appendices, tables, diagrams and figures, references, bibliography, footnotes and endnotes)

Abstract

Heart failure is a common and debilitating disease. In recent years, improved diagnosis and treatment have resulted in more people than ever living with the condition. Accurate quantification of cardiac function is essential in the diagnosis and monitoring of heart failure. A good diagnostic test must reflect cardiac contractile state and is insensitive to physiological changes in load.

This thesis investigated the effects of changing load on existing and novel indices of cardiac function obtained using echocardiography. Firstly, breathless patients on maintenance haemodialysis underwent echocardiography immediately before and after a session of dialysis (large preload change). Secondly, healthy blood donors underwent echocardiography immediately before and after a session of venesection (moderate preload change).

Indices of cardiac function showed differential preload sensitivity during the above experiments. Conventional indices (EF, MAPSE) were relatively preload resistant. Longitudinal and radial tissue Doppler velocities and left ventricular apical rotation were more load-sensitive and tracked moderate preload change. Mid left ventricular circumferential strain was resistant to moderate preload change but was sensitive to a large preload change. Mid left ventricular radial strain, basal rotation and longitudinal strain and strain rate were unaffected by these changes in preload.

The key result from this thesis is that many echocardiographic indices of cardiac function are sensitive to changes in preload. Therefore, clinical interpretation of these results must take into account the loading status at the time of study.

Dedication

To James and Grace,

Thank you for your continuous patience, understanding, and encouragement

And

In loving memory of baby Harry

Acknowledgements

St Jude Medical supported this research through a fellowship programme.

I thank the Welsh Blood Service and the Nephrology Department at the University Hospital of Wales for hosting this study. I am grateful to Professor Rob Shave at Cardiff Metropolitan University for the loan of research equipment. I am also thankful to Dr Keith Morris at Cardiff Metropolitan University for his advice on statistical methods.

A special thank you goes to my clinical supervisor, Professor Zaheer Yousef, for the faith he placed in me in seeing this through to fruition. My heart felt gratitude to my academic supervisor, Professor Alan Fraser, for the thought provoking exchanges and much needed guidance I have received to the completion of this thesis.

Commonly used abbreviations

2DSTE	two-dimension speckle tracking
6MWT	6-minute walk test
A	peak trans-mitral filling velocity in late diastole
AVC	aortic valve closure
AVO	aortic valve opening
BP	blood pressure
CO	cardiac output
CPEX	cardio-pulmonary exercise testing
DBP	diastolic blood pressure
dp/dt	change in pressure over time
DT	early mitral filling deceleration time
E	peak trans-mitral diastolic filling velocity in early systole
e’	peak early diastolic tissue velocity
EDP	end diastolic pressure
EDV	end diastolic volume
E_{es}	end systolic elastance
EF	ejection fraction
E_{NDavg}	normalised population-averaged left ventricular elastance
ESBP	end systolic blood pressure
ESV	end systolic volume
ET	ejection time
HFpEF	heart failure with preserved ejection fraction
HR	heart rate
ICC	intra-class correlation
IVA	isovolumetric acceleration velocity
IVC	isovolumetric contraction
IVRT	isovolumetric relaxation time
LA	left atrium
LAD	left anterior descending artery
LAV	left atrial volume
LAVI	left atrial volume index
LV	left ventricle
LV Tor	LV torsion
LVIDd	left ventricular internal dimension in diastole
LVIDs	left ventricular internal dimension in systole
LVOT	left ventricular outflow tract
MAPSE	Mitral annular planar systolic excursion
MPI	myocardial performance index
MRI	magnetic resonance imaging
MVC	mitral valve closure
MVO	mitral valve opening
NT-proBNP	N-terminal pro-B-type natriuretic peptide
PCWP	pulmonary capillary wedge pressure
PEP	pre-ejection period
PV	pressure-volume

PW	pulsed-wave
RA	right atrium
Rot	rotation
RV	right ventricle
RVOT	right ventricular outflow tract
s’	peak systolic tissue velocity
SBP	systolic blood pressure
S_{circ}	peak circumferential strain at mid LV
SD	standard deviation
S_{long}	peak longitudinal strain at systole
SR	strain rate
S_{rad}	peak radial strain at mid LV
SR_E	strain rate at early diastole
SR_{IVR}	strain rate at isovolumetric relaxation time
$S_{systole}$	Peak longitudinal strain
SV	stroke volume
Tau	isovolumetric relaxation time constant
TDI	tissue Doppler imaging
Tor	LV torsion
VTI	velocity time integral

Table of Contents

List of Tables

List of Figures

1 Introduction

1.1 The burden of heart failure with preserved ejection fraction (HFpEF)

Heart failure is a complex clinical syndrome, resulting from the inability of the heart to meet the demands of major organs, despite normal or high filling pressure. It is common, affecting up to 1 in 20 adults in developed countries (1). An expanding ageing population, improved diagnosis, treatment and survival for those with heart diseases (2) have resulted in rising incidence (3) and prevalence, especially amongst older people(1). This poses a significant burden on health care budget (4,5), accounting for 2% of in-patient bed days and 5% of all emergency admissions to NHS hospitals (6).

In the 1980's, 36% of patients presenting with acute congestive heart failure were found to have preserved ejection fraction (HFpEF) on subsequent investigations (7). In the following decade, the prevalence of HFpEF in an out-patient population was found to be 22% (8). Contemporary registries have reported that as many as half of those with heart failure have HFpEF (2,9–16).

Five-year survival amongst people with HFpEF is significantly worse compared to the age- and gender-matched general population (11). In-hospital mortality following acute de-compensation has been reported at 4.2% in two studies (12,17). From index hospitalisation, population-based registry studies (2,12,15,16,18–21) reported an average annual mortality of 10-25%, although clinical trial participants fared better with an annual mortality of 5-14% (22–26).

The available treatment is different for those with reduced ejection fraction and for those with preserved ejection fraction. Hence, correct clinical diagnosis and characterisation using available investigations are essential in the management of these patients.

1.2 Current diagnostic criteria for HFpEF and limitations

The majority of patients meeting the criteria for the clinical diagnosis of HFpEF were found to have elevated left ventricular end-diastolic pressure (LVEDP) and impaired left ventricular (LV) relaxation, at the time of cardiac catheterisation (13,27,28). Echocardiography, which is easily accessible and non-invasive, has been widely accepted to be an invaluable diagnostic test for this condition.

The literature shows many studies identifying abnormalities in patients with HFpEF using echocardiography. Tissue Doppler Imaging (both pulsed wave tissue Doppler; and processed velocities from colour tissue Doppler), 2-dimensional speckle tracking (2DSTE) strain, blood flow Doppler velocities and diastolic filling pattern, non-invasively quantified left ventricle elastance (E_{es}) are amongst the many methods reported. Compared to asymptomatic subjects, patients with HFpEF have lower longitudinal TDI systolic (s') (29–34) and early diastolic (e') (29,31–34) velocities, lower MAPSE (mitral annular planar systolic excursion) (35). They also have reduced global longitudinal strain (30,36,37), reduced radial strain (33,36), reduced circumferential strain (33,36) and reduced left ventricular torsion (37,38) when compared to asymptomatic subjects. Left ventricular relaxation index (*Tau*)

(31) is prolonged, left ventricular filling index E/e' (31,34) is high and left ventricular elastance E_{es} (31,33,36) is low compared to healthy volunteers.

Whilst the European Society of Cardiology (38) adopts a stepwise clinical approach for the diagnosis of HFpEF, the American Society of Echocardiography (39) focuses on the assessment of LV diastolic function and estimation of LV filling pressure by echocardiography. Both societies agree on the primary findings of abnormal cardiac structure and evidence of elevated LV filling pressures, in the diagnosis of HFpEF. The similarities and differences are summarised in Table 1-1.

Table 1-1 Comparison of current international guidelines on the diagnosis of HFpEF

	European (38)	American (39)
EF	> 50%	> 50%
LAVI	> 34 ml/m^2	> 34 ml/m^2
LVMI	♂ > 115 g/m^2 ♀ > 95 g/m^2	Not included
E/e’	Mean >13	Mean > 14 cm/s
e’		Septal e’< 7 cm/s Lateral e’ < 10 cm/s
Peak TR velocity		TR velocity > 2.8 m/s

To meet the European criteria for a clinical diagnosis of HFpEF, a patient must have symptoms and signs of HF, EF ≥ 50%, elevated level of natriuretic peptides and either cardiac structural abnormality (LA dilatation, LVH) and/or functional alteration (abnormal E/e', e', global longitudinal strain, tricuspid regurgitation). When there is uncertainty, a diastolic stress test is recommended to demonstrate changes in E/e', TR velocity, SV and CO and global longitudinal strain. Alternatively, invasive assessment of LV filling pressures can be performed at rest and with exercise to detect changes in LVEDP, PCWP, SV and CO.

At least 2 of the 4 criteria have to be present (LA enlargement, elevated E/e', low e', elevated TR velocity) to meet the American Society of Echocardiography's requirement for diagnosis of diastolic dysfunction. In addition, the society also recommends using Valsalva manoeuvre during echocardiography to evaluate changes in E/A which helps unmask diastolic dysfunction.

Whilst the positive predictive value of a single parameter (E/e') is poor (40,41), the combined use of a panel of indices (TR velocity, E/A, E/e', e'), increases the diagnostic accuracy for elevated LVEDP (42). Some investigators studied their subjects at rest (29–31,36), others have studied their subjects at rest and during stress using upright ergometer(43), supine ergometer (33,35,37,44) and dobutamine infusion (32,34). Therefore, although these studies identified abnormalities, it is difficult to ascertain how much of the observed effects and differences might be related to changes in loading conditions. Before we can use these parameters as a diagnostic tool, we must first understand how each of these indices respond to a preload change. In the following sections, I shall first discuss

how contractile indices respond to changes in preload that were observed using PV loops (section 1.3), and then I shall review studies in which the effects of altering load were investigated using echocardiography (section 1.4).

1.3 Frank-Starling mechanism & Pressure-volume (PV) relationship of the left ventricle

The Frank-Starling mechanism (45,46) is central to our understanding of cardiac mechanics. An increase in preload and a larger LVEDV lead to an increase in cardiac contractile force. This is mediated by heightened sarcomere responsiveness at a given calcium concentration (47). In other words, a longer end-diastolic length of the myocyte within the physiological range causes increased systolic shortening. Figure 1, adapted from elsewhere (48) shows this graphically. It is worth noting that there is an initial linear relationship between LVEDP and SV/CO, until a plateau is reached whereby SV/CO remain static and subsequently fall despite further increase in LVEDV. Failure of actin/myosin filaments to form cross bridges at long myocyte lengths above the physiological range, and also the development of ventricular interaction and pericardial constraint (49) at larger LVEDV, are probable causes of the descending limb of the Frank Starling curve. At any given preload (LVEDV), inotropic stimulation increases SV/CO but this is reduced in a failing heart. This is in part due to reduced sarcoplasmic endoplasmic reticulum calcium ATPase expression, resulting in a depressed contractile state at a given calcium concentration (50).

Bearing these principles in mind, one would expect an ideal marker of cardiac function to distinguish intrinsic contractile properties in health from that of a

diseased state. It should also track and reflect contractile state following positive and negative inotropic stimulation. A predictable response to load change is also essential to aid meaningful clinical interpretation. Many parameters derived from invasive conductance catheter studies and echocardiography are used as markers of cardiac contractile function. It is therefore reasonable to expect these parameters to respond to changes in preload and to reflect the Frank-Starling mechanism. Some parameters (Ees, IVA) are considered preload-independent markers of contractile properties, whilst most other parameters (SV, CO, EF, TDI s', 2DSTE strain, LV torsion) are sensitive to changes in preload. In the following sections, I shall discuss how these indices respond to changes in preload that were observed using PV loops (section 1.3.1), and then I shall review studies in which the effects of altering load were investigated using echocardiography (section 1.4).

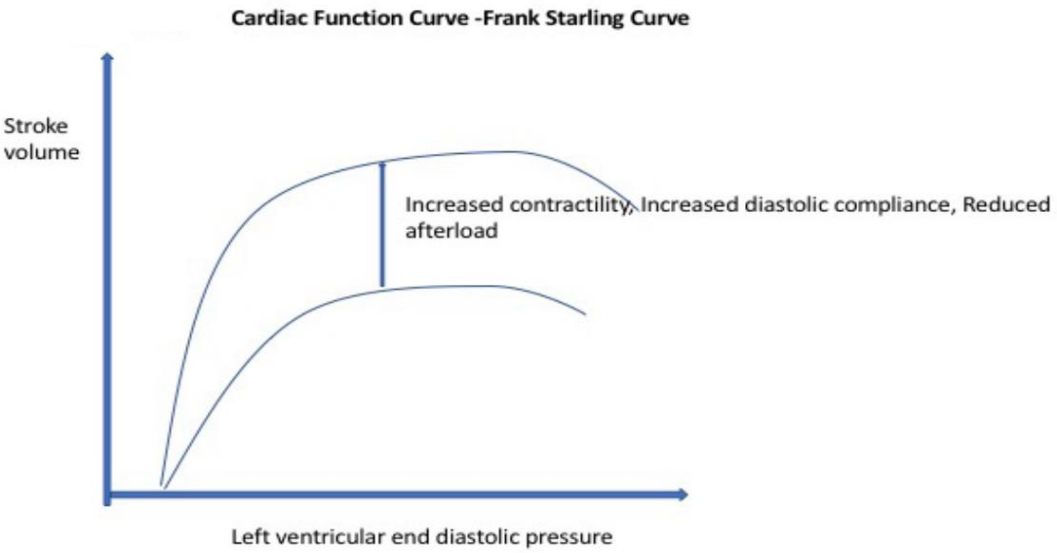

Figure 1 Schematic representation of Frank-Starling curve, adapted from Anesth Pain Res (48).

Data from pressure-volume (PV) loops obtained using conductance catheters during invasive studies were long considered the working standard in the investigation and diagnosis of heart disease. To describe the pressure-volume (PV) relation (51) of the heart briefly, at end-diastole mitral valve closure is followed by isovolumetric pressure rise. Maximal positive pressure change (max positive dp/dt) occurs before or at aortic valve opening, and left ventricular ejection follows. At end-systole, aortic valve closure precedes isovolumetric pressure decline until mitral valve opens and left ventricular diastolic filling occurs. Maximum negative pressure decline (max negative dp/dt) occurs after aortic valve closure and isovolumetric relaxation of the left ventricle follows. The time course of this isovolumetric pressure decline is exponential (52–54) and the pressure decay can be characterised by a time constant (55) *Tau*. The end-systolic pressure-volume intercept point is $E_{max.}$ The slope of serial readings of E_{max}, produced by altering afterload and inotropic status in consecutive experiments, is the end-systolic pressure volume relationship (ESPVR) or end-systolic elastance (E_{es}). Stroke volume (SV) is the difference of end-diastolic volume (LVEDV) and end-systolic volume (LVESV). Ejection fraction (EF) is the percentage of SV/LVEDV. LVEDP and LVEDV are widely accepted as markers of left ventricular filling (preload). EF, maximal positive dp/dt and E_{es} are markers of LV contractile function. Maximal negative dp/dt and *Tau* are markers of diastolic function of the LV.

Figure 2 shows a schematic representation of the left ventricular PV loop, adapted from *Comprehensive Physiology* (56). Point A denotes end-diastole, mitral valve closure, and the onset of isovolumetric contraction (ICT). Point B denotes the

point whereby LV pressure exceeds that is necessary for aortic valve opening and the onset of ejection. Point C denotes end-systole and aortic valve closure. This point, the end-systolic pressure-volume point, is used to develop the end-systolic pressure volume relation (ESPVR). Point C is also the onset of isovolumetric relaxation (IVRT). Point D denotes the end of the isovolumetric relaxation phase, opening of the mitral valve, and the onset of diastolic filling. This phase of diastole can be used to develop the diastolic pressure-volume relation. Both the end-systolic and end-diastolic pressure-volume relationships are determined by plotting values with acute changes in LV loading conditions to develop a family of LV pressure-volume loops and are shown here for illustrative purpose only.

In the following section, I will discuss the pressure-volume/time relationship of the heart and its response to changing load within a physiological range.

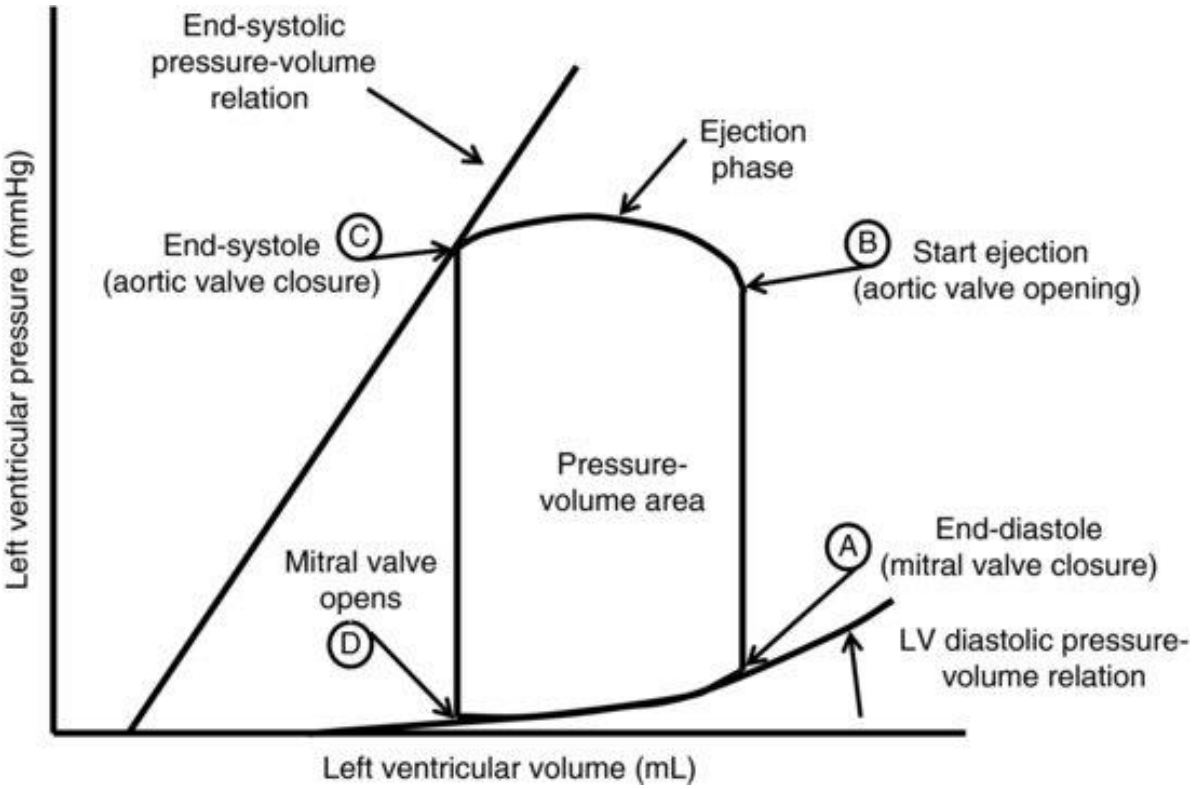

Figure 2 Schematic representation of a left ventricle pressure-volume loop. Adapted from Spinale FG. Compr Physiol. 2015 Sep 20;5(4):1911-46. doi: 10.1002/cphy.c140054.

1.3.1 Effect of load on PV loop measurements

1.3.1.1 Animal models

In an isolated canine heart model, Weiss et al (55) demonstrated the effect of changing heart rate, preload and inotropy on left ventricular pressure in isovolumetric hearts. Following maximal negative dp/dt, the pressure-time-course relationship of the left ventricle proved to be exponential, and it is characterised by the index *Tau*. A shortened *Tau* from the control state would indicate an increase in active left ventricular relaxation. Maximum negative dp/dt was sensitive to change in preload, heart rate, inotropy and ischaemia. Unlike maximal negative dp/dt, *Tau* index did not change with alteration in preload and heart rate, but was sensitive to the altered inotropy and ischaemia. This study concluded that *Tau* index reflects the intrinsic active relaxation property of the heart. Its insensitivity to physiological changes (preload and heart rate) makes it a more robust index compared to maximal negative dp/dt in the assessment of early diastolic cardiac function.

Using a similar canine model, Kass et al (57) studied the effects of changing load and altered inotropy on systolic contractile indices. They used right atrial pacing to maintain a constant heart rate and to eliminate the *Treppe* effect (force-frequency relationship) on these measurements. They studied the effects of altering preload and afterload by manipulating a balloon in the vena cava and descending aorta. The authors reported preload dependency of left ventricular end-diastolic volume (LVEDV) and pressure (LVEDP), stroke volume (SV), ejection fraction (EF) and maximal positive dp/dt. Afterload change had an inverse relationship with stroke volume (SV), ejection fraction (EF) and maximal positive

dp/dt. Altered inotropy changed ejection fraction (EF), maximal positive dp/dt and LV end-systolic elastance (E_{es}). E_{es} tracks inotropy change but was insensitive to changes in preload and afterload in the range studied in this experiment.

In summary, the above animal experiments (55,57) demonstrated preload dependence of LVEDP, LVEDV and SV. Systolic indices (maximal positive dp/dt, EF) and diastolic indices (maximal negative dp/dt) are both preload and afterload sensitive. Two indices (E_{es} and *Tau*) are load insensitive and reflect changes in contractile state. Human studies have since replicated these findings from animal studies. I will discuss these studies in the next section.

1.3.1.2 Human models

Quinones et al (58) studied the effect of changing load in 14 patients undergoing cardiac catheterisation. The majority of these patients (12/14) had normal LV systolic function and all had normal coronary arteries. Right atrial pacing kept heart rate constant during the study. They used fluid (dextran or normal saline) infusion to increase preload (LVEDP) to >10-15mmHg, an increase of 7-10mmHg from baseline value. Afterload was increased (a rise in LV systolic pressure of 15-60mmHg) by infusion of angiotensin. Maximal positive dp/dt was sensitive to changes in preload and afterload (an inverse relationship).

Penicka et al (13) performed cardiac catheterisation and echocardiography in 30 subjects with stable symptoms of dyspnoea who had normal left ventricular ejection fraction >50%. To study the effect of different loading conditions and contractile states, the subjects were studied at rest, during handgrip exercise (an

increase of afterload), leg lift (an increase of preload), nitroprusside infusion (a decrease of preload and afterload) and dobutamine infusion (an increase in contractile state) consecutively. Following manipulation of preload and afterload it was clear that left ventricular volumes (LVEDV) and pressures (LVEDP), cardiac output (CO), ejection fraction (EF), heart rate and end systolic blood pressure were responsive to a change in load with different sensitivity. However, only following dobutamine infusion was an increase seen in the end systolic left ventricular elastance (E_{es}) and maximal positive pressure change of the left ventricle (max positive dp/dt). Their results are summarised in Table 1-2.

Table 1-2 Effect of load and inotropy on PV loop derived measurements (13)

	↑ preload by leg lift	**↑ afterload by hand grip**	**↓ preload and afterload by nitroprusside infusion**	**↑ contractile state by dobutamine infusion**
Change in LVEDP	↔	↑ 7 mmHg	↓ 8 mmHg	↓ 5 mmHg
Change in LVESV	↔	↑ 8 ml	↓ 11 ml	↓ 17 ml
Change in LVEDV	↔	↔	↓ 19 ml	↓ 23 ml
Change in HR	↔	↔	↔	↑ 16 bpm
Change in CO	↔	↔	↔	↑ 1.2 l/min
Change in EF	↔	↔	↑ 6 %	↑ 8 %
Change in ESBP	↔	↑ 29 mmHg	↓ 30 mmHg	↓ 18 mmHg
Change in E_{es}	↔	↔	↔	↑ 1.2 mmHg/ml
Change in maximal +dp/dt	↔	↔	↔	> two fold ↑
Change in *Tau*	↔	↔	↔	↔

In summary, PV loop studies in humans showed identical results to those in animals. Contractile indices, E_{es} (systole) and *Tau* (diastole), are load insensitive. Other PV loop derived measurements (LVEDP, LVEDV, SV, EF, and maximal positive/negative dp/dt) reflect LV filling pressure, systolic and diastolic function but are preload and afterload sensitive even within a physiological range. The effects of load manipulation, changing heart rate and altered inotropy on pressure-volume loop derived measurements in animals and humans are summarised in Table 1-3.

Therefore, clinical interpretation of these (derived from PV loops) measurements must take into account the state of loading, before drawing a meaningful conclusion. Because they are invasive measurements, however, that are time-consuming to acquire and that need considerable expertise for interpretation, they are not relevant for routine use in elderly patients with suspected HFpEF. Echocardiography, a non-invasive and easily accessible investigation, is widely accepted as a diagnostic tool. In the following section, I will discuss validation studies using echocardiography compared with cardiac catheterisation.

Table 1-3 Effect of heart rate, load, and inotropy on PV loop derived measurements.

Study	**Intervention**	**LV VOLUME**		**LV PRESSURE**	**SYSTOLIC INDICES**		**DIASTOLIC INDICES**		**Ees**
		EDV	SV	LVEDP	EF	+dp/dt	-dp/dt	Tau	
(55)	Preload ↑	↑	↑	↑	Not studied		↑	↔	Not studied
	Heart rate↑	Not studied			Not studied		↑	↓	Not studied
	Inotropy↑	Not studied			Not studied		↑	↓	Not studied
(57)	Preload ↑	↑	↑	↑	↔	↑	Not studied		
	Afterload ↑	↔	↓	↔	↓	↓	Not studied		
	Inotropy↑	↔	↑	↔	↑	↑	Not studied		↑
(58)	Preload ↑	Not studied		↑	Not studied	↑	Not studied		
	Afterload ↑	Not studied		↔		↓	Not studied		
(13)	Preload↑	↔	↔	↔	↔	↔	Not studied	↔	↔
	Afterload↑	↔	↓	↔	↔	↔		↔	↔
	Nitroprusside	↓	↔	↓	↔	↔		↔	↔
	Dobutamine	↓	↑	↓	↑	↑		↔	↑

1.4 Validation of echocardiography against PV loop measurements

As mentioned before, echocardiography is non-invasive. Direct visualisation of the cardiac structures is possible with high temporal and spatial resolution. Doppler flow study, tissue Doppler imaging and speckle tracking add further useful information regarding the structure and function of the heart. In this section, I will review validation studies using invasive catheters and echocardiography. For ease of narration, I will discuss first systolic indices and then diastolic indices.

1.4.1 Echocardiography in the assessment of left ventricular systolic function

As discussed in previous sections (section 1.2.2), invasively derived left ventricular end systolic elastance (E_{es}) from PV loop studies is a good marker of underlying contractile state. It tracks changes across a range of contractile states predictably and is preload and afterload insensitive, at a constant heart rate. Hence, the search for a similarly robust index using non-invasive modality such as echocardiography is at the heart of many studies.

1.4.1.1 Non-invasive estimation of E_{es}

In this section, I shall first discuss briefly the gold standard of invasive estimation of E_{es}, followed by the single beat method of invasive E_{es} estimation, and finally the non-invasive estimation of E_{es}. Suga et al (59) used a supported excised

denervated canine heart model to study the instantaneous pressure-volume relationship (ESPVR) of an ejecting left ventricle. They used an infusion of epinephrine to alter inotropy and atrial pacing to alter heart rate. They produced consecutive pressure-volume curves under different loading conditions. The group found that the end-systolic left ventricular pressure-volume intercept (E_{max}) is load independent and tracks contractile state change. Later, Suga and Sugawa (60) reported on another experiment using an excised, supported canine heart model. They studied the instantaneous pressure-volume relationship of the left ventricle during isovolumic and auxobaric (constant volume with varying load) contraction. Repeated experiments with inotropes and various loads produced consecutive pressure-volume curves of the left ventricle. The authors again found that E_{max} is load independent and tracks contractile state of the left ventricle.

E_{max}, end-systolic pressure-volume intercept of the left ventricle thus provides a useful assessment of the contractile state independent of loading condition. Linear regression of E_{max} from consecutive PV loops produces a line of ESPVR and its slope is E_{es}. E_{es} is a load independent contractile index of the left ventricle. However, the main limitation of quantifying E_{max} and E_{es} by the methods (59,60) described above is the cumbersome need to acquire multiple cardiac cycles at varying loading conditions.

Sunagawa et al (61) in 1980 were the first to have developed a line fitting mechanism for estimating the pressure-volume intercept at end diastole in a canine model using a single beat. Igarashi et al (62) took this further and used another canine open chest model to develop a method for estimation of E_{max} and E_{es} by assuming the linearity of ESPVR line within a physiological range of loads. Takeuchi

et al (63) tested this single-beat estimation method of E_{es} in human subjects against the conventional method of performing serial PV loops. They found the single beat PV loop study estimated E_{es} has good correlation and agreement to the actual measured E_{es} by conventional iterative PV loop method. The studies (59–63) described so far only included human and animal subjects with normal hearts. For this method of single beat estimation of E_{es} to be of clinical relevance, it needs to be applicable to subjects with normal and impaired cardiac function.

Senzaki et al (64) developed a different single beat method of estimation of E_{es} in human subjects, by deriving the normalised time-varying elastance($E_N(t_N)$) curves. The left ventricle is an elastic structure that stiffens and relaxes during the cardiac cycle in a predictable time course. This changing pressure-time relationship in a cardiac cycle is the time-varying elastance. The authors found that $E_N(t_N)$, normalised time-varying elastance, in humans was consistent across a wide spectrum of cardiac disease, contractility, loading and heart rate. They then used this normalised time-varying elastance to estimate E_{max} and E_{es} in a single PV loop. The values estimated by this method were well correlated and agreed with the values produced by serial PV loop measurements.

Another canine model study (65) reported by Shishido et al used the time-varying elastance to estimate E_{es} in a single beat PV loop and found similar results to that of the Senzaki group. Estimated E_{es} was well correlated and agreed with the values produced by serial PV loops. It is also afterload insensitive, and tracks change in cardiac contractile state. These studies (64,65) laid the path for non-invasive estimation of E_{es} with the knowledge of a constant $E_N(t_N)$.

Kim et al (66) modified the single beat method estimation of E_{es} developed by Shishido et al (65) using echocardiography. They assumed an EDP value of 10mmHg. A combination of arm cuff blood pressure readings, biplane method EF and stroke volume, Doppler flow derived pre ejection period (PEP) and ejection time (ET) produced an estimated E_{es} reading. They validated this method in juvenile sheep against the gold standard method of producing E_{es} with iterative PV loops. They found that non-invasively estimated E_{es} has good correlation (Pearson's R=0.79) and agreement (mean difference of 0.1 ± 0.6 mmHg/ml) with invasively derived E_{es}.

Tanoue et al (67–70) first derived a much simpler single beat estimation of E_{es} in canines and later validated this non-invasively in children undergoing cardiac surgery. Only arm cuff systolic blood pressure and biplane ESV from echocardiography are required for this calculation. Estimated E_{es} correlated well (Pearson's R=0.966) with gold standard E_{es} with a small mean difference between the measurements.

Chen et al (71) derived a non-invasive method for E_{es} estimation, assuming the constant normalised left ventricular elastance $E_N(t_N)$ described before (64,65). They made an empirical estimation of normalized population-average elastance at the onset of ejection fitted by a 7-degree polynomial to the ratio of pre ejection time (PEP) to total systolic ejection time (ET) measured by spectral Doppler. This, in combination with arm cuff blood pressure, left ventricular volumes and EF derived from echocardiography yielded the non-invasive single beat estimated E_{es}. The estimated E_{es} showed good correlation and agreement with the gold standard E_{es} measured from PV loop studies. In addition, non-invasive single beat estimated E_{es}

has the same resistance to load change and tracks contractile state reliably as invasive E_{es}. Redfield et al (72) studied the E_{es} using this method (71) in a community dwelling group of asymptomatic people of older than 45 years, with no established cardiovascular disease. They found a range of E_{es} 1.74 mmHg/ml to 2.46 mmHg/ml in this group. Sasso et al (73) showed the single beat estimation (71) of E_{es} is feasible in dialysis patients. These values remained unchanged following dialysis.

Although several studies (66,67,71) have validated the non-invasive E_{es} estimation against the single beat methods (61–65), the methodology in using 2D echocardiography cannot be truly 'single beat'. Biplane left ventricular volumes quantification using 2D echocardiography requires image acquisition in separate beats. Herberg et al (74) used 3D echo and validated the single beat method against conventional iterative method for E_{es}. They found good agreement and correlation with the two methods. Scali et al (75) used 3D echo and quantified E_{es} in normotensive, hypertensive and heart failure subjects using a single beat method as previously described (67). They found normotensive and hypertensive subjects have higher E_{es} compared to subjects with heart failure. Gayat el al (76) estimated E_{es} using 3D echo and compared the previous methods (65,66,71) of non-invasive quantification. They found significant difference in E_{es} in the two groups (healthy volunteers and subjects with dilated cardiomyopathy). One method (66) was superior in providing clear cut-off values for separating the clinical subgroups.

1.4.1.2 Other systolic indices using echocardiography

Greenberg et al (77) validated peak systolic tissue Doppler velocity (s') and strain rate (SR) against PV loop in a closed-chest anaesthetised canine model. Low then high dose infusion of dobutamine and esmolol consecutively produced modulation of contractile states. At each contractile state, inflation of a balloon in the inferior vena cava was used to obtain the ESPVR and measure E_{es}. Using tissue Doppler imaging at the septal annulus, they measured peak tissue Doppler velocity in systole (s') and peak systolic strain rate (SR). Their study found that expectedly, end systolic elastance E_{es} tracked the changes in inotropy at every stage of the experiment. Septal annular s' and peak systolic SR correlated well with E_{es} with Pearson's R=0.75 and R=0.94 respectively. Measurements of s' and SR were in good agreement with measurements of E_{es}, as tested by the Bland-Altman method. Similarly, Gorcsan at al (78) found good correlation of radial s' (r=0.85) with E_{es} measurements in a PV loop validation study in open-chest dogs using dobutamine and esmolol infusion to alter contractile state.

Understandably, the invasive nature of PV loops limits its use in subsequent validation studies with echocardiography. In addition, E_{es} is a global contractile index and does not provide specific information on regional cardiac function. Hence, TDI derived strain (S) and strain rate (SR) have been validated using alternative techniques such as sonomicrometry (79,80) in animals and MRI tagging (80,81) in humans.

Urheim et al (79) used an intact anaesthetised canine model whereby sub-endocardial ultrasonic crystals were implanted and connected to a

sonomicrometer. Instantaneous change in dimension and length during the cardiac cycle was used to calculate strain (S), strain rate (SR) and LV volumes. Strain (S), by definition, is the percentage change per unit length and tt can be expressed in absolute terms or as a percentage. Strain rate is the rate of this change expressed in 1/s. Conductance catheters generated LV pressure-volume loops for the study. Standard apical images were acquired using echocardiography. Tissue Doppler imaging (TDI) generated a time-velocity graph, from which a measurement of peak systolic tissue Doppler velocities (s') was possible. Time-integration of the TDI graph produced a strain (S)-time graph and peak longitudinal strain (Ssystole) can be measured. The integration of the strain graph against time produced the strain rate (SR) graph. They then compared the values of S and SR measured by sonomicrometry to those derived from tissue Doppler imaging. Pericardial dissection of the heart and brief balloon occlusion of the left anterior descending artery (LAD) allowed assessment of the effect of ischaemia on these indices. At baseline, S and SR values measured by sonomicrometry were no different from that derived using TDI echocardiography, provided the images were in the same axis orientation. These measurements showed a good (r=0.92) correlation. During transient LAD occlusion, the left ventricular apex became dyskinetic. Apical s' changed from a positive to negative value. S and SR graphs showed systolic expansion rather than compression. Basal (circumflex territory) S and SR remained unchanged. Basal s' decreased significantly possibly reflecting the loss of function in the apical segments. The authors concluded that non-invasive TDI derived S and SR measurements are comparable to those measured invasively using

sonomicrometer. In addition, these regional indices of LV contractile function are sensitive to track change in regional perfusion and inotropy.

Edvardsen et al (81) validated the use of TDI derived radial and longitudinal strain (S) measurements against 3-dimensional MRI tagging. They studied healthy subjects, patients with ischaemic regional wall motion abnormality, and patients undergoing dobutamine stress echocardiography for investigation of chest pain. Across a range of values in all groups, there was a strong correlation for radial (r=0.92) and longitudinal (r=0.84) strain derived using the two methods. Measurements obtained using these two modalities as tested (Bland Altman method) were in good agreement.

A major limitation of using TDI and the derived s', S and SR measurements, is its dependency on the axis orientation at time of image acquisition. Two dimensional speckle tracking (2DSTE) provides a solution independent of the axis orientation during image acquisition. Amundsen et al (80) validated 2DSTE longitudinal strain against sonomicrometry in animals and found good correlation (r=0.9) and agreement between the two modalities. In humans, they validated 2DSTE longitudinal strain against MRI tagging and found similar correlation (r=0.87) and good agreement. Langeland et al (82) validated 2DSTE longitudinal and radial strain against sonomicrometry in an open-chest sheep model. They used an infusion of esmolol or dobutamine to induce altered cardiac inotropy. 2DSTE strain had good correlation and agreement (by Bland Altman method) with sonomicrometry strain. Strain derived from both methods (sonomicrometry and 2DSTE) reliably tracked the altered contractile states produced in their experiments.

The helical structure (83) of the left ventricle has fibres gradually changing orientation from the sub-endocardium to the mid-wall and the epicardium (84,85). The opposite orientations of the sub-endocardial and epicardial fibres result in the clockwise rotation in the base, anti-clockwise rotation in the apex, and shortening of the left ventricle major axis in systole. This systolic wringing motion causes left ventricular ejection, followed by rapid untwisting of the fibres in diastole, allowing subsequent filling. Non-invasive assessment of left ventricular torsion (86) using 2DSTE correlates well and agrees with sonomicrometry in dogs (r=0.94) and MRI tagging in humans (r=0.85).

In summary, TDI derived systolic indices like septal annular longitudinal s', peak systolic longitudinal SR and radial s' showed good correlation and agreement with the E_{es} when validated against PV loop studies. Later, validation studies of sonomicrometry in animals and MRI tagging in humans showed good correlation and agreement for tissue Doppler longitudinal s' and SR in detecting regional differences in cardiac function. However, its accuracy is dependent on the axis orientation of the image at time of acquisition. 2DSTE and its angle independent derived longitudinal strain, strain rate and left ventricular torsion measurements correlated well with measurements from sonomicrometry in animals and MRI tagging in humans. In the following section, I will turn our focus to the diastolic parameters and validation studies in the diagnosis of HFpEF.

1.4.2 Echocardiography in the assessment of left ventricular diastolic function

Zile et al (27,28), studied stable patients with a previous clinical diagnosis of congestive heart failure using cardiac catheterisation and concomitant echocardiography. These subjects had normal left ventricular dimensions, ejection fraction (>50%) and left ventricular hypertrophy. At the time of cardiac catheterisation, almost all (92%) had elevated LVEDP (>16mmHg) and a majority (79%) had prolonged *Tau* (>48ms). However, fewer had abnormal echocardiographic indices consistent with diastolic dysfunction (isovolumetric relaxation time IVRT 38%, early diastolic filling velocity E 40%, late diastolic filling velocity A 50%, ratio E/A 40% and early diastolic filling deceleration time DT 64%). Since all the subjects were fasted for twelve hours prior to catheterisation, the 'diagnostic insensitivity' of the echocardiographic filling indices was perhaps down to the 'load sensitivity' of these indices.

Kasner et al (87) studied 43 subjects with symptoms of HFpEF by PV loop analysis followed by echocardiography 3-5 hours later. They recorded transmitral Doppler blood flow velocities and tissue Doppler (TDI) velocities at the lateral annulus. All the patients had elevated LVEDP (>12mmHg) and prolonged *Tau* (>48ms). Fewer patients had abnormal conventional Doppler indices consistent with diastolic dysfunction: 50% E/A, 44% IVRT and 49% DT. Moderate correlation of *Tau* was found with E/A (r=-0.36) and IVRT(r=0.31) respectively. DT correlated moderately with LVEDP (r=0.30). A filling ratio of early diastolic blood flow velocity to early diastolic tissue velocity, E/e', correlated with LVEDP (r=0.71), *Tau* (r=0.34) and was abnormal in 86% of the patients. The authors therefore proposed that the

combined tissue Doppler and transmitral blood flow Doppler velocities (filling ratio E/e') increase detection (ROC 84% sensitivity) of elevated left ventricular end diastolic pressure and impaired active LV relaxation.

Kasner et al (88) later studied similar patients with concomitant PV loop and echocardiography. Conventional and tissue Doppler imaging, 2 dimensional speckle tracking (2DSTE) were used. They noted the strain rate at isovolumetric relaxation time (SR_{IVR}), early diastole (SR_E) and late diastole (SR_L). Similar to previous studies, they found elevated LVEDP (>16mmHg) and prolonged *Tau* (>48ms) were apparent in these patients. The diagnostic sensitivity of the conventional and tissue Doppler velocities was identical to the previous studies(27,28,87). Using 2DSTE and strain rate (SR_{IVR}, SR_E and SR_L) did not improve the detection beyond that of combined tissue and conventional Doppler indices.

Much later, in a European multi-centre study (42), patients with normal and reduced EF were studied simultaneously using conductance catheter and echocardiography. Patients with elevated LVEDP had a LVEDP of ≥15mmHg.Several echocardiographic indices were used in combination to estimate LV filling pressure. In asymptomatic patients with normal EF, LV filling pressure was considered elevated if >2 parameters (septal e'<7cm/s or lateral e'<10cm/s, averaged E/e'>14, LAVI >34ml/m^2, tricuspid regurgitation velocity jet >2.8m/s) are present. In patients with symptom of heart failure regardless of EF, LV filling pressure was estimated to be elevated if E/A ≥2. For those with intermediate values (E/A <0.8 and E>0.5m/s or E/A >0.8 but <2), LV filling pressure was considered elevated if >2 parameters were present (averaged E/e'>14, LAVI>34ml/m^2, TR velocity >2.8m/s). The study found that these criteria correctly identify patients with elevated LVEDP 79% of the

time. Amongst patients with LVEF>50%, each of the echocardiographic parameters showed modest correlation with LVEDP, E (r=0.27), E/A (r=0.23), DT (r=0.32), e' (r=0.17) and lateral E/e' (r=0.20).

Thus far, studies(27,28,87,88) suggest that patients with HFpEF are characterised by elevated LVEDP and abnormal diastolic relaxation (prolonged *Tau*), despite normal EF. Doppler blood flow velocities and derived measurements (E/A, IVRT, DT) showed moderate correlation with *Tau* and LVEDP but lacked diagnostic sensitivity (40-50%). Filling index (lateral E/e') has improved diagnostic sensitivity (86%) and correlates with PV loop measurements of LVEDP and *Tau*. 2DSTE and strain rate did not improve the diagnostic sensitivity beyond what was previously shown using filling index of E/e'. Using a combination of echocardiographic indices (e', E/e', LAVI, TR velocity, E/A and E) improves the correct diagnosis of elevated LVEDP to 79% (42).

None of the validation studies (discussed in section 1.2.3) examined the effect of preload on the studied indices. Since echocardiography indices correlated and were in good agreement with those indices obtained from PV loop studies, it would be logical to assume similar preload dependency, as demonstrated separately with the PV loop indices. To perform well as a diagnostic tool, an index would have to reflect and track contractile state, across a range of physiological conditions, in a constant or a predictable manner so that useful clinical conclusion may be drawn. In the next section, I will discuss how changes in preload affect these echocardiographic indices in animal and human studies.

1.5 Effect of load on echocardiographic assessment of cardiac function

Many animal and human models demonstrated the effect of changing load on echocardiographic assessment of cardiac function. In this section, I will first discuss the findings in animal models, followed by the findings in human models.

1.5.1 Animal models

Using invasive pressure volume loop and simultaneous tissue Doppler echocardiography, Vogel et al (89) studied the effects of reducing preload (inferior vena cava occlusion), increasing afterload (intra-aortic balloon inflation)and altering inotropy (by infusion of esmolol and dobutamine) at a constant heart rate (right atrial pacing at 130bpm) in pigs. They also studied the force frequency relationship by pacing the right atrium at a heart rate range of 120-180bpm at constant preload and afterload. The authors used Tissue Doppler imaging at the lateral annulus of the left ventricle and produced a velocity time graph. Two indices: peak systolic tissue Doppler velocity (s') and isovolumetric acceleration (IVA) were measured from the graph. IVA occurs before or at the onset of mitral valve closure and precedes s'. The rate of change of tissue velocity during this isovolumetric time is IVA and it is expressed in cm/s^2. Left ventricular pressure, volume and the maximal rate of pressure change (maximal positive dp/dt) before or at onset of systole were determined from the pressure-volume loop. Left ventricular ESPVR or left ventricular end-systolic elastance (E_{es} in mmHg/ml) were derived from serial pressure volume intercept at the left corner of the PV loops. A small (↓ LVEDV by 5ml or 10%) preload reduction reduced LVEDP, maximal positive dp/dt and systolic

peak myocardial tissue velocity (s'). There was no change in E_{es} and IVA. A modest (↑ 30mmHg or 30%) afterload rise increased LVEDP, and maximal positive dp/dt but reduced s'. There was no change in IVA. The authors did not report the effect this had on E_{es} in their experiment. IVA, s', max positive dp/dt and E_{es} reliably tracked and reflected the pharmacologically imposed and altered inotropy. Increasing heart rate had the expected effect on IVA, s', and maximal positive dp/dt, all of which showed an increase. E_{es} did not change.

Urheim at al (79) studied effect of preload change in a canine model validated against implanted sonomicrometer. Saline infusion was used to increase preload (LVEDP) by 60% (around 10mmHg). They took measurements of TDI derived longitudinal s', S, SR at baseline and after preload increase. They produced E_{es} using the iterative method at baseline and after preload manipulation by balloon venal caval occlusion. They found preload increase did not affect the contractile index E_{es} but there was an increase in s', S and SR.

In another porcine intact heart model, A'roch et al (90) studied the effect of changing preload at different contractile states. Balloon vena caval occlusion produced a physiological range (within 10% of the baseline LVEDV) of preload changes. They altered cardiac contractility either by using an infusion of adrenaline (enhanced contractile state) or an infusion of beta-blocker (depressed contractile state). Radial and longitudinal peak systolic velocities (s') and strain rate (SR) were assessed using tissue Doppler imaging. The basal inferior wall in the parasternal long axis view provided s' and SR for radial function assessment. The basal septal wall in the apical 4-chamber view yielded s' and SR for longitudinal function

assessment. The authors found that at a constant preload and heart rate, radial and longitudinal s' tracks changes in inotropy but SR did not. Preload reduction at baseline contractile state did not change radial and longitudinal s', radial SR but there is a decrease in longitudinal SR. Similarly, preload reduction in an increased contractile state, did not change radial and longitudinal s' and SR. However, preload reduction in a depressed contractile state, caused a reduction in longitudinal s' and SR, and reduced radial SR but radial s' remained unchanged. The study concluded that radial s' is preload insensitive within a normal physiological range (10% of baseline LVEDP). Longitudinal s' and SR are sensitive even to a small preload reduction.

Another study used an isolated canine heart model, MRI tagging and echocardiography (91). The authors demonstrated that left ventricular torsion was sensitive to change in inotropy (dobutamine infusion), as well as to a small change in preload (increase of 3 mmHg LVEDP) and afterload (5 mmHg increase in peak systolic pressure). Preload increase led to an increase in left ventricular torsion whilst afterload increase led to a reduction in left ventricular torsion.

In summary, animal models have shown some echocardiographic indices of cardiac contractile function (torsion, TDI derived longitudinal s', S and SR) are preload sensitive to a differential degree, detecting even a small reduction/rise in preload. TDI derived IVA, radial s' and SR are resistant to preload changes within a normal physiological range.

In the following section, I will discuss findings in humans using different clinical models. Unlike animal studies, which were designed for a specific purpose,

human studies have often been opportunistic, used existing clinical situations, for example recruiting blood donors, dialysis patients, and symptomatic patients undergoing clinical investigations to evaluate the effect of changing preload on cardiac indices.

1.5.2 Human: Healthy volunteer models

Various clinical models exist in humans to investigate the effect of changing load on echocardiographic indices. In this section, studies involving healthy volunteers are discussed first, followed by studies in symptomatic patients and finally by studies in dialysis subjects.

Nineteen subjects with no cardiac history undergoing elective surgery indicated for non-cardiac reasons (49) were studied after preload expansion, given as hypervolaemic haemodilution to reduce blood loss in Jehovah's witnesses. After induction of anaesthesia, the investigators recorded transgastric images (end-diastolic area and end systolic area) of the left ventricle mid-cavity short axis. A radial arterial line and pulmonary wedge catheter provided invasive measurements of cardiac output (CO), stroke volume (SV), pulmonary capillary wedge pressure (PCWP) and blood pressure. Fluid infusion of 3 litres over 45 minutes, done in three stages of 1 litre over 10 minutes consecutively produced rapid and significant volume expansion. After the first litre, there was a decrease in heart rate and an increase in blood pressure. These did not change with subsequent fluid volume expansion. PCWP increased linearly with volume expansion. End-diastolic area of

the LV, SV and CO increased initially but remained unchanged thereafter suggesting pericardial constraint.

Another study (92) used rapid infusion of isotonic saline (rate of 30ml/kg over 15 minutes), administering between 1.5 to 3 litres to healthy subjects. This did not produce a change in heart rate or blood pressure (constant afterload and heart rate). Stroke volume (SV) was calculated by velocity time integral method and cardiac output was calculated from SV and heart rate. EF was calculated from the modified area and length method in the apical 4-chamber view. The increase in preload produced an increase in left atrial volume (LAV), left ventricular end-diastolic volume (LVEDV), cardiac output (CO), stroke volume (SV), septal and lateral mitral annular early diastolic velocities (e'), and the ratio of E/e' at septal and lateral annuli. However, there was no change in ejection fraction (EF), isovolumetric acceleration (IVA) in septal and lateral annuli, tissue Doppler derived septal and lateral annular strain rate (SR). Peak longitudinal strain (S) in the basal septum increased significantly but did not change in the other segments (mid septum, basal and mid lateral segments).

Healthy subjects undergoing saline infusion at resuscitative rate (3Ls over 3 hours followed by 1L over 2 hours) have demonstrated expected results of load dependency using conventional echocardiographic parameters (93). There is an increase in LVEDV, a reduction of LVESV and subsequently an increase in SV and EF. These observed results were independent of heart rate or blood pressure changes at the end of the first 3 hours.

Healthy blood donors undergoing venesection (94) showed that a modest preload reduction (500ml over 10 minutes) did not change heart rate and systolic blood pressure. The investigators performed echocardiography using Doppler blood flow and tissue Doppler velocities whilst the subjects maintained the same position immediately before and after venesection. There was a significant reduction in early (E) and late (A) diastolic left ventricular filling and TDI derived longitudinal strain (S) in the basal septum. In contrast, TDI velocities in basal septum (s', e' and a') and SR did not change. Other studies showed a small reduction of circulating volume in healthy population may produce transient change in heart rate and blood pressure, but is well tolerated(95–97). The effect of blood donation on non-invasively derived cardiac output, heart rate and its effect on neuro-hormonal cascade has been previously studied (96–99).

Following the combined results of the above studies(92,94,100) in healthy subjects, we are able to conclude that heart rate and blood pressure remain unchanged within a wide physiological range of preload (500ml reduction to 5L increase). Echocardiographic parameters are preload sensitive to various degrees. Diastolic Doppler flow (E, A) and basal septum longitudinal strain (S) are sensitive to even a small (500ml) reduction in preload. Some echocardiographic indices (s', e', EF) become load sensitive at larger preload change (1.5 L- 3 L) when an increase in LVEDV and E/e' are also apparent. Some indices (IVA, longitudinal TDI derived SR) are load insensitive even at significant preload change (3 L). I will discussed studies in breathless patients undergoing catheterisation in the following section.

1.5.3 Human: Breathless patient models

Another conductance catheter validated study (101) used 2DSTE in patients with normal ejection fraction (>50%) and normal regional wall motion. They performed echocardiography before and after intervention. Nitroprusside infusion caused a significant change in LVEDP, LV peak systolic pressure, *Tau*, E_{es} and LV torsion. Filling ratios (E/e', E/A), tissue Doppler velocity (e') and LV internal dimension in diastole ($LVID_d$) did not change. The authors concluded that 2DSTE derived left ventricular torsion is preload and afterload sensitive. However, as $LVID_d$, E/e' and E/A remained unchanged despite drop in LVEDP, we are just as likely to conclude that torsion is sensitive to afterload manipulation at constant preload.

Burns at al (102) examined the effects of sublingual GTN and rapid infusion of 750ml normal saline in elderly subjects undergoing investigations for chest pain. These subjects had a history of hypertension and relatively preserved ejection fraction (LVEF>45%). Concomitant invasive pressure-volume data and echocardiography were performed. Conductance catheter derived measurements including maximal positive dp/dt, *Tau* and LVEDP were used to estimate the systolic, diastolic contractile properties and left ventricular filling pressure. Afterload was estimated by calculating wall stress which is derived from left ventricular internal dimension, posterior wall thickness and left ventricular end systolic pressure. In addition to previously discussed echocardiographic parameters (EDV, ESV, EF, E, A, E/A, e', E/e'), left ventricular torsion was assessed using speckle tracking imaging (2DSTE). Rotation and rotation velocity graphs were obtained using speckle tracking at the left ventricular apex and base. To normalise for data

acquired at different cardiac cycles, all measurements were interpolated and expressed at percentage of cardiac cycle. The difference of rotation and rotational velocities from the apex to base is the torsion and torsion velocities of the left ventricle. Peak torsion, systolic torsion velocity, diastolic untwisting velocity were calculated from the graphs. Subjects were studied in a fasting state, followed by sublingual GTN administration. Following GTN administration, a steady state was reached for 15 minutes before data was acquired to serve as baseline for the fluid infusion.

GTN reduced LVEDP by 7mmHg and fluid infusion increased LVEDP by 7mmHg. Heart rate did not change after fluid infusion but increased after GTN. Maximal positive dp/dt, increased following GTN although *Tau* was unchanged. Fluid infusion caused a decrease in maximal positive dp/dt but an increase in *Tau.* Both modes of manipulation had the expected effect on echocardiographic indices. GTN produced a reduction in end diastolic and systolic volumes, a reduction of diastolic filling and ratio (E, A, E/A, e'), a reduction in wall stress, an increase in peak torsion and systolic twisting velocity but no change in diastolic untwisting velocity. Fluid infusion produced the opposite effect in left ventricular volumes and Doppler flow and tissue Doppler velocities. No change in peak torsion and systolic twisting velocity were seen, but there was a reduction in diastolic untwisting velocity. Although EF increased following GTN administration, it did not change after fluid infusion.

Burns at al concluded that their experiment reproduced similar and expected findings in the pressure-volume and echocardiography (volume, Doppler

and tissue Doppler studies) data. They claimed that left ventricular torsion, systolic twisting velocity, and diastolic untwisting velocity are sensitive to change in load. Although the design of this experiment reflects real life clinical practice, it is difficult to isolate the independent effect of preload and afterload on these indices.

Published separately, Burns et al (103) also reported on the change in 2-dimenisonal circumferential and longitudinal S and SR. Parasternal short axis LV view and apical 4-chamber LV view were post-processed using 2DSTE. Circumferential and longitudinal systolic S, SR were averaged over the 6 segments in the respective views. Following sublingual GTN, heart rate increased, LVEDP decreased, and peak systolic pressure decreased significantly. Systolic S and SR both increased circumferentially and longitudinally. Following fluid infusion, heart rate was unchanged, LVEDP and peak systolic pressure increased significantly. Circumferential and longitudinal S did not change but SR decreased significantly. These results suggest that provided heart rate is constant, increasing preload produces no change in 2-dimensional circumferential and longitudinal systolic strain. Strain rate, however was sensitive to this small preload increase.

1.5.4 Human: Haemodialysis patients model

Haemodialysis patients undergo regular change in load at times of dialysis. They render themselves suitable subjects for investigation of the effect of load on echocardiographic parameters. Bornstein et al (104) studied 10 dialysis patients with normal ejection fraction and no symptom of heart failure. Echocardiography and carotid pulse tracing were done simultaneously immediately before and after a

session of haemodialysis. Left ventricular internal dimensions at end diastole (LVIDd) and systole (LVIDs) were measured from echocardiography. Fractional shortening (FS) was calculated as (LVIDd-LVIDs)/LVIDs. Ejection fraction (EF) and stroke volume (SV) were calculated using Teichholz method. Left ventricular ejection time (LVET) and pre ejection time (PEP) were calculated from the carotid pulse tracing. Following 4-5 hours of dialysis at a flow rate of 250-300ml/min, there was significant weight loss, reduction in LVIDd, SV and LVET. No change was seen in heart rate, systolic blood pressure, EF and FS. No change in PEP was seen. The study concluded that at constant heart rate and afterload, left ventricular volume and dimension, and ejection time are preload sensitive. Indices of systolic function (EF, FS) were not preload sensitive at this given load change.

Hung et al (105) studied 128 patients with no cardiac symptoms 1 hour before and after a session of haemodialysis using 2 dimensional echocardiography, Doppler flow and tissue Doppler imaging. Despite identical flow rate as the above study, there was a significant drop in systolic blood pressure and increase in heart rate after dialysis. There was a predictable reduction in LVIDd, LVIDs, LVEDV, LVESV, SV, E, A, E/A, E/e', e'. They found a significant drop in septal (8%) and lateral (11%) e', early diastolic filling velocity E (26%), septal E/e' (11%) and lateral E/e' (15%) following dialysis. However there was no change in contractile indices (FS, EF) and late diastolic annular tissue velocity a'. The effect of preload could not be separated from that of afterload and heart rate in this study. However it seems FS, EF and basal annular a' are load/heart rate insensitive.

Assa et al (106) studied subjects with normal range of brain natriuretic peptide before, during (60 minutes and 180 minutes into dialysis) and 30 min following a session of haemodialysis. Heart rate increased and systolic blood pressure fell significantly during and remained so following dialysis. Diastolic mitral inflow Doppler velocities (E, A,), filling ratio (E/A, E/e') followed the same trend and reached significance. Doppler flow timing (DT and IVRT) were significantly prolonged. Similar to the study by Hung et al, this study reported the combined effect of preload/afterload reduction and increased heart rate.

Drighill et al (107) studied asymptomatic uraemic patients using echocardiography before and after haemodialysis. There was no change in systolic blood pressure but heart rate rose significantly. Diastolic mitral inflow velocities (E and A) and timing (DT), filling ratio (E/A, E/e') behaved same as the above study. Their study showed a significant change in TDI systolic (17% and 13% in lateral and septal s') and diastolic (4% and 23% in lateral and septal e') velocities following dialysis. The small change of lateral e' is insignificant; this coupled with the large (31%) change of early diastolic blood pooled filling velocity E, resulted in the significant change in filling pressure, estimated using E/e' in the lateral mitral annulus. Septal E/e' however remained unchanged. Global contractile index (EF) remained unchanged but regional systolic velocity (s') was significantly lower. We may conclude that these changes are independent of afterload but it is impossible to separate the effect of preload from that of increased heart rate.

Park et al (108) studied patients following a session of dialysis. They had significantly lower systolic blood pressure but unchanged heart rate following

dialysis. LV dimension, volume, stroke volume, mitral inflow Doppler flow rate (E, A) and timing (IVRT, DT), filling pressure (E/A, E/e'), septal and lateral annular s', septal annular e' all decreased, perhaps unsurprisingly. Ejection fraction (EF), lateral annular e', septal and lateral annular a' were unchanged.

Vignon et al (109) studied the effect of differential load change following dialysis on cardiac function. They studied stable subjects undergoing routine scheduled haemodialysis (3L volume loss) and compared their response to those of critically ill patients maintained on vasopressor infusion. The critically ill patients underwent ultrafiltration and lost 1.9l in volume although their blood pressure and heart rate did not change. The stable subjects dropped their blood pressure after dialysis but had unchanged heart rate. A 1.9l load change did not have an impact on E and mitral annular e' but a 3l load change significantly reduced E (24%), septal e' (17%) and E/e'. Lateral e' remained unchanged however. Their results were similar to other studies that I have already summarised. Although the results in the two groups cannot be compared directly, these results suggest that lateral annular e' is resistant to reduction in preload (up to 3L). In addition, septal annular e' only becomes preload sensitive beyond 2L load change.

Gerede et al (110) studied the effect of changing preload in dialysis patients. There was a small but significant change in systolic blood pressure (drop of 7mmHg), heart rate (rise of 2 bpm) and an average weight loss of 2.8kg over 4 hours. They used conventional Doppler (E, A, DT, IVRT, MPI) and tissue Doppler imaging (lateral annular s', e',a', modified MPI). Modified MPI was calculated by measuring the time intervals from a TDI pulsed wave trace in the lateral annulus.

Duration of s' was used in place of LVET, and isovolumetric time was calculated by subtracting duration of s' from the cycle length. They found consistent results in the preload dependency of LV dimension and conventional Doppler indices. LVEDD, LVESD, E, A decreased significantly, whilst IVRT, DT and MPI increased significantly. Using TDI, lateral s' increased significantly but e', a' and modified MPI remained unchanged. There was a small increase in isovolumetric time but no change in LVET. They concluded that TDI indices (e', a') and modified MPI are resistant to change in preload compared to conventional echocardiographic indices. However, it is possible that if there was a bigger change in heart rate, modified MPI too will show load sensitivity.

Hayashi et al (111) studied 13 patients before and after one session of haemodialysis. They used conventional Doppler indices and colour tissue velocity imaging (TVI). There was an average weight loss of 2.3kg over 3-4.5hours. The authors did not report heart rate and blood pressure before and following dialysis. Tissue velocities in eight segments (apical basal to mid septal, lateral, inferior and anterior walls) were averaged and reported as global systolic and diastolic functional indices. Systolic indices included were tissue velocity at time of isovolumetric contraction (IVC_v), peak systolic velocity (s'), and systolic strain rate (SR). Diastolic indices were early and late diastolic tissue velocities (e' and a'). Lateral mitral annular e' was used to calculate E/e'. Following dialysis, there was significant reduction in E, LVEDD, a', e', E/e' whilst IVC_v, s' and SR increased significantly. The authors concluded that tissue velocities are just as preload

sensitive as conventional Doppler indices. However, as heart rate and blood pressure were not reported, it is difficult to generalise the results of this study.

Sztajzel et al (112) studied the effect of dialysis on the LV filling pattern. Early diastolic blood flow velocity E dropped by 34% following dialysis. Chakko et al (113) studied the effect of differential load on cardiac function on the same patients undergoing dialysis. There was no change in the LV dimension and early diastolic filling E following dialysis without fluid removal (average weight loss of 0.5kg). LV dimension (6%) and E (16%) were significantly lower following dialysis with fluid removal (average weight loss 3.4kg). Fijalowski et al (114) studied dialysis patients and found septal e' remained unchanged, but septal E/e' dropped by 13% as E dropped by 15%.

Amongst patients undergoing a single session of dialysis (115), with baseline normal EF (EF>50%), there was a reduction in filling ratio E/e'. A differential response was apparent in the systolic (s') and diastolic (e') TDI velocities amongst patient with diabetes and coronary artery disease.

Galetta et al (116) studied the effect of dialysis on cardiac function. Following dialysis, there were no significant change in global EF, E, E/A. However, a significant reduction in lateral and septal s' (25% and 22%), a significant reduction in lateral and septal e' (31% and 24%) followed. It is possible that a small change in E was not detected due to the high measurement variability.

1.6 Summary of effect of load on echocardiography indices in humans

Thus far, studies in non-uraemic subjects have demonstrated that left ventricular contractile state is dependent on heart rate (force frequency relationship) at a given preload. Assessment of cardiac function is complicated by the load sensitivity of routinely used indices. Compared to echocardiographic indices (s', IVA, MPI, SR), invasively derived contractile indices (*Tau*, E_{es}), are relatively load insensitive across a physiological range, but they are ultimately load dependent. Provided loading and heart rate are taken into consideration, echocardiographic assessment provides good approximation to the underlying contractile state. At a constant heart rate and afterload, echocardiography measurements for volumes (LVEDV, LVESV, LAV), dimensions (LVIDd, LVIDs), Doppler blood flow rate (E, A) and filling ratio (E/e', E/A) are preload dependent. Some indices (TDI longitudinal s', TDI e', EF) are preload insensitive provided the change is small (500ml). Other indices (MPI, SR and IVA) may be more useful if the change in preload is significant (1.5 to 3 L).

Amongst asymptomatic stable haemodialysis patients, given constant afterload and heart rate, LV dimension is preload sensitive but regional and global contractile indices (FS and EF) are not. There is a differential load sensitivity using echocardiographic parameters (E, A, E/A, DT, IVRT, E/e', s', e') at various combination of preload, afterload and heart rate change. Some tissue Doppler velocities (lateral annular e', septal and lateral annular a') appear relatively load insensitive compared to others (septal e', septal and lateral s'). Some global

contractile indices (EF and FS) are load insensitive across a range of preload, afterload, and heart rate. They may track changes in contractile state relatively independent of load. Although indices like SR, IVA proved to be load insensitive in non-uraemic subjects, we know little of how these indices may change following dialysis.

1.7 Conflicting results of load dependency of echocardiographic indices in clinical models

Echocardiography provides good assessment of cardiac contractile function when validated against pressure-volume loop, sonomicrometry, and MRI tagging in a range of clinical models. However, its use for deriving clinical conclusion must take into account the loading conditions at the time of the study. The extensive literature shared many similar findings but also some inconsistencies. These are summarised in the following paragraphs.

The shared findings of animal and human studies are:

1. Left ventricular end diastolic volume and pressure (LVEDV, LVEDP), Doppler flow diastolic cardiac filling and its derived timings (E, A, E/A, DT, IVRT) are preload dependent. Measurements of these indices are sensitive to even a small change of preload, at a constant heart rate and afterload.
2. Tissue Doppler systolic velocities (s'), in particular longitudinal basal septal annular s' are sensitive to even a small change in preload, from as little as 10% or 500ml reduction in preload.

3. Tissue Doppler derived longitudinal strain (S) in basal septum is sensitive to a small change in preload, from as little as 500ml preload reduction and up to 60% increase in preload.
4. Tissue Doppler derived longitudinal strain rate (SR) in basal septum is resistant to a modest change in preload (from 500ml to up to 3l) but becomes load sensitive beyond this range.
5. Tissue Doppler derived septal e' is resistant to a small preload change (500ml reduction) but becomes load dependent at greater preload change (>1.5l).
6. Tissue Doppler derived lateral e' is resistant to a modest preload change (1.5-3l).
7. 2DSTE derived left ventricular torsion is preload sensitive and increases with a small preload reduction (up to 750ml).
8. Global systolic function index EF is resistant to preload change of up to 3l but becomes load sensitive beyond 5l of change in preload.

Despite the shared findings, there are some contradicting results:

1. Tissue Doppler derived basal septal s' may be resistant to a small change in preload (10% change or 500ml), as shown in two studies(90,94).
2. Tissue Doppler derived basal septal longitudinal SR may be sensitive to a small (10% reduction) change in preload (90).
3. Tissue Doppler derived lateral annular e' may be load sensitive at modest preload change of 1.5-3 L, as reported by two studies(92,111).

4. Pressure-volume loop studies have previously demonstrated load dependency of EF. This is not the case in many dialysis studies(101,104,105,107) where preload change of up to 3l was present.

There are findings that require further investigation and confirmation:

1. Tissue Doppler derived radial SR is less load sensitive compared to longitudinal SR, a reported finding by A'Roch et al (90).
2. Vogel and Dalsgaard et al (89,92) reported no change in IVA at a preload change of up to 3 L in two separate studies. However, IVA has an unacceptably high measurement variability as demonstrated in another study (117): intra-observer variability of 12-30% and inter-observer variability of 21-28%. This can limit the routine clinical application of IVA. Therefore, further confirmation of the load insensitive property of IVA, if proved to have acceptable repeatability in subsequent studies, can render it a useful clinical tool.
3. E_{es} is load insensitive in PV loop studies. Despite the availability of several methods (65–67,71) of single beat echocardiography estimation of E_{es}, the effect of load dependency on this index can be tested in further studies.

1.8 Research Aim

To evaluate the effect of preload change on a comprehensive range of echocardiographic indices using two readily available clinical models. Dialysis patients with symptoms of HFpEF serve as a model to study the effect of slow but large preload change (reduction of 3L circulating blood volume over 2 to 4 hours). Asymptomatic blood donors undergoing venesection serve as a model to study the effect of rapid small preload change (reduction of 500ml circulating blood volume over 10 minutes) in health.

I planned to answer the following questions posed by the existing literature:

1. Given a small (500ml) preload change, is TDI derived basal septal and lateral s' load sensitive?
2. Is TDI derived lateral e' load-resistant at a small (500ml) and large (3l) preload change?
3. Is TDI derived IVA preload insensitive, at a small (500ml) and large (3l) preload change?
4. Is TDI radial s' load insensitive at a small (500ml) and large (3l) preload change?
5. Is 2DSTE longitudinal S, radial S, and circumferential S load-resistant at a small and large preload change?
6. Is LV torsion resistant to small and large load change?
7. Is EF load-resistant at a small (500ml) and large (3l) preload change?
8. Is non-invasive quantification of E_{es} by single beat method feasible in clinical use?

9. Is non-invasive E_{es} load insensitive, given a small and large preload change?

1.9 Hypotheses

To summarise what I have discussed so far, the Frank Starling mechanism underpins our understanding of cardiac mechanics. At a given contractile state, cardiac function (SV) increases linearly with preload (LVEDV) increase, until the exhaustion of actin/myosin cross bridges and pericardial constraint occur. A good echocardiographic index should inform on the contractile property, and respond to a change in load predictably across a physiological range.

The existing literature suggests that two indices (IVA and E_{es}) are markers of contractile state and that they are unaffected by a change in preload and afterload. Although regional markers like TDI s', e', EF, LV rotation and torsion, 2DSTE radial/circumferential/longitudinal strain reflect contractile state, they behave heterogeneously in response to a change in preload. This makes clinical interpretation of these results challenging. Therefore, I aimed to investigate the following hypotheses:

1. It is feasible to adopt the use of non-invasive quantification of E_{es} clinically.
2. Non-invasively estimated E_{es} does not change following preload reduction.
3. IVA does not change following preload reduction.

4. Regional (TDI s', e', 2DSTE longitudinal strain, circumferential strain, radial strain and apical rotation, LV torsion) and global (EF, CO) cardiac function markers may change (increase or decrease) following preload reduction to an extent that is dependent on the magnitude of preload change.

2 Methods

2.1 Ethics Approval

Cardiff University was the sponsor (reference SPON 1150-12) of this study. The Research Ethics Committee (REC) for Wales first received this application in August 2012. The committee met in September 2012 and granted permission for this study in October 2012 (reference 12/WA/0288), following receipt of further clarification. Minor amendments were submitted to the committee notifying changes to the patient information leaflets in December 2012 and February 2013, with favourable outcome. The host organisation was Cardiff and Vale University Hospital Health Board for the dialysis patients. A separate site-specific application (reference 2013/VCC/0045) was made to the Welsh Blood Service for hosting the study in the blood donor group in April 2013. Permission was granted in September 2013. The study completed recruitment in May 2014.

2.2 Determination of study sample size

I used a statistical software G*Power (March 28, 2001) for sample size and power calculation. Previous published data (31,33,36,105,118–120) were used to calculate the sample size required to detect a 30% difference with 80% power. The published mean ± SD, sample size required for each of the parameters are shown in the table below (Table 2-1).

A sample size of 30 in the dialysis group was calculated to have a power of >80% in detecting a 30% change in each measured parameter after a change in preload.

The magnitude of preload change in studies (105,118) used for this calculation was 3.1 ± 0.9 L or up to 5% change of body weight.

For detecting a difference between the dialysis and blood donor groups, a sample size of 30 in the dialysis group and a sample size of 15 in the blood donor group were calculated to have achieved a power of >80% in detecting a 30% difference in each of the listed parameters.

Table 2-1 Sample size and power calculation

Studies	Measure	Published mean ± SD	Sample size required to detect a 30% difference following dialysis with 80% power	Sample size required to detect a 30% difference between dialysis and blood donor groups at baseline
Hung et al (105)	LVEDV (ml)	115 ± 29	8	13
	LVMI (g/m^2)	140 ± 44	11	18
	LAA (cm^2)	39 ± 6	5	6
	LVIDd (mm)	49 ± 6	4	4
	SV (ml)	78 ± 17	7	9
	E (cm/s)	91 ± 19	7	9
	A (cm/s)	105 ± 21	6	9
	E/A	0.9 ± 0.2	8	12
	DT (ms)	191 ± 49	9	13
	IVRT (ms)	88 ± 24	9	14
	e’ (cm/s)	8 ± 2	9	15
	a’(cm/s)	10 ± 2	5	7
	E/e'	13 ± 4	10	17
	LVEF (%)	73 ± 7	4	4
Choi et al (118)	LAVI (ml/m^2)	44 ± 14	12	20
	$S_{systole}$	18 ± 3	5	6
	s’ (cm/s)	7 ± 1	3	8
Wang et al (120)	S_{circ}	17 ± 3	5	6
	S_{rad}	41 ± 16	16	30
Chen et al (119)	E_{es} (mmHg/ml)	2.8 ± 1.0	14	24
Yip et al (36)	LV Torsion (^{0})	16 ± 7	19	34
Tan et al (33)	Apical Rot (^{0})	10 ± 4	15	27

2.3 Subjects recruitment

2.3.1 Inclusion criteria

2.3.1.1 Dialysis group

All stable patients on established regular haemodialysis at the University Hospital of Wales Health Board were eligible to take part in the study. To participate, each subject must be aged 18-85 years, be able to give informed consent, be able to adhere to study protocol and be on established haemodialysis. In addition, each subject must have symptoms of heart failure and have an EF>50%.

2.3.1.2 Blood donor group

Healthy blood donors from student and staff groups at Cardiff University and Cardiff Metropolitan University were invited to take part. To participate, each subject must be aged 18-85 years, be able to give informed consent, be able to adhere to study protocol. In addition, subjects with pre-existing renal disease and symptoms of heart failure were not eligible to take part.

2.3.2 Exclusion criteria:

Subjects aged <18 years or >85 years were ineligible to take part. Subjects who were unable or unwilling to give informed consent and who were unable to adhere to study protocol were excluded from taking part in this study. For the dialysis group, the presence of an alternative explanation for their symptoms would also exclude their participation in this study. The following diagram (Figure 3) outlines the recruitment process for the two groups of study subjects.

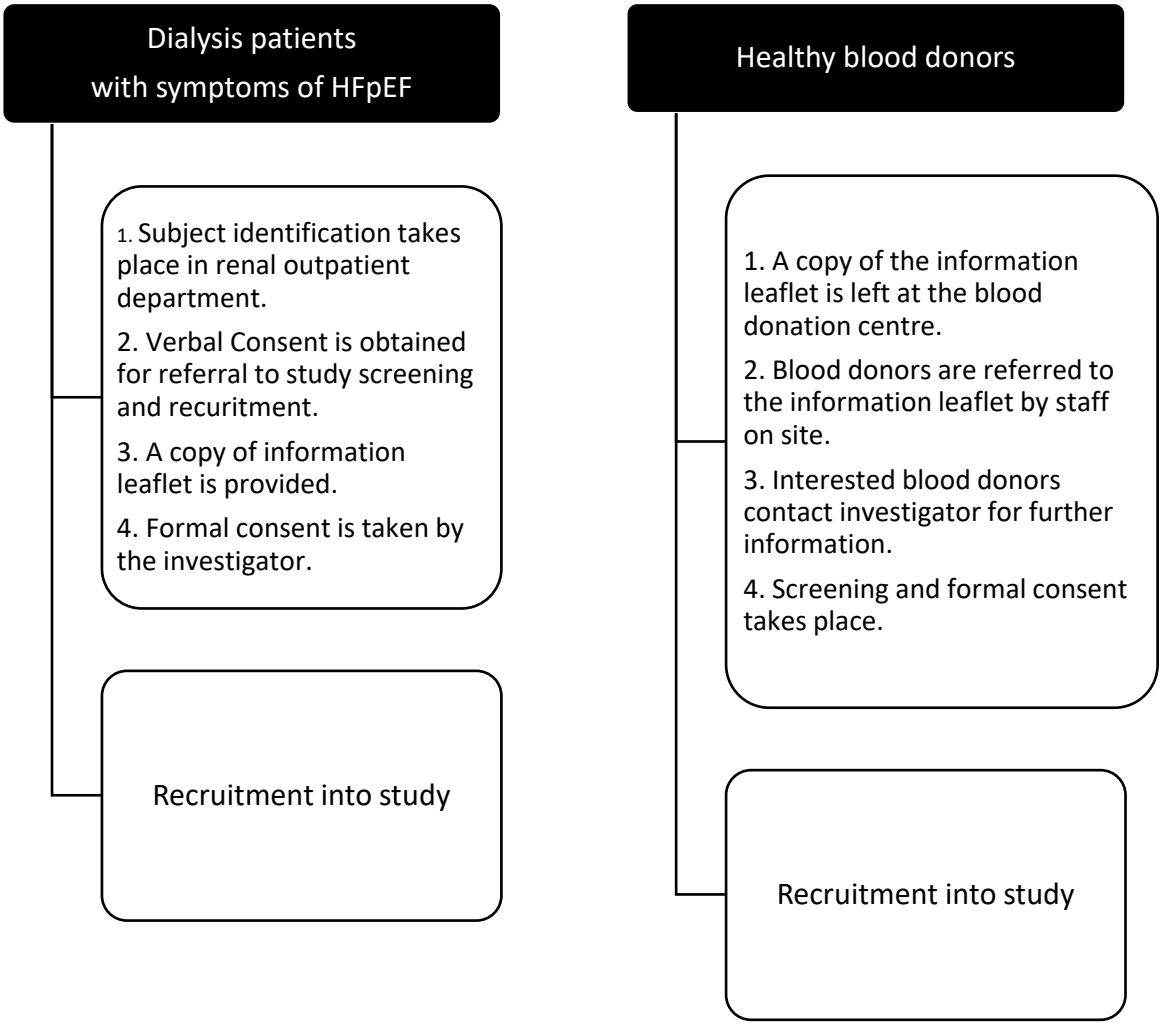

Figure 3 Subject identification and recruitment

2.4 Subject testing

Anonymisation of each subject occurred at the time of enrolment. The dialysis subjects took part on a mid-week dialysis day. Healthy subjects took part on their day of blood donation. Each subject maintained the same position (supine on a bed) throughout the experiment and had echocardiography performed immediately before and after dialysis or blood donation. One operator acquired all images using a portable echocardiography machine (Vivid I, GE Healthcare) for offline analysis later. Immediately before and after dialysis or blood donation, arm cuff blood pressure and heart rate were measured.

In addition, all subjects filled in a quality of life questionnaire (Minnesota Living with Heart Failure Questionnaire). Subjects who were able were also invited to perform a 6-minute walk test and a cardiopulmonary exercise test as per existing standards (121,122).

2.5 Assessing repeatability of study measurements

To determine the required number of repeated measurements for repeatability assessment, I first chose an exemplar parameter from each of the measurement groups, as shown in the following table (Table 2-2). I measured each parameter using the same image and same loop, at least 2 weeks apart from the first measurement. As per previously described by Bland Altman (123), the standard deviation (Sω) of the mean difference of the two repeated measurements

are determined. Sω is then plotted graphically against the magnitude of the mean difference, to confirm no significant correlation (rank correlation coefficient, Kendall's tau, p>0.05). When there was a significant correlation of Sω with magnitude of mean, I used Log transformation of scale.

Subsequently, standard error (SE) for the two repeated measurements was calculated using the formula:

$$SE = \frac{\mathrm{S}\omega}{\sqrt{2\mathrm{n} * (\mathrm{m} - 1)}}$$

where

n=number of subjects

m=number of repeated measurements per subject

Of the 45 recruited subjects, I used a random number generator available online (https://www.random.org) to select 30 subjects, for repeat measurements. Hence, having repeated the measurements twice in thirty subjects, this would yield a power of 87% to estimate within 13% of the SE of each measurement.

Table 2-2 Exemplar indices used for repeatability assessment

Measurement group	**Measurement**	**Measurement used for repeatability assessment**
Dimension (cm)	LVIDd, LVIDs, LVOT diameter, LV VTI, MAPSE, IVSd, PWd, LV length	LVIDd
Volume	LV EDV, LV ESV, LAV	LV ESV
Blood flow velocities	E, A.	E
Tissue Doppler velocities	Longitudinal and radial s', e', a'	Longitudinal s'
2-dimension strain	$S_{systole}$, S_{rad}, S_{circ}, apical Rot, basal Rot	Apical Rot

Once these five pairs of repeat measurements were available, I firstly explored the paired measurements graphically using a simple scatterplot. I then performed a bivariate linear correlation analysis using a statistical software SPSS (*IBM Corp. Released 2017. IBM SPSS Statistics for Windows, Version 25.0. Armonk, NY: IBM Corp.*). Measurement 1 is considered to be significantly correlated to measurement 2 when the p value is <0.05. I report this using Pearson's R and the corresponding p value.

Secondly, I plotted a Bland-Altman graph of bias, by showing the difference from mean (y-axis) against the calculated mean of repeated measurements (x-axis). I report the bias from mean with a constructed 95% confidence interval. The figures (Figures 4-8, page 61-65) show the graphic representation of these analyses for LVIDd, s', E, apical ROT and LV ESV.

Thirdly and finally, I used the root mean square (RMS) method to estimate the coefficient of variation (CV), for each measured parameter. I report the intra-observer variability (repeatability) for each measured parameter as CV with a constructed 95% confidence interval. The results for my study measurements' repeatability are shown in Table 2-3.

Table 2-3 Intra-observer variability for measurements obtained from echocardiography

Measurements	Pearson's linear correlation between paired measurements	Mean values	Bland-Altman analysis: Bias (95% CI)	Coefficient of variation (95% CI)
LVIDd (cm)	R=0.96 P<0.001	4.2	0.03 (-0.04 to 0.11)	3.8% (2.3-4.9%)
LV ESV (ml)	R=0.87 P<0.001	34.2	1.67 (-1.20 to 4.53)	18% (13-22%)
E (cm/s)	R=0.99 P<0.001	77.4	1.27 (-0.05 to 2.58)	3.6% (1.4-4.9%)
s' (cm/s)	R=0.94 P<0.001	8.4	0.18 (-0.01 to 0.38)	6.8% (4.7-8.5%)
Apex Rot (^{0})	R=0.99 P<0.001	9.5	0.32 (-0.03 to 0.68)	7.1% (0-10%)

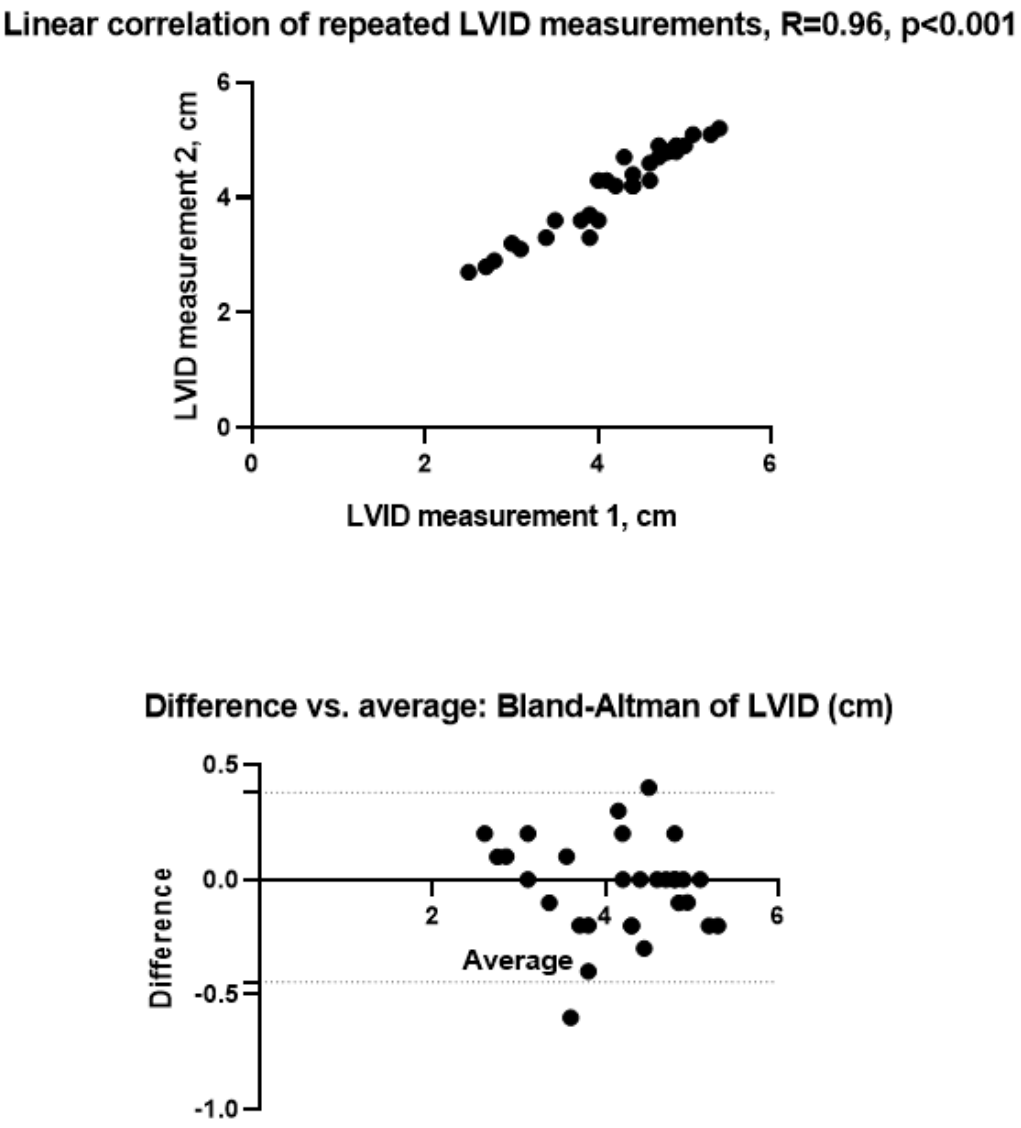

Figure 4 *Linear correlation (top panel) and BA (bottom panel) graphs for LVID*

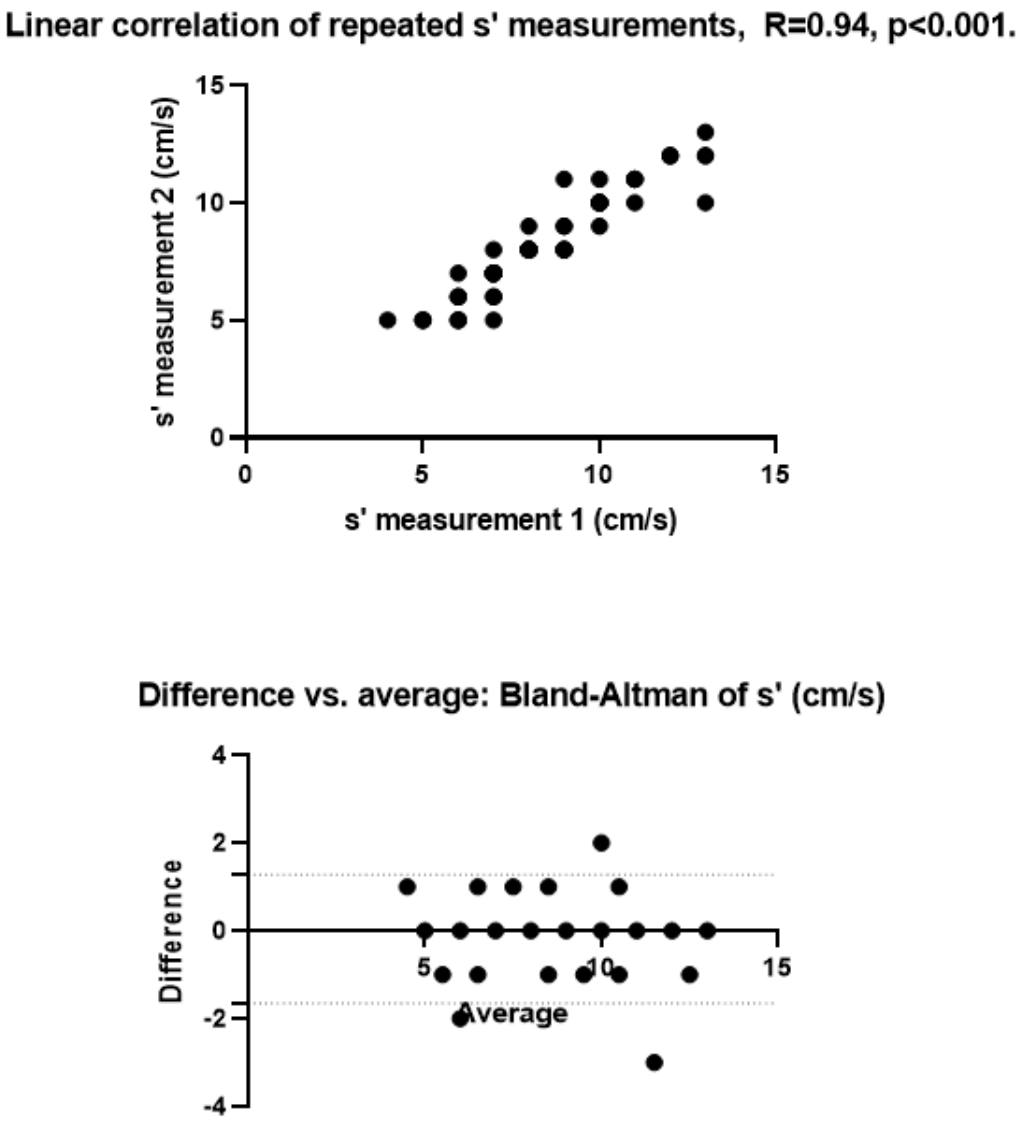

Figure 5 *Linear correlation (top panel) and BA (bottom panel) graphs for s'*

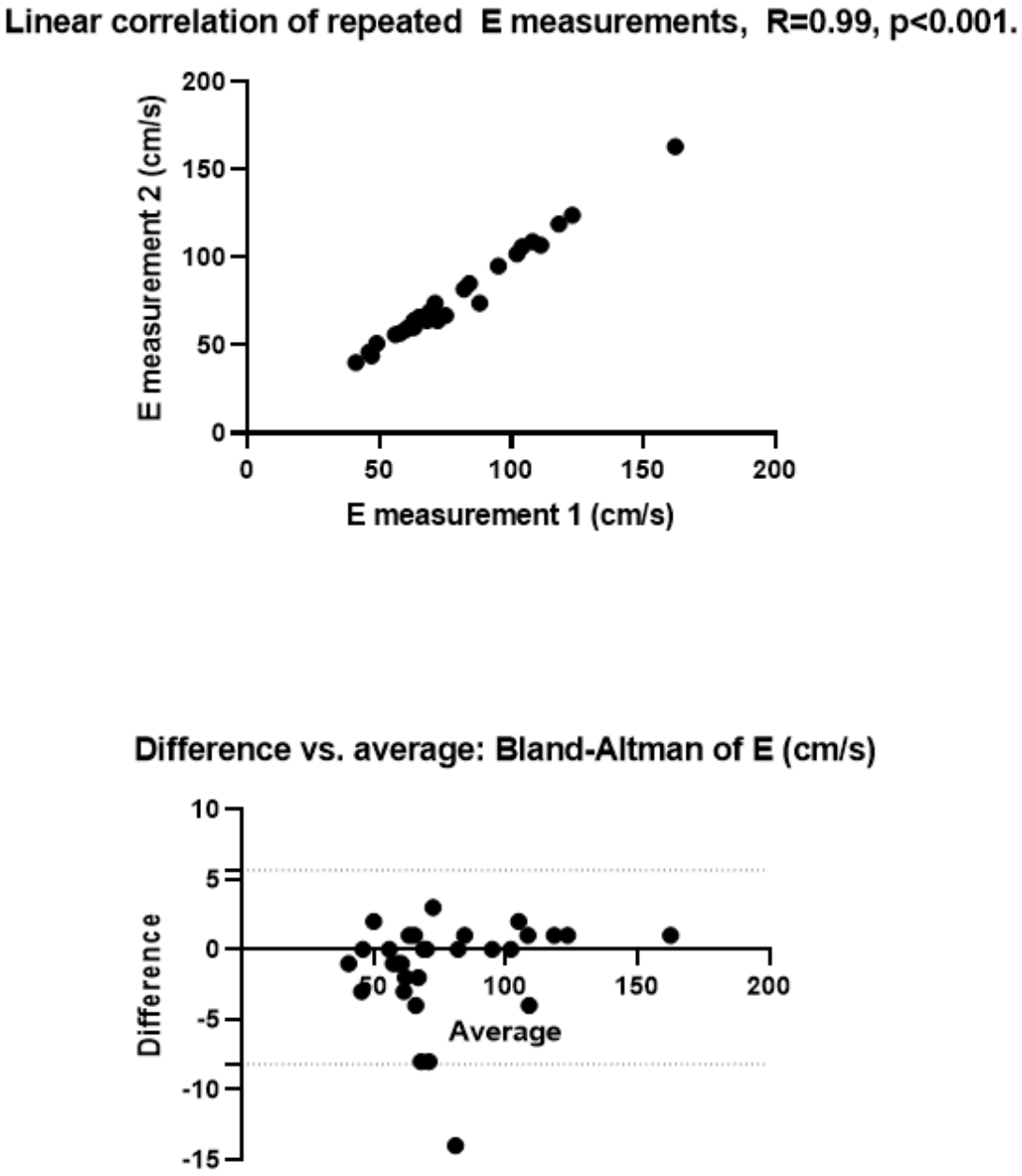

Figure 6 *Linear correlation (top panel) and BA (bottom panel) graphs for E*

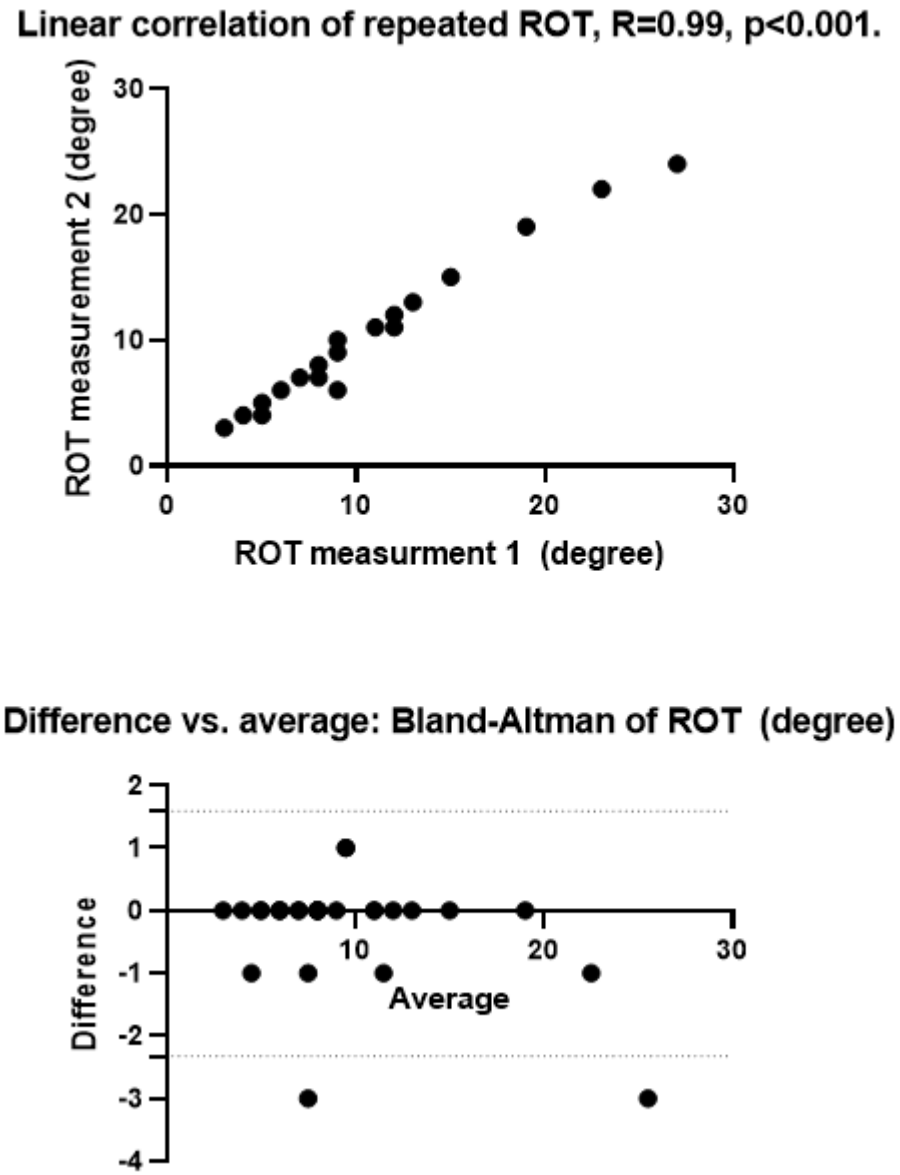

Figure 7 *Linear correlation (top panel) and BA (bottom panel) graphs for ROT*

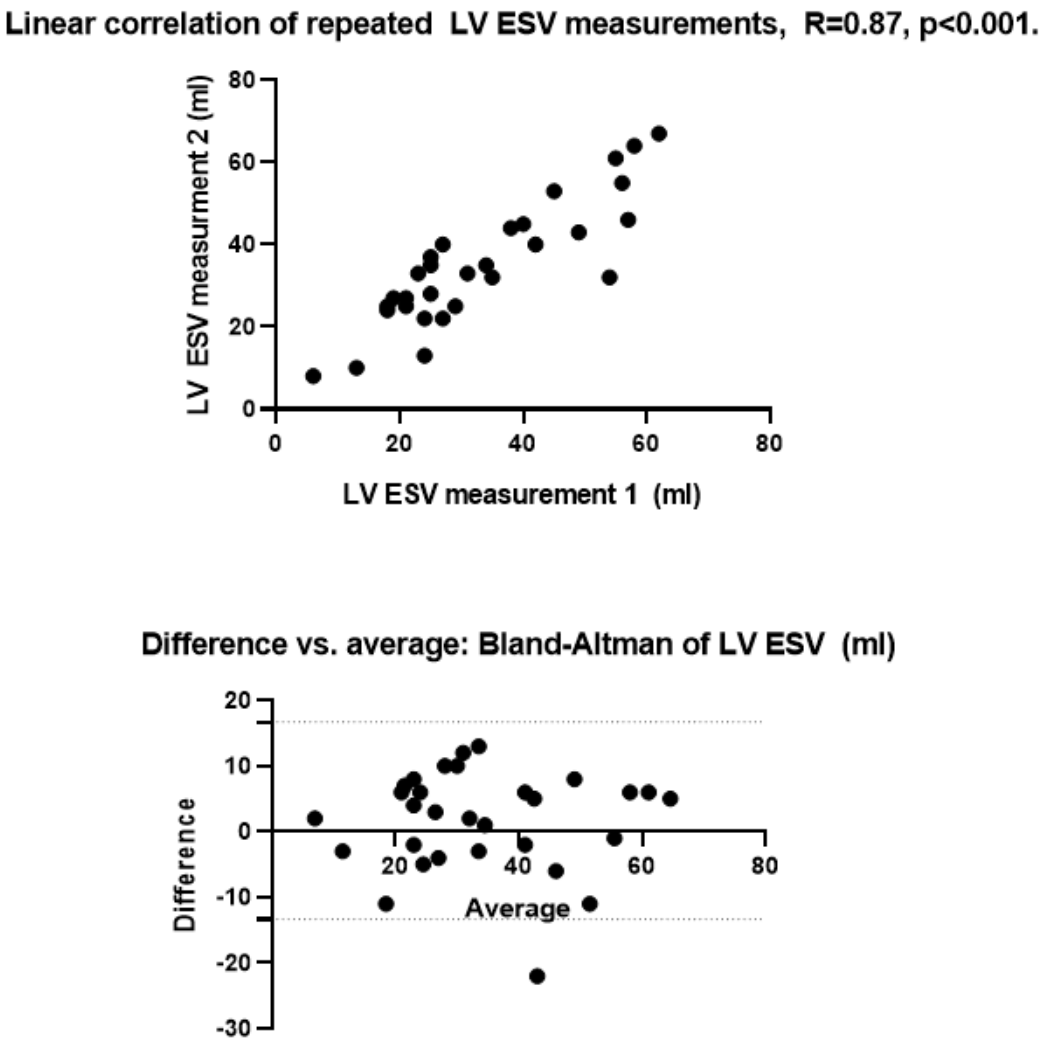

Figure 8 Linear correlation (top panel) and BA (bottom panel) graphs for LV ESV

2.6 Echocardiography

Each subject lay supine on a bed and maintained the same position whilst echocardiography images were acquired as per current standards (124). Images were acquired immediately before and after dialysis or blood donation. These images were stored digitally and analysed offline later. At least three consecutive cardiac cycles were stored for subjects in sinus rhythm. At least five consecutive cardiac cycles were stored for subjects in atrial fibrillation. Each subject was asked to hold his or her breath at passive end expiration during image acquisition. I used a 5 mm sample volume size (factory preset for Vivid I, GE Healthcare) for pulsed wave Doppler sampling. I optimised the frame rate to be >25/s for colour flow mapping, >150/s for tissue velocity imaging and 40-60/s for 2DSTE.

Two-dimensional echocardiography images were stored in the following sequences for the respective measurements:

1. Parasternal long-axis window grey scale image of mid left ventricle and ascending aorta (LVIDd, LVIDs, LVOT diameter)
2. Parasternal long-axis window colour tissue Doppler encoded image of the left ventricle (radial s', e', a' in septum and infero-lateral walls)
3. Parasternal short-axis window grey scale images at base, mid and apex levels of left ventricle (2 dimensional radial and circumferential strain in mid LV, apical rotation and basal rotation and LV torsion)
4. Apical window grey scale 4-chamber image including both atria (LAA and LAV)

5. Apical window grey scale 2-chamber image including left atrium (LAV)
6. Apical window grey scale 4-chamber image of left ventricle (LVEF, LV volumes, LV length, 2-dimensional longitudinal strain)
7. M-mode of the lateral annulus of LV in apical 4-chamber view (MAPSE)
8. Apical 2-chamber image of left ventricle (LVEF, LV volumes, LV length)
9. Apical window 4-chamber pulsed wave Doppler velocities at the mitral leaflet tips (E, A, DT)
10. Apical window 4-chamber pulsed wave Doppler velocities at the mitral annulus (timing of MV opening and closure)
11. Apical window 5-chamber pulsed wave Doppler velocities at the LVOT (timing of AV opening and closure)
12. Apical window 4-chamber view, real time pulsed-wave Doppler tissue velocities at the lateral mitral annulus, medial mitral annulus (systolic and diastolic tissue velocities of left ventricular lateral, septal annuli)

Measurements routinely used in clinical practice such as chamber quantification and blood flow Doppler velocities were measured and quantified as recommended by current standards (124). Figure 9 shows examples of these measurements. In the following sections (2.6.1 to 2.6.5), I shall elaborate and illustrate the measurements of indices that are not yet adopted into routine clinical use.

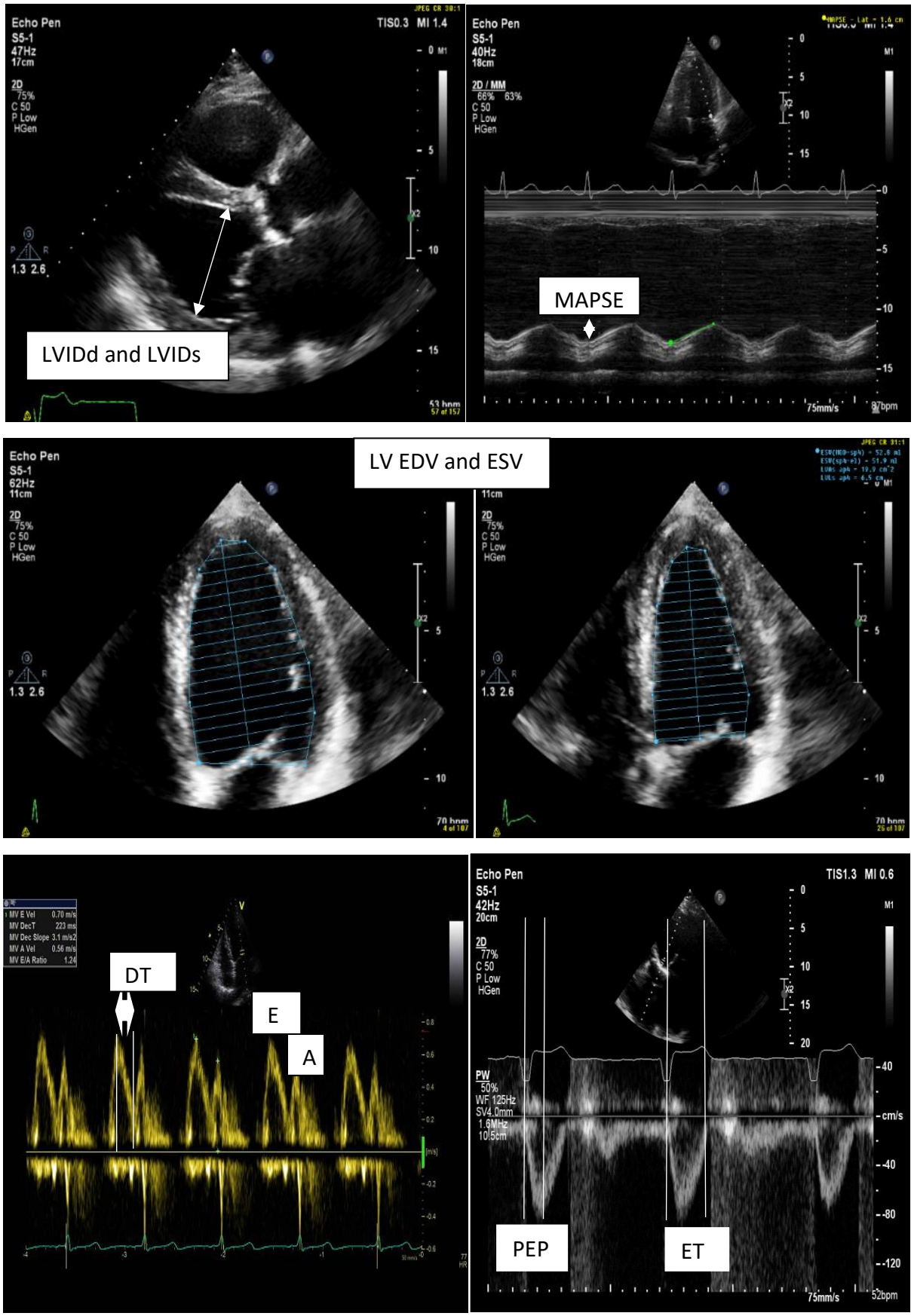

Figure 9 Echocardiographic measurements for LVIDd, LVIDs (parasternal long axis view), MAPSE (lateral annulus, 4-chamber view), LV EDV, LD ESV (Apical 4-chamber view),

2.6.1 Tissue Doppler velocities

I recorded at the time of the study, pulsed-wave tissue Doppler velocities in the septal and lateral annuli. Later, I analysed processed colour tissue Doppler velocities in the basal septal and basal lateral walls from a digitally stored four-chamber LV image. Sector width during image acquisition was adjusted to maintain a frame rate >150/s. In addition, I aligned images to the angle of the Doppler interrogation to minimise sampling error. Figure 10 illustrates a typical time velocity graph generated. Figure 11 shows the measurements for calculation of IVA, reproduced from Margulescu A, JASE 2010:23:423-31. Isovolumetric acceleration, IVA (cm/s^2) is calculated from the peak amplitude of velocity (cm/s) divided by the time (s) to the peak velocity, during left ventricular isovolumetric contraction (also known as the pre-ejection period).

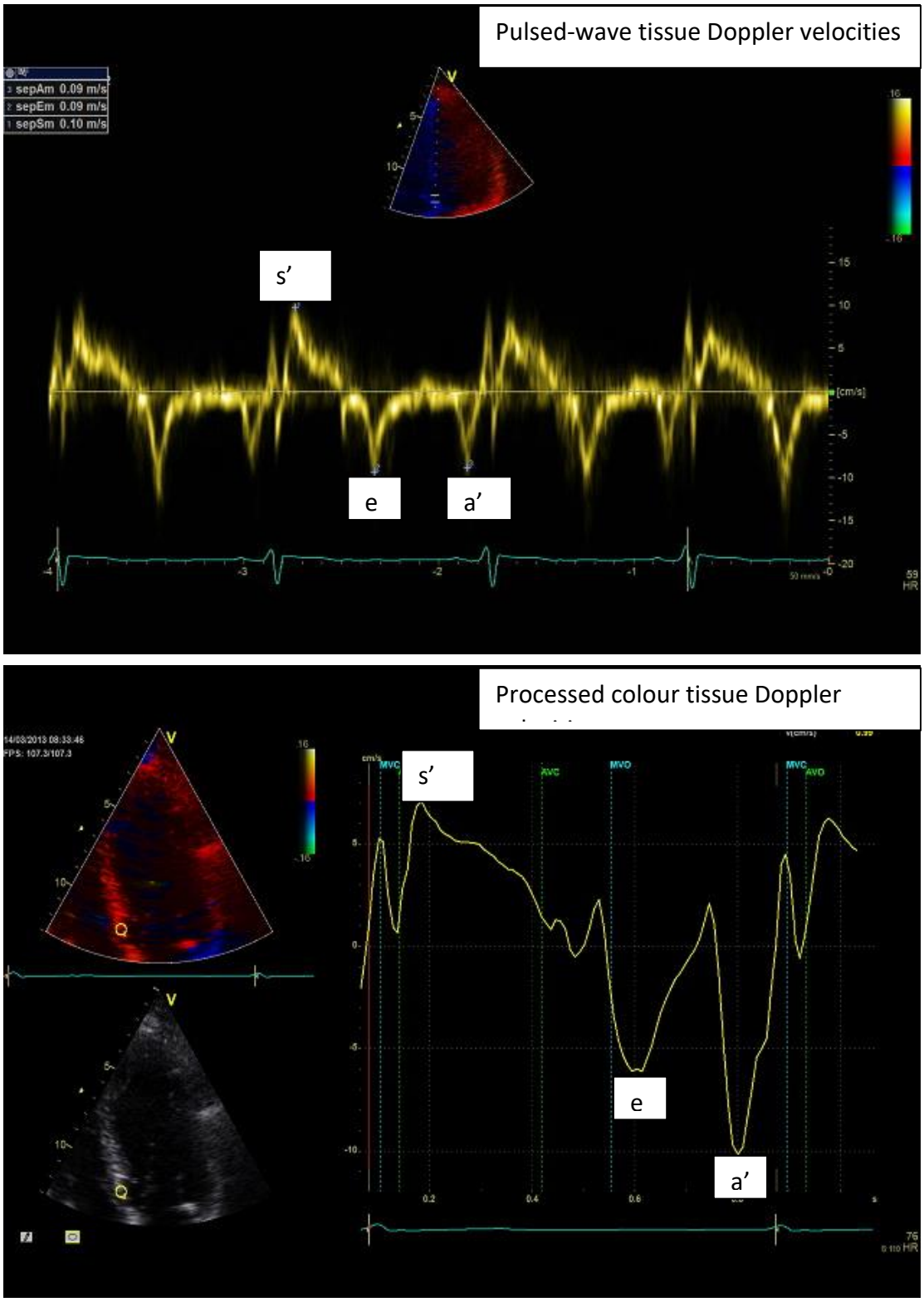

Figure 10 Pulsed-wave (top) and processed colour (bottom) tissue Doppler velocities and its derived measurements. s' denotes peak systolic tissue velocity, e' denotes early diastolic tissue velocity, a' denotes late diastolic tissue velocity.

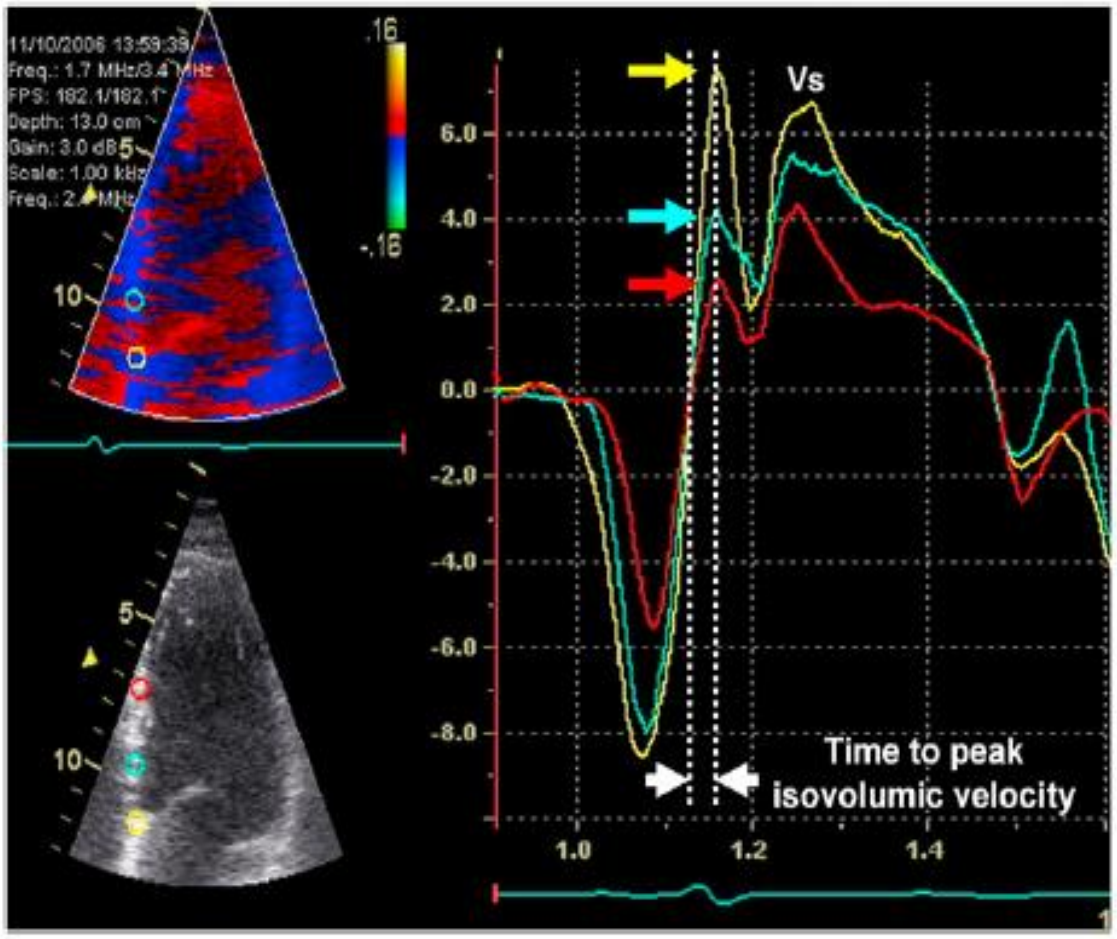

Figure 11 IVA measurement, reproduced from Margulescu A, JASE, 2010:23:423-31.

2.6.2 Global longitudinal strain of the left ventricle

I used 2DSTE as previously described (125) to derive global longitudinal strain of the left ventricle. An image of the left ventricle was stored in the 4-chamber view for speckle-tracking analysis. Strain (S) is the percentage change in left ventricular length from diastole to systole. As the left ventricle shortens in systole, peak longitudinal strain has a negative value and its change during a cardiac cycle is displayed in a strain-time graph (Figure 12 top panel). Each of the six segments (basal septum, mid septum, apical septum, basal lateral, mid lateral and apical lateral), denoted by a different colour, is analysed and the average (denoted by the white dotted line) is taken as the peak global longitudinal strain ($S_{systole}$).

The rate of change of left ventricular strain (S) during a cardiac cycle is strain rate (SR). This is displayed in a SR-time graph (Figure 12 bottom panel). The white dotted line denotes the global SR plotted against time in a cardiac cycle. The following denote peak SR corresponding to the respective time in the cardiac cycle: systole $SR_{systole}$, isovolumetric relaxation time SR_{IVRT} and early diastole SR_E.

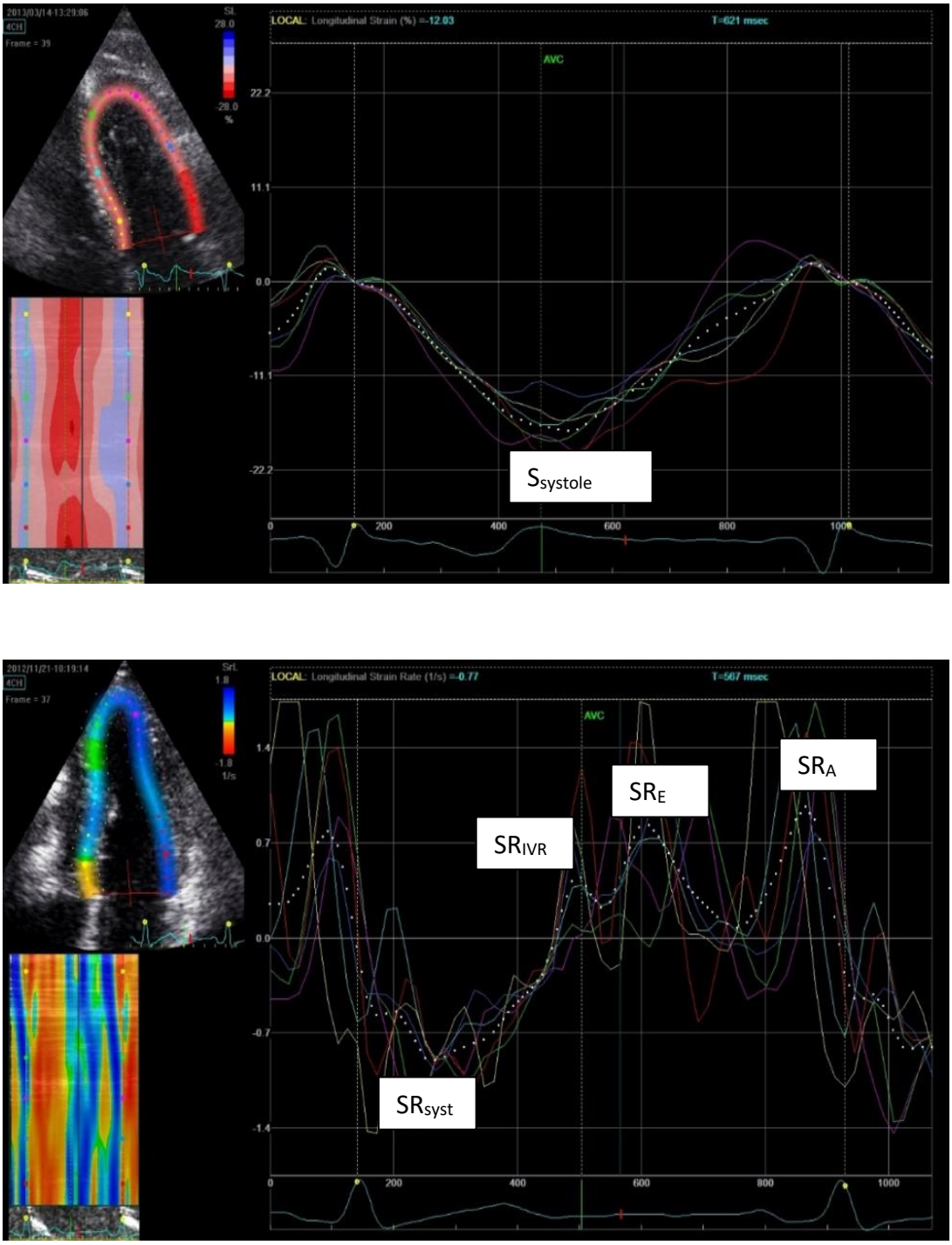

Figure 12 2DSTE trace from apical 4-chamber view of LV: longitudinal strain (top panel) and strain rate (bottom panel) graphs.

2.6.3 Mid left ventricular radial and circumferential strain

I used 2DSTE, similarly to the method described in section 2.6.2 to derive radial and circumferential strain at the mid LV. I acquired an image at the left ventricle mid cavity at the time of the study for speckle-tracking analysis. A typical radial and circumferential strain graph at the mid LV is shown in Figure 13. Each of the six segments at left ventricle mid cavity (anterior, antero-lateral, infero-lateral, inferior, infero-septum, and antero-septum) is denoted by a different colour in the graph. The average of these segments represents global radial (S_{rad}) and circumferential ($S_{circ.}$) strain

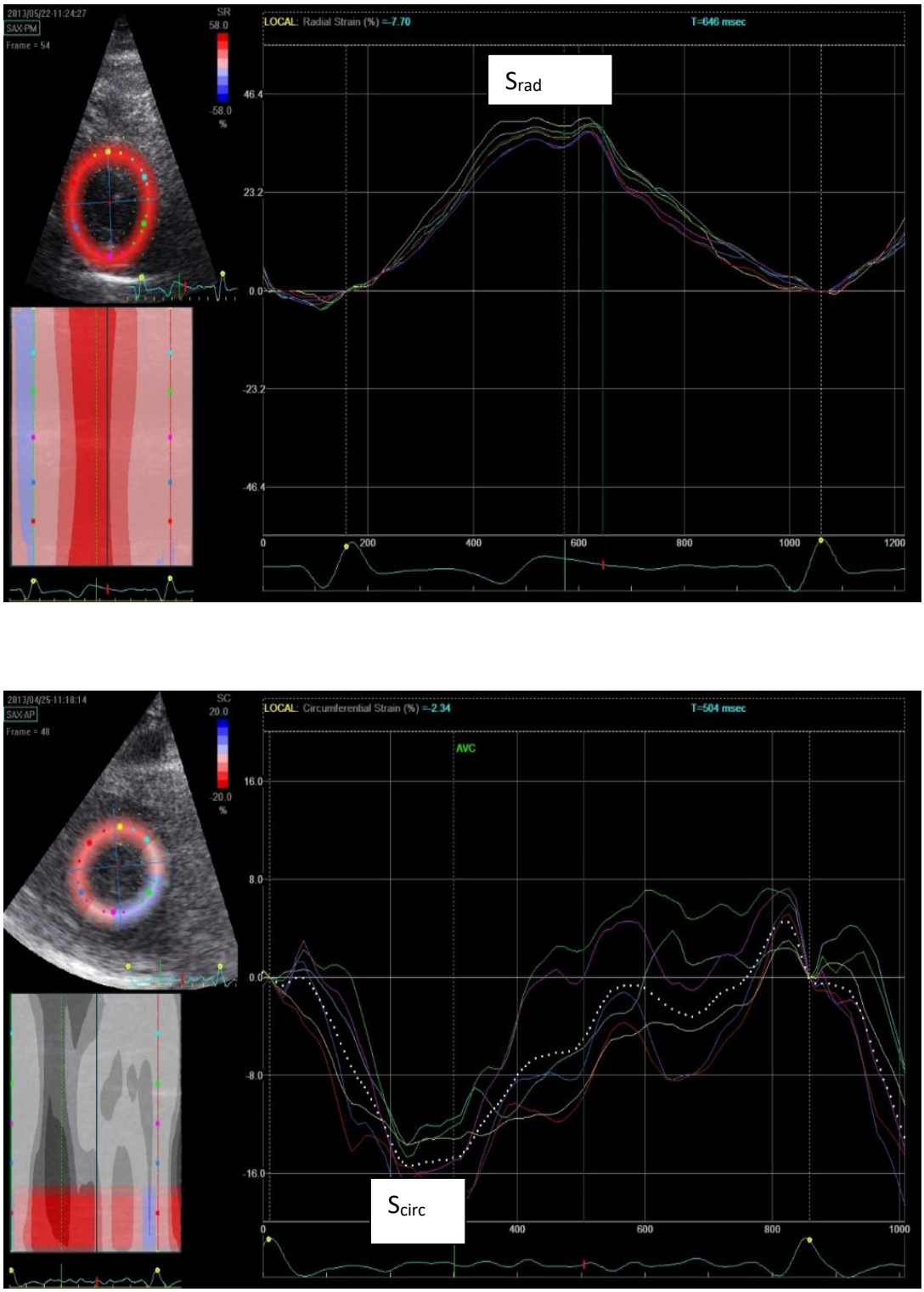

Figure 13 Radial (top) and circumferential (bottom) 2DSTE strain graphs at mid LV (parasternal short-axis view).

2.6.4 Apical and basal rotation, and left ventricular torsion

I used 2DSTE as previously (33) described to derive left ventricular apical rotation and basal rotation graphs. I acquired an image of the left ventricular apex and an image of left ventricular base for later analysis with speckle tracking. Figure 14 illustrates a typical rotation-time graph and rotation rate-time graph obtained from the apex (top and bottom panels) and base (middle panel) of the left ventricle. The left ventricular apex rotates in the opposite direction from the base and the left ventricle shortens from the apex towards the base in systole. During diastole, the left ventricle actively untwists in the opposite direction to allow rapid diastolic filling. The difference in peak apical rotation and basal rotation is left ventricle twist. Left ventricle torsion (degrees/length) is LV twist corrected by LV length. The rate of rotational change at the apex provides a strain rate-time graph as illustrated in the bottom panel of figure 14. Time to peak apical rotation, total untwisting time (UTT), time to peak untwisting rate (Time to peak UTR) were noted and expressed as a percentage of the cardiac cycle to allow comparison between subjects.

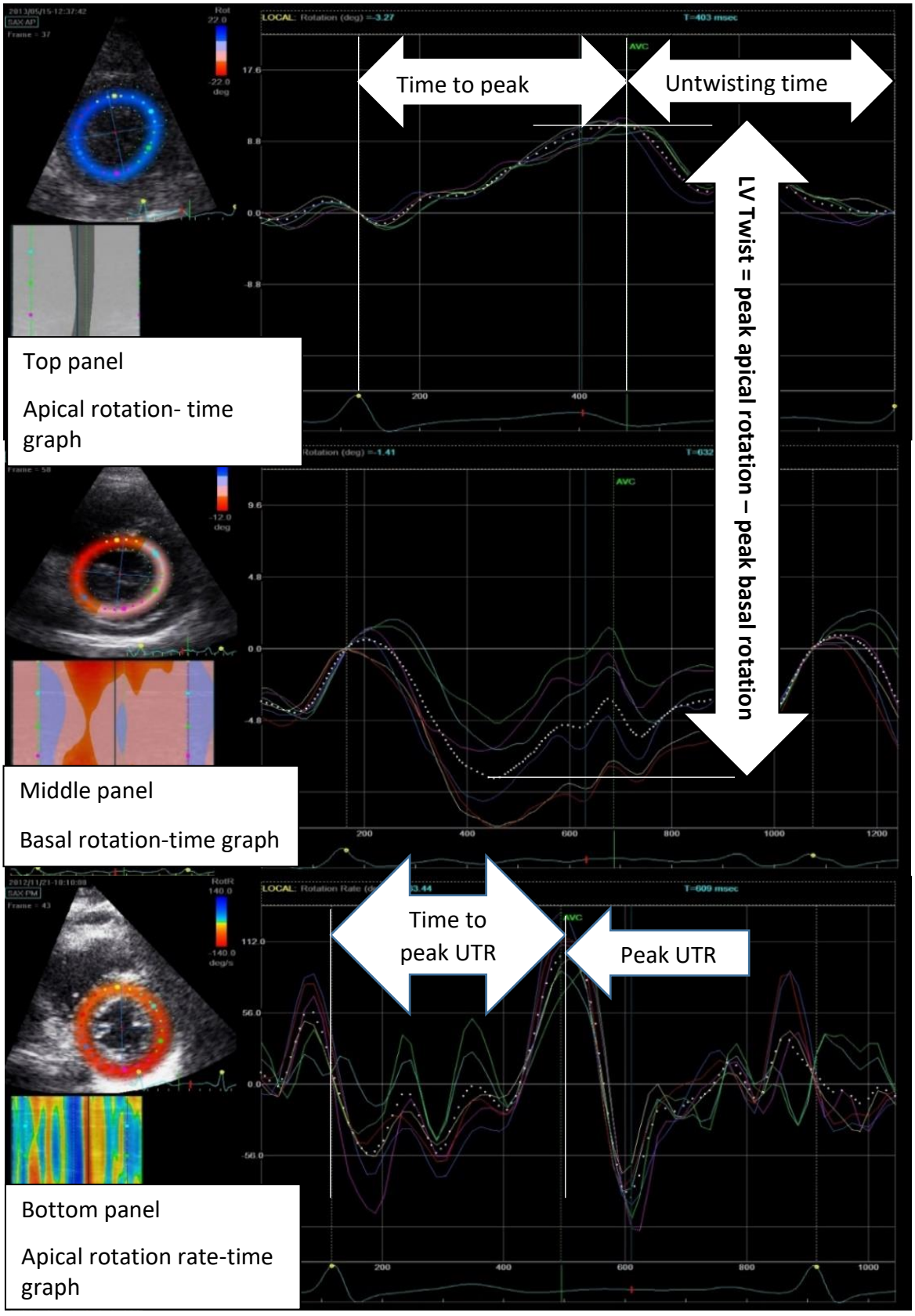

Figure 14 Apex (top panel) and base (middle panel) of LV rotation graphs and apical rotation rate graph (bottom panel).

2.6.5 Non-invasive estimation of pressure-volume relationship slope (E_{es}) of the left ventricle

Several methods (65–67,71) as discussed in section 1.2.3.1, Chapter 1, have been used to estimate the E_{es} non-invasively. These methods have various degrees of complexity in their estimation of E_{es}. Chowdhury et al (126) validated these methods in a paediatric population against PV loop study and found the method described by Tanoue et al (67) produced non-invasively estimated E_{es} most consistent with the invasively measured E_{es}. For the purpose of this study, I have used three methods (66,67,71) previously described for non-invasive estimation of E_{es} in my participants. The formulas used are listed below here.

$$1.\ Ees = \frac{\left(DBP - (0.9 * SBP) + \propto * (\mathrm{DBP} - \mathrm{EDP}) * \frac{ET}{PEP}\right)}{SV}$$

$$\alpha = 1.171 * EF + 0.022$$

(66)

Where

DBP is arm cuff diastolic blood pressure

SBP is arm cuff systolic blood pressure

EF is left ventricular ejection fraction by biplane method

EDP is end diastolic LV pressure, assumed as 10mmHg in this cohort

ET is left ventricular ejection time, measured from the spectral Doppler trace of LVOT

PEP is left ventricular pre-ejection time, measured from the spectral Doppler trace of LVOT

SV is left ventricle stroke volume, by biplane method

$$2.\ Ees = \frac{\mathrm{DBP} - (\mathrm{ENDest} * \mathrm{SBP} * 0.9)}{SV * ENDest}$$

$$ENDest = 0.0275 - (0.165 * EF) + 0.3656 * \left(\frac{DBP}{SBP * 0.9}\right) + (0.515 * ENDavg)$$

(71)

Where

DBP is arm cuff diastolic blood pressure

SBP is arm cuff systolic blood pressure

SV is left ventricular stroke volume, by biplane method

EF is left ventricular ejection fraction by biplane method

E_{NDest} is group-averaged normalised elastance

E_{NDavg} is empirical estimation of group-averaged normalised elastance at onset of ejection, fitted by a 7-degree polynomial equation.

3. $$Ees = 0.9 * \frac{SBP}{ESV}$$

(67)

Where

SBP is arm cuff systolic blood pressure

ESV is left ventricular end systolic volume by biplane method

2.6.6 Non-invasive estimation of LV filling pressure (LAP) using echocardiography

Several research groups have described different methods for non-invasive estimation of LV filling pressure with echocardiography. In this section, I shall explore these methods briefly.

Temporelli et al (127) recruited stable subjects with ischaemic or non-ischaemic heart failure (age 62 ± 9 years, LVEF 22 ± 5%) in atrial fibrillation whilst they underwent cardiac catheterisation for clinically indicated investigation. They performed simultaneous invasive cardiac catheter and trans-thoracic echocardiogram. Transmitral Doppler blood flow velocities (E) and its timings (IVRT, DT), and left atrial dimension were recorded and used in a stepwise multivariate linear regression analysis. They found DT was an independent predictor of invasively measured LAP. The range of DT and invasively measured pulmonary

capillary wedge pressure (PCWP) in this study were 60-180ms and 5-35mmHg respectively. DT was found to have an inverse linear relationship (Pearson's R=0.95, p<0.001) with invasive LAP measurements. A DT<120ms has a 100% sensitivity and 96% specificity in detecting LAP>20mmHg. Estimated LAP was calculated based on the formula below, DT was measured in milliseconds.

$$Estimated\ LAP = 51 - 0.26 * DT \qquad (127)$$

Sohn et al (128) studied only subjects in atrial fibrillation with or without depressed ejection fraction (LVEF 53 ± 11%, age 63 ± 11 years). These subjects had elective cardiac catheterisation for investigations of atypical chest pain, dyspnoea, angina, dilated cardiomyopathy, and arrhythmias. The reported E/e' and PCWP were 5-25 and 10-25mmHg respectively. They found good linear correlation of E/e' with invasively measured LAP, Pearson's R=0.79, p<0.001. A ratio of E/e' of ≥11 has a 75% sensitivity and 93% specificity for detecting a LAP≥15mmHg in their subjects. They estimated LAP by the formula given below.

$$Estimated\ LAP = 6.489 + 0.821 * \left(\frac{E}{e'}\right) \qquad (128)$$

Garcia et al (129) included 45 subjects admitted to an intensive care unit, mostly for a cardiac indication (acute ischaemia, aortic stenosis, congestive heart

failure) but they also included patients admitted following peripheral vascular surgery, trauma and sepsis. These subjects (mean age 64 ± 14 years) were in sinus rhythm and included both patients with impaired and patients with normal global left ventricular systolic function (LVEF 40 ± 15 %). They underwent invasive haemodynamic monitoring including the insertion of a pulmonary artery catheter for the measurement of pulmonary capillary wedge pressure (PWCP). Trans-thoracic echocardiogram was performed within 5 minutes of obtaining the PWCP. Transmitral Doppler blood flow velocities (E, A, E/A) and their timings (DT, IVRT), LVEF, mitral valve diastolic propagation velocity (Vp) and age were parameters used in a stepwise multilinear regression analysis to estimate the invasively measured LAP. They found that the ratio (E/Vp) was an independent predictor of the invasively measured LAP. Estimated LAP correlated well (Pearson's R=0.80, $p<0.001$) with the invasively measured LAP. In addition, a majority (87%) of the subjects had estimated LAP within 5mmHg of the invasively measured LAP. Only one subject had a difference of >10mmHg in these two measurements. The range of E/Vp in this study was 1-3.5 and the range of LAP/PCWP was 5-30mmHg. The authors proposed that LAP can be estimated non-invasively using the formula given below.

$$Estimated\ LAP = 5.27 * (\frac{E}{Vp}) + 4.66 \qquad (129)$$

Nagueh et al (130) recruited stable subjects in sinus rhythm, with or without depressed ejection fraction. They underwent routine cardiac catheterisation for investigation of breathlessness and consented to have concomitant echocardiography. Lateral mitral annular tissue Doppler early diastolic velocity (lateral e') was used in combination with mitral Doppler velocity (E) in the estimation of LAP as shown in the formula below. The range of reported E/e' and PCWP in their study were 3-35 and 7-35mmHg respectively. They found the non-invasively estimated LAP correlated well with that invasively measured LAP (Pearson's R=0.87, p<0.01). The mean difference from the two measurements were 0.1 ± 3.8mmHg.

$$LAP = 1.9 + 1.24 * \left(\frac{E}{e'}\right) \qquad (130)$$

Whilst Sohn et al (128)and Temporelli et al (127) only included stable subjects in atrial fibrillation, Garcia et al (129) only included unstable subjects requiring intensive care admission in their non-invasive methods of LAP estimation. In addition, the method proposed by Temporelli et al (127) would produce a negative value for estimated LAP, when DT > 196ms (range of DT in their study was 60-180ms). I therefore did not use this method for estimation of LAP in my subjects. The results of estimated LAP derived by using the other methods discussed (128–130) were well correlated in my study subjects, as shown in Figure 11. LAP estimated using the methods described by Sohn et al and Nagueh et al are almost

identical (mean difference of the two estimates of 4mmHg, $p<0.001$). As my subjects were stable and did not have atrial fibrillation, I therefore used the method described by Nagueh et al(130) to estimate filling pressure (LAP) in my study.

2.7 Blood pressure and heart rate

Blood pressure was recorded immediately (within 5 minutes) before and after dialysis/venesection using a standard automated arm cuff blood pressure equipment (Procare 420, Dinamap (131)). Heart rate was monitored using surface electrodes placed in the three standard limb lead positions. Heart rate before and after preload reduction from the last and first echo images respectively, was recorded as displayed on the echo equipment (Vivid I, GE Healthcare, Horten, Norway). The subjects maintained the semi-supine position before, during, and after the experiments whilst these measurements were taken.

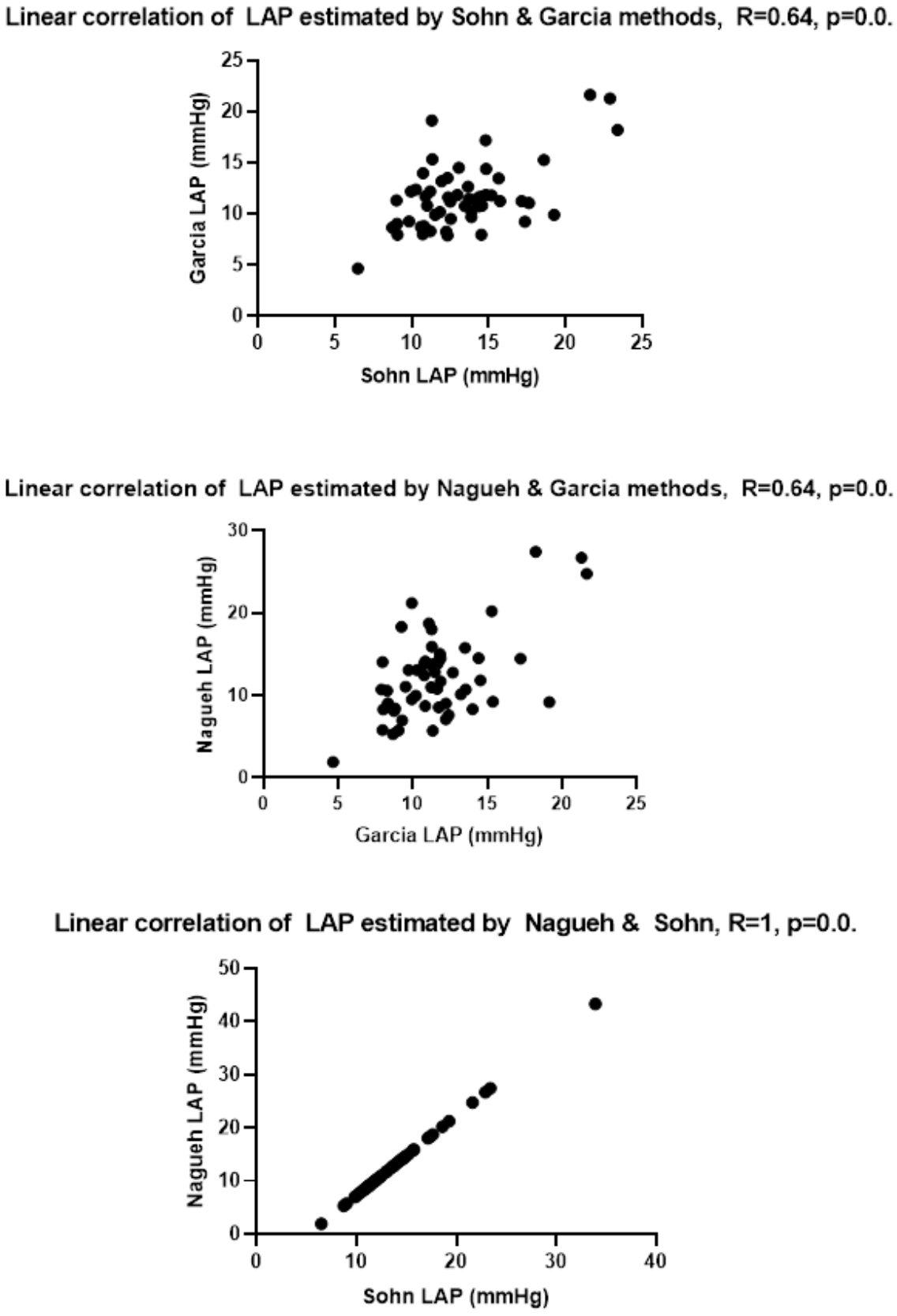

Figure 15 Linear correlation graphs of LAP estimated using Sohn, Garcia and Nagueh methods, as described in text.

2.8 Data analysis

I analysed all the images offline using a dedicated software (EchoPAC, GE Healthcare). Each measurement was an average of at least three cardiac cycles (five cardiac cycles for those in atrial fibrillation). I used a statistical software SPSS (*IBM Corp. Released 2017. IBM SPSS Statistics for Windows, Version 25.0. Armonk, NY: IBM Corp.*) to perform analysis of my data. Data were first explored and tested for normal distribution before statistical analysis were performed. For data with a skewed distribution, I performed log transformation to approximate normal distribution before conducting statistical testing. I reported continuous data as mean ± SD (for normally distributed data) or median and interquartile range (for skewed distribution). Categorical data were reported as percentages.

I used paired t-test (for normally distributed measurements) or Wilcoxon's sign rank test (for measurements with a skewed distribution) for comparison of measurements within the same subject before and after the experiment (preload reduction). Statistical significance was set at $p<0.05$. A 95% confidence interval of the mean difference following the experiment was constructed for each measurement.

I used independent t-test (for normally distributed measurements) or rank-sum test (for measurements with skewed distribution) for comparison of mean/median between the dialysis subjects and blood donors. Statistical significance was set at $p<0.05$. A 95% confidence interval of the mean difference following the experiment was listed for each measurement.

ANCOVA analysis was used to perform covariate adjusted analysis to compare the group difference in parameters. Statistical significance was set at $p<0.05$. A 95% confidence interval of the mean difference following the experiment was listed for each measurement.

To minimise the impact of multiple testing, I will make all inferences based primarily on the size of difference found, with a constructed 95% confidence interval, either as an absolute measure and/or as a percentage of change, as a relative measure.

3 Baseline characteristics of the subjects

3.1 Dialysis subjects

Thirty stable patients on established haemodialysis consented to take part in the study. Causes of end-stage renal failure for the group were hypertension (63%), diabetes (20%) and obstructive uropathy (27%). Significant comorbidities of participants were diabetes mellitus (30%), hypertension (93%), stable ischaemic heart disease (13%), and paroxysmal or persistent atrial fibrillation (10%). The median length on established dialysis of the group was 25.5 months and the median duration of the dialysis session was 4 hours.

All participants on cardiovascular medications took their medication in the previous evening before the study session as per their usual practice. Table 3-1 shows the prevalence of use and median dosage of each group of cardiovascular medications amongst the study subjects.

Table 3-1 Medication use of dialysis subjects

Class of medication	Exemplar medication	Prevalence of use & median dose
Beta blocker	bisoprolol	23% (2.5 mg)
Diuretics	furosemide	23% (160 mg)
ACE/ARBs	ramipril	16% (10 mg)
Alpha receptor antagonist	doxazosin	10% (16 mg)
Calcium antagonist	diltiazem	1% (120mg)

Before the study dialysis session, the mean inter-dialytic weight gain for the group was 1.7 ± 1.3kg. Following dialysis, the mean weight loss of the group was 1.6 ± 1.3kg. The mean weight before and dialysis was 83 ± 22kg and 81 ± 22kg respectively, paired t-test $p<0.01$.

3.2 Blood Donors

Fifteen experienced blood donors, with no past medical history of note and on no regular medication consented to take part in the study. Each donor gave 480ml of blood via venesection over ten minutes.

The following table (Table 3-2) shows the baseline characteristics of the two groups.

Table 3-2 Baseline characteristics for both groups (continued on next page)

Category of **measurements**		Dialysis patients N = 30	Blood donors N = 15	p value
General	Age (years)	59 ± 18	45 ± 15	0.015
	Gender	68% men	80% women	Not applicable
	SBP(mmHg)	138 ± 24	127 ± 17	0.138
	DBP(mmHg)	72 ± 13	77 ± 12	0.180
	BMI(kg/m^2)	29 ± 7	26 ± 4	0.176
Dimension	LVMI(g/m^2)	119 ± 44	70 ± 44	0.000
	LAVI(ml/m^2)	43 ± 19	22 ± 6	0.000
	LVEDVI(ml/m^2)	49 ± 10	48 ± 10	0.419
Diastolic function	E(cm/s)	81.7 ± 29.2	69.0 ± 11.6	0.058
	A(cm/s)	77.3 ± 24.6	52.1 ± 11.6	0.001
	E/A	1.1 ± 0.4	1.4 ± 0.4	0.008
	DT(ms)	228 ± 58	218 ± 42	0.541
	IVRT(ms)	99 ± 21	96 ± 13	0.586
	E/e’	13 ± 7	6.8 ± 1.4	0.001

	lateral e'(cm/s)	8.8 ± 2.7	11.1 ± 2.4	0.010
Systolic function	Septal s'(cm/s)	7.2 ± 1.7	8.8 ± 1.6	0.017
	Lateral s'(cm/s)	7.6 ± 1.9	8.7 ± 2.2	0.199
	$S_{systole}$	14.3 ± 3.4	15.1 ± 1.2	0.739
	Apical Rot(^{0})	7.7 ± 4.2	6.5 ± 2.2	0.356
	LVEF(%)	58 ± 7	64 ± 5	0.008

3.3 NT-proBNP results of dialysis subjects

As the dialysis group comprised of subjects with symptoms of heart failure and preserved ejection fraction, they underwent blood test at the time of dialysis for quantification of serum NT-proBNP. All the subjects had age-adjusted values of NT-proBNP above the diagnostic cut-off value (132) for diagnosis of heart failure. The median value of NT-proBNP in this group was 1635 ng/L, inter-quartile range 3623 ng/L.

3.4 Exercise tolerance and symptom burden of the dialysis subjects

To assess their exercise capacity, all subjects were invited to attend on a separate occasion for exercise testing, within 2 weeks from the time of the echocardiographic study. Dialysis patients attended on a mid-week non-dialysis day for the exercise capacity assessment. Not all the dialysis subjects were able to perform either of the exercise tests. Twelve of the thirty (12/30) dialysis participants and twelve of the fifteen (12/15) blood donors agreed to undergo exercise testing.

Cardiopulmonary (CPEX) exercise testing was performed using a semi-supine ergometer and 6-minute walk test (6MWT) was performed according to the current standards (121,122).

A portable cardiopulmonary stress testing system (Oxycon mobile, Vyaire Medical) analysed breath-to-breath inhaled oxygen (VO_2, ml/min), exhaled carbon

dioxide (VCO_2, ml/min), and ventilatory effort (VE, minute ventilation, ml) via a facemask. During incremental exercise testing, there is a continuous rise in both VO_2 and VCO_2 reflecting physiological demand of exercise. As the subject reaches his or her aerobic or ventilatory threshold (AT, ml/min), there is an inflection of the VE/VO_2 slope whilst the VE/VCO_2 slope remains constant. Maximal oxygen uptake (VO_2 max) is the highest measured VO_2 when a plateau is reached. The inflection point helps determine the aerobic threshold (AT). Respiratory exchange ratio (RER) is the ratio of VCO2/VO2, with a value of >1 generally regarded as a mark of adequate effort during testing. I compared the actual AT to reference normal values proposed by Shvartz and Reibold (133) to estimate each subject's exercise capacity. A ratio (AT/reference VO_2 max) of 60-80 is considered athletic, 50-60 is considered sedentary, 40-50 is considered deconditioned and <40 is considered diseased.

There are published reference data (134) for 6MWT distance. A 40-year-old can manage 600 metres. This capacity decreases by 50 metres per decade. I compared each subject's results to their age predicted norm to assess their exercise endurance.

To assess their symptom burden and limitation, I used a validated questionnaire (MLHFQ, The University of Minnesota). The total score of the questionnaire is 125, 0 indicating no symptoms and 125 indicating maximal limitation.

Table 3-3 summarises the baseline characteristics of the twelve dialysis subjects able to perform exercise testing, compared to the twelve blood donors.

No complication or adverse event occurred during cardiopulmonary exercise testing and 6MWT. The tests were terminated at the subjects' request due to leg fatigue. All subjects in both groups exercised to and past their respective anaerobic threshold (AT). They demonstrated good effort during the test as evident by the measured peak RER ≥1.1. The dialysis group had moderately reduced maximal oxygen uptake (54% of reference values) whilst the blood donors had normal capacity (93% of reference values). Table 3-4 shows the results of exercise testing in dialysis patients and blood donors.

Table 3-3 Baseline characteristics of study subjects undergoing exercise capacity assessment

	Dialysis patients N=12	**Blood donors N=12**	**p values**
Baseline characteristics			
Age (years)	54 ± 19	46 ± 12	>0.05
Gender	17 % female	75 % female	<0.01
BMI (kg/m^2)	31 ± 8	26 ± 3	>0.05
median NYHA class	II	I	<0.001
Blood pressure (mmHg)	131 ± 25 / 68 ± 16	127 ± 17 / 77 ± 12	>0.05
Echocardiography parameters			
EF (%)	60 ± 5	64 ± 5	0.012
LVEDVI (ml/m^2)	44 ± 11	46 ± 9	0.515
LVMI (g/m^2)	114 ± 45	69 ± 20	<0.001
LAVI (ml/m^2)	38 ± 17	20 ± 6	<0.001
E/A	1.0 ± 0.3	1.4 ± 0.4	<0.01
Average E/e'	12 ± 7	7 ± 1	<0.01

Table 3-4 Results of CPEX testing in dialysis patients and blood donors

	Dialysis patients N=12	**Blood donors N=12**	**p values**
Exercise duration(min)	7.8 ± 1.9	9.2 ± 1.6	0.05
Time to AT (min)	4.6 ± 1.5	6.5 ± 1.2	<0.01
HR at rest (bpm)	84 ± 13	76 ± 18	>0.05
HR at peak (bpm)	116 ± 26	158 ± 23	<0.01
Rise in HR (bpm)	32 ± 23	82 ± 16	<0.01
Max work load (watt)	92 ± 43	174 ± 40	<0.01
Resting systolic BP (mmHg)	123 ± 22	116 ± 16	>0.05
Peak systolic BP (mmHg)	160 ± 31	151 ± 19	>0.05
Rise in systolic BP (mmHg)	37 ± 18	35 ± 18	>0.05
Peak VO_2 (ml/min)	1254 ± 358	1689 ± 478	0.02
Peak VO_2 (ml/kg/min)	15 ± 5	24 ± 8	<0.01
% predicted VO_2 (%)	54 ± 20	93 ± 24	<0.01
VO_2_AT (ml/min)	869 ± 267	1241 ± 380	0.01
% predicted VO_2_AT (%)	37 ± 14	69 ± 23	<0.01
RER peak	1.2 ± 0.1	1.2 ± 0.1	>0.05
RER AT	1.1 ± 0.1	1.0 ± 0.1	>0.05
Perception of exertion at peak, Borg scale (/20)	14 ± 5	6 ± 8	<0.05
Perception of SOB at peak, VAS scale (/100)	58 ± 30	11 ± 10	<0.01

The 6MWT distance walked was 344 ± 76 metres in the dialysis group and 549 ± 84 metres in the blood donors (independent t-test, $p<0.01$). Compared to their age-predicted capacity, the dialysis group achieved 64 ± 13% and the blood donors achieved 106 ± 26% respectively, independent t-test $p<0.01$. The mean quality of life (MLHFQ, The University of Minnesota) score for the participants was 58 ± 21, out of a maximum of 125. None of the blood donors reported any symptom.

3.5 Comparison of the two groups

The main findings at baseline are:

1. Compared to the blood donors, the dialysis patients were older, they had more comorbidities and had a higher usage of cardiovascular medication.
2. Both the groups had comparable blood pressure at baseline.
3. Dialysis patients had higher LAP (E/e'), left ventricular mass (LVMI), larger left atrial volume (LAVI), and diastolic dysfunction (E/A, lateral e') compared to the blood donors despite both groups having comparable indexed left ventricular dimension (LVEDVI).
4. Some indices of systolic function (EF and pulsed-wave septal s') were significantly lower in the dialysis patients, whilst some indices of systolic function were comparable in both groups (Apical rotation and $S_{systole}$).
5. At peak exercise, although both groups exhibited good effort related to exercise, the dialysis patients achieved a lower workload and were breathless, compared to the blood donors. Dialysis patients showed a lower

rise in heart rate, lower age and gender predicted peak oxygen consumption.

6. Compared to the blood donors, the dialysis subjects achieved lower age-predicted capacity in their 6MWT distance.

These results confirmed that the blood donors are healthy and the dialysis group behave like HFpEF subjects. Together they provide 2 well-characterised groups in which the effects of altering preload can be assessed (in a healthy model and in a diseased group of patients)

4 Effect of preload reduction on cardiac function following haemodialysis

4.1 Aims of this chapter

In this chapter, I aimed to investigate the effect of a large preload change on echocardiographic indices of cardiac function. I studied this in a group of subjects with symptoms of HFpEF, evidence of left ventricular hypertrophy and limited exercise tolerance. I tested the hypothesis that most echocardiographic indices are preload sensitive.

As discussed in chapter one, previous animal and human studies (13,57,79) concurred that E_{es}, a measure of left ventricle contractile state derived from repeated PV loop studies, is load insensitive and tracks contractile status change. Development of a single beat non-invasive estimation (65–67,71) of E_{es} has subsequently allowed estimation of E_{es} using echocardiography. IVA, another marker of LV contractile state (89,92) was previously shown to be preload independent.

In this chapter, I shall evaluate the feasibility of E_{es} and IVA quantification in my subjects using the previously discussed methods (66,67,71,117) previously described. I will find out if values of estimated E_{es} using the three methods are in good agreement with each other. I also test the hypothesis that non-invasively quantified E_{es} and IVA are insensitive to changes in preload.

4.2 Subjects testing

Thirty subjects consented to take part in the study at the Cardiff and Vale University Hospitals. Each subject lay semi supine in the left lateral position and underwent echocardiography immediately before dialysis. During dialysis, all subjects maintained the semi supine position. Immediately after dialysis, each subject resumed the semi supine left lateral position whilst I performed echocardiography.

All images were stored digitally for offline analysis on a separate occasion. I assigned each subject a study identification number for anonymization. I performed all the data analysis.

4.3 Preload reduction and its effect on cardiac dimension and volume

All data pre and post dialysis were explored graphically using Kolmogorov-Smirnov test of normality. All data were normally distributed.

Dialysis achieved a mean weight loss of 1.6 ± 1.3 kg (one sample t-test $p<0.01$) in my subjects. Previous studies in dialysis patients (105,106,118) have shown that a reduction in weight closely approximated the reduction in LV preload/ultra-filtration volume during dialysis, as demonstrated in the reduction in LV and LA dimensions. Therefore, from this point onwards, I shall refer to this 'mean weight loss of 1.6 ± 1.3 kg' as 'mean preload reduction of 1.6 ± 1.3 L'. Blood pressure and

heart rate (median HR 73bpm and HR 75bpm, Wilcoxon sign rank test $p > 0.05$) did not change following dialysis.

There was a reduction in LV internal dimension (by 13%), LA volume and area (LAV 21%, LAA 13% reduction) but no change in LV wall thickness and LV mass. A geometry/shape change of the left ventricle, driven by a reduction in radial dimension but unchanged length, resulted in an increase of the sphericity index by 17%. Table 4-1 shows the detailed results.

Table 4-1 Cardiac dimension and volume following dialysis.

	Number	Pre dialysis	Post dialysis	Change 95% CI	P value
LVIDd (cm)	26	4.4 ± 0.7	3.7 ± 0.8	↓0.6 ± 0.6 14% (0.4-0.9)	<0.001
LVIDs (cm)	26	3.1 ± 0.7	2.6 ± 0.7	↓0.4 ± 0.5 13% (0.2-0.7)	<0.001
Sphericity Index	20	1.8 ± 0.3	2.2 ± 0.5	↑0.4 ± 0.4 (-0.6 to -0.2)	0.01
LVEDV(ml)	23	83 ± 23	79 ± 27	4.4 ± 16.7 (-2.8-11.6)	0.22
LVESV(ml)	23	35 ± 11	30 ± 11	↓4 2 ± 7.4 12% (1.0-7.4)	0.01
SV (ml)	23	48 ± 15	48 ± 18	0.2 ± 13.5 (-5.7-6.0)	0.95
LAA (cm2)	25	23 ± 7	21 ± 8	↓2.7 ± 4.1 12% (1-4)	<0.01
LAV (ml)	25	78 ± 33	63 ± 28	↓15.5 ± 13.5 20% (9.9-21.1)	<0.001

4.4 Preload reduction and its effect on diastolic filling and estimated LAP

The following table (Table 4-2) shows the effect on diastolic blood flow velocities and timing following dialysis. There was a drop in early diastolic filling (E), late diastolic filling (A), deceleration time (DT) and early to late diastolic filling ratio (E/A). This reflects 'normalisation' of the diastolic filling profile or 'down grading' of the severity of diastolic dysfunction (grade II to grade I) observed and described elsewhere (135) following load change.

In addition, using method (130) described earlier in Chapter 2, I calculated the estimated left atrial pressure before and following dialysis. There was a significant drop in filling pressure following dialysis. Nonetheless, estimated LAP remains elevated at a mean of 13 ± 6 following dialysis. Table 4-3 shows the results.

Table 4-2 Diastolic filling (blood flow velocities) and timing following dialysis.

	Number	**Pre dialysis**	**Post dialysis**	**Change 95% CI**	**P value**
E(m/s)	25	0.82 ± 0.29	0.69 ± 0.21	↓0.13 (15%) (0.04-0.22)	0.005
A(m/s)	21	0.79 ± 0.25	0.73 ± 0.22	↓0.06 (8%) (0.02-0.11)	0.010
DT (ms)	25	229 ± 60	264 ± 67	↑36 (16%) (9-62)	0.011
E/A	24	1.11 ± 0.39	0.97 ± 0.29	↓0.15 (14%) (0.04-0.26))	0.014
IVRT (ms)	28	99 ± 22	103 ± 25	↑4 (4%) (-5-13)	0.348

Table 4-3 Estimated LAP following dialysis

	Number	**Pre dialysis**	**Post dialysis**	**Change** **95% CI**	**P value**
LAP, mmHg (130)	20	16 ± 9	13 ± 6	↓ 2.4 ± 5.6 ↓ 15% (-0.3-5)	0.03
E/e'	21	13 ± 7	10 ± 4	↓ 2 ± 5 ↓ 15% (0.3 – 4.4)	0.01

4.5 Preload reduction and its effect on indices of global and regional cardiac function

4.5.1 Global & regional cardiac function using conventional echo indices

Table 4-4 shows the results following dialysis. There were no significant changes in left ventricular (LV VTI) stroke distance, mitral (MAPSE), biplane left ventricular ejection fraction (EF), and cardiac output (CO) by stroke distance (VTI) or stroke volume (SV) methods.

Table 4-4 Conventional echo indices for global and regional cardiac function following dialysis.

	Number	Pre dialysis mean/median	Post dialysis Mean/median	P value
Fraction shortening (%)	26	28 ± 9	30 ± 6	0.40
LV VTI(cm)	27	21 ± 5	23 ± 9	0.36
MAPSE(cm)	22	1.4 ± 0.3	1.3 ± 0.3	0.58
Biplane EF (%)	23	57	63	0.06
CO by SV method (l/min)	23	3.5 ± 1.0	3.5 ± 1.1	0.88
CO by VTI method (l/min)	27	5.8 ± 1.8	5.5 ± 1.7	0.38
HR (bpm)	30	73 ± 14	76 ± 15	0.15
SBP (mmHg)	30	137 ± 24	131 ± 25	0.11
DBP (mmHg)	30	72 ± 13	76 ± 15	0.11

In addition, cardiac output derived by the two methods (biplane method and VTI method) are seemingly different. I calculated cardiac output both by multiplying the heart rate by the VTI of flow in the LV outflow tract (VTI method) and by multiplying it by SV measured as the difference between LV end-diastolic and systolic volumes (biplane method). Heart rate, taken at the same time as blood pressure reading immediately after dialysis, was unchanged (median HR 73bpm and HR 75bpm, Wilcoxon sign rank test $p>0.05$) following dialysis. Using the two methods, cardiac output before and after dialysis correlated moderately well despite there being no significant difference following dialysis. Cardiac output (VTI method): 5.8 ± 1.8 and 5.5 ± 1.7, Pearson's $R = 0.54$, $p=0.004$. Cardiac output (biplane method): 3.5 ± 1.0 and 3.5 ± 1.1, Pearson's $R=0.50$, $p=0.017$. To explore this further, I used Pearson's linear correlation and Bland Altman graph to assess the difference of cardiac output as derived by the two methods. There is a significant linear correlation between measurements derived from the two methods, Pearson's $R=0.65$, $p=0.00$ although the mean measurements using VTI and biplane methods were significantly different (independent t-test $p<0.01$). More over there appeared to be a systematic error in the measurements as the difference of the two measurements differed increasingly as the mean increased in a linear manner. Figure 16 shows this graphically.

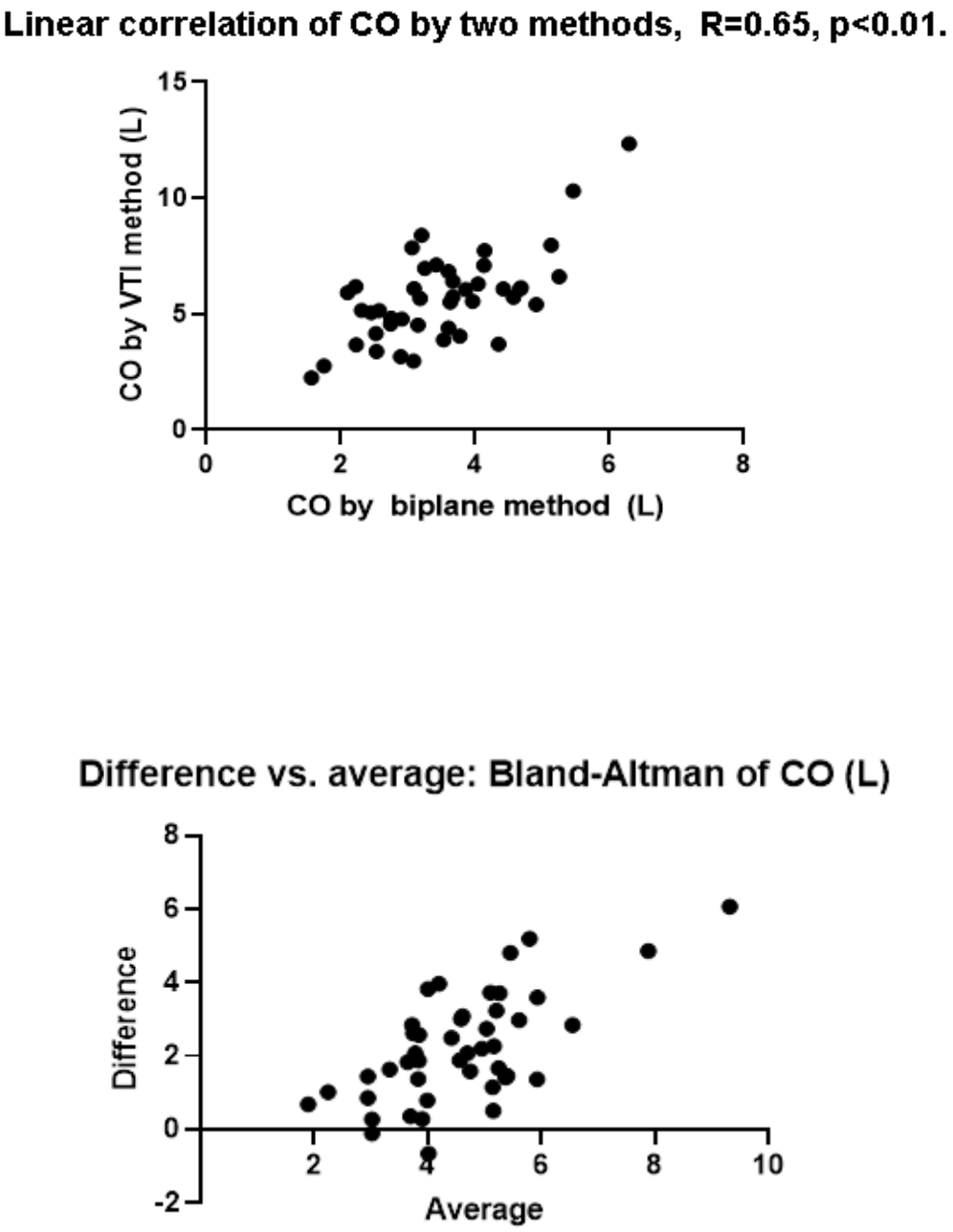

Figure 16 Comparison of CO derived by biplane and VTI methods. Top panel, linear correlation graph. Bottom panel, BA plot of difference and average measurement.

4.5.2 Global and regional cardiac function using novel indices

4.5.2.1 Longitudinal cardiac function indices

I used tissue Doppler velocities to assess regional longitudinal cardiac function. I used 2 dimensional speckled tracking to assess global longitudinal cardiac function.

4.5.2.1.1 Longitudinal tissue Doppler velocities

I recorded at the time of the study, real-time pulsed tissue Doppler velocities of the septal and lateral annuli. Later, I analysed processed colour tissue Doppler velocities in the basal septal and basal lateral walls from a digitally stored image obtained from the time of the study. Sector width during image acquisition was adjusted to maintain a frame rate >60 Hz. In addition, I aligned images to the angle of the Doppler interrogation to minimise sampling error. Table 4-5 summaries the effects of dialysis on longitudinal tissue Doppler velocities. As shown, following dialysis, there is an increase in systolic longitudinal mitral annular tissue velocities. However no change is noted in early and late diastolic longitudinal mitral annular tissue velocities.

Table 4-5 TDI velocities following dialysis

	Number	Pre dialysis	Post dialysis	P value
Pulsed-wave TDI velocities (cm/s)				
Septal s’	25	7.2 ± 1.7	8.5 ± 3.6	0.07
Lateral s’	23	7.6 ± 1.9	8.5 ± 2.3	0.04
Septal e’	22	6.7 ± 2.3	6.0 ± 1.7	0.19
Lateral e’	20	8.9 ± 2.8	8.7 ± 2.5	0.68
Septal a’	21	7.8 ± 2.7	8.3 ± 2.0	0.15
Lateral a’	19	8.6 ± 2.8	8.3 ± 2.7	0.49
Septal e’/a’	21	0.9 ± 0.3	0.8 ± 0.3	0.09
Lateral e’/a’	19	1.1 ± 0.3	1.1 ± 0.4	0.58
Colour processed TDI velocities (cm/s)				
Septal s’	26	5.3 ± 1.9	5.7 ± 1.6	0.08
Lateral s’	24	5.3 ± 1.4	5.9 ± 1.9	0.06
Septal e’	23	4.8 ± 2.1	4.4 ± 2.1	0.27
Lateral e’	20	5.8 ± 2.1	5.5 ± 2.1	0.49
Septal a’	20	5.1 ± 1.8	5.2 ± 1.98	0.43
Lateral a’	20	5.3 ± 1.4	5.9 ± 1.9	0.08
Septal e’/a’	22	1.0 ± 0.7	0.9 ± 0.6	0.21
Lateral e’/a’	19	1.3 ± 0.7	1.7 ± 1.9	0.43

4.5.2.1.2 Two-dimensional longitudinal strain and strain rate

An image of the left ventricle was stored in the 4-chamber view for speckle tracking analysis as illustrated in Chapter 2, section 2.6.2.

Table 4-6 shows the results following dialysis. Following dialysis, there was no change in global longitudinal systolic strain ($S_{systole}$) and systolic strain rate ($SR_{systole}$).

Table 4-6 longitudinal strain following dialysis

	Number	**Pre dialysis mean**	**Post dialysis mean**	**P value**
$S_{systole}$ (%)	24	-14.3 ± 3.4	-14.0 ± 3.7	>0.05
SR $_{systole}$ (/second)	24	0.79 ± 0.24	0.83 ± 0.26	>0.05

4.5.2.2 Radial tissue Doppler velocities

I recorded at the time of the study a tissue Doppler-encoded clip of the parasternal long-axis image of the left ventricle. These loops were only stored in a subset (6) of subjects during the latter part of the study recruitment. This was a protocol change in order to study the differential effect of preload reduction on radial and longitudinal TDI velocities. Later, I analysed radial velocities in the basal septum and basal infero-lateral walls using colour processed TDI data. Sector width during image acquisition was adjusted to maintain a frame rate >60 fpm. In addition, I aligned images to the angle of the Doppler interrogation to minimise sampling error. As illustrated in Chapter 2, section 2.6.1, s' (peak systolic tissue velocity), e' (early diastolic tissue velocity) and a' (late diastolic tissue velocity) were measured.

The results are shown in Table 4-7. Only 6 of the 30 participants had available images for this analysis and therefore the results are to be interpreted with caution. Given the limited sample, no change was seen in peak radial systolic (s') and early diastolic (e') tissue velocities in both the basal septum and basal infero-lateral walls. Nonetheless, there is a small increase in radial late diastolic velocities (a').

Table 4-7 Radial tissue Doppler velocities pre and post dialysis

Colour processed TDI velocities (cm/s)		**Number**	**Pre dialysis**	**Post dialysis**	**P value**
LV basal infero-lateral wall	s’	6	3.9 ± 1.2	4.2 ± 0.6	>0.05
	e’	6	4.0 ± 1.7	5.1 ± 0.9	0.09
	a’	4	3.1 ± 1.1	4.0 ± 0.7	0.03
LV basal septal wall	s’	2	2.3 ± 0.4	2.3 ± 0.2	>0.05
	e’	2	2.9 ± 0.0	2.2 ± 0.1	0.05
	a’	1	1	1.2	

4.5.2.3 Radial strain & circumferential strain at mid left ventricle

Table 4-8 shows the results following dialysis. There was no change in radial strain following dialysis. The large standard deviation of radial strain in these subjects was comparable to reported data from a previous study (36). Circumferential strain increased following preload reduction.

Table 4-8 Radial and circumferential strain following dialysis

	number	**Pre dialysis**	**Post dialysis**	**P value**
S_{rad} (%)	18	34.2 ± 16.3	33.4 ± 14.9	0.70
S_{circ} (%)	18	17.9 ± 3.9	18.6 ± 3.8	0.03

4.5.2.4 Left ventricular apex rotation & torsion

I acquired an image of left ventricular apex and an image of left ventricular base for later analysis with speckle tracking. An illustrated diagram can be found in Chapter 2, section 2.6.4. The results are shown in the following table (Table 4-9). Although there was no change in basal rotation and LV length, there was an increase in apex rotation leading to an increase in LV untwisting and torsion. Nonetheless, there was no change in the peak UTR and time to peak rotation following dialysis.

Table 4-9 LV rotation, torsion and timing

	number	Pre dialysis mean	Post dialysis mean/median	P value
Apex Rotation (^{0})	26	6.9	8.5	0.01
Basal Rotation (^{0})	17	6.0 ± 2.5	6.4 ± 2.6	0.63
LV length (cm)	25	6.61 ± 0.82	6.52 ± 0.84	0.46
Torsion (^{0}/cm)	15	2.3 ± 1.1	2.8 ± 1.1	0.03
Time to Peak Apex Rotation (% cycle length)	26	40 ± 10	41 ± 8	0.45
Peak UTR (/second)	26	73 ± 30	76 ± 27	0.69

4.6 Preload reduction and its effect on E_{es}

4.6.1 Non-invasive single beat estimation of E_{es}

Several non-invasive methods (66,67,71) previously validated well against PV loop studies for single beat estimation of E_{es}. I quantified the E_{es} in my study subjects using the three methods described in page 66-68 (section 2.6.5), Chapter 2.

The results of estimated E_{es} using the three methods and the comparison between the healthy blood donors and the dialysis patients are as shown in the table below (Table 4-10). E_{es} estimated by using the Kim's and Chen's methods were significantly different between the two groups of subjects. E_{es} estimated by Tanoue's method did not distinguish the two groups, unsurprisingly due to the simplicity of the method.

Although the estimated values of E_{es} by the three methods were widely different, measurements of pre and post load change combined together, showed significant linear correlation between each of the three methods. Figure 17 shows this graphically.

Table 4-10 Non-invasive single beat estimated E_{es} by different methods

		Blood donors N=15	Dialysis patients N=30	P value
Ees mmHg/ml	**Chen** (71)	2.8 ± 0.9	1.7 ± 0.7	0.00
	Kim (66)	4.3 ± 2.2	1.6 ± 1.2	0.00
	Tanoue (67)	4.0 ± 1.3	3.9 ± 1.2	0.70

4.6.2 Non-invasive single beat estimation of E_{es} following preload reduction

There was no change in the non-invasively estimated LV end-systolic elastance E_{es} following dialysis. Figure 18 illustrates the pre and post load change measurements and correlation for each of the three methods. Table 4-11 shows the results of E_{es}, and its component measurements pre and post load change. ET, left ventricular ejection time was affected by preload reduction, which is expected and consistent with what was previously reported (104).

Linear correlation of E_{es} estimated by Chen & Tanoue methods, R=0.231, p=0.047.

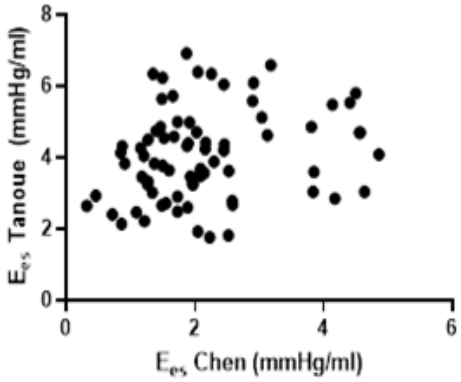

Linear correlation of E_{es} estimated by Kim & Chen methods, R=0.893, p<0.01.

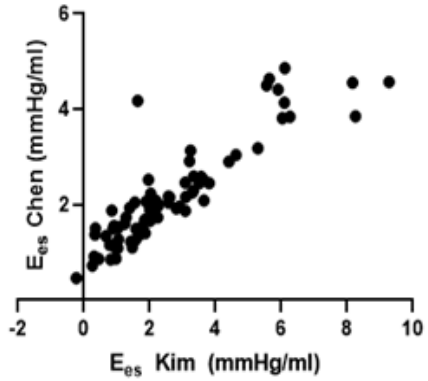

Linear correlation of E_{es} estimated by Kim & Tanoue methods, R=0.29, p=0.012.

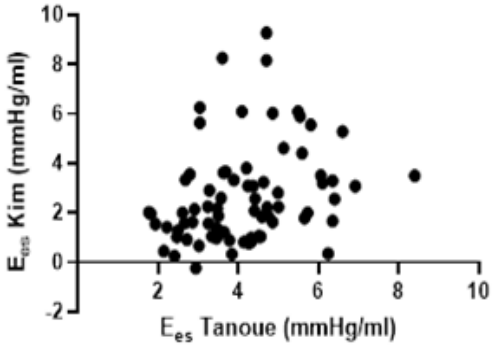

Figure 17 Linear correlation of estimated Ees by different methods

Table 4-11 Non-invasive Ees and its component measurements following dialysis

	Dialysis patients		
	pre	**post**	**P value**
E_{es} Chen (71) **mmHg/ml**	1.6 ± 0.5	1.6 ± 1.0	0.703
E_{es} Kim (66) **mmHg/ml**	1.7 ± 1.3	1.8 ± 1.3	0.613
E_{es} Tanoue (67) **mmHg/ml**	3.9 ± 1.2	4.3 ± 1.5	0.085
DBP mmHg	72 ± 13	68 ± 16	0.116
SBP mmHg	138 ± 24	131 ± 25	0.117
ET Milliseconds	292 ± 7	268 ± 51	0.001
PEP Milliseconds	79 ± 21	74 ± 18	0.365
SV ml	48 ± 15	48 ± 18	0.951
EF %	58 ± 7	61 ± 6	0.060
E_{NDavg}	0.3 ± 0.1	0.3 ± 0.1	0.496
ESV ml	35 ± 11	31 ± 11	0.012

4.6.3 Feasibility of non-invasive quantification of E_{es} measurements

Non-invasive quantification of E_{es} was feasible in my study subjects using the previously described methods (66,67,71). I found that non-invasive E_{es} was unaffected by a large (1.6 L) preload reduction. Similar to earlier findings (126), although the calculated E_{es} obtained using these methods differed, there was good correlation between any given two methods in my subjects. See Table 4-10, page 122 and Figure 17, page 124 for details.

Previous studies have reportedly that E_{es} is around 2 mmHg/ml in normal hearts (136), 4 mmgHg/ml in hypertrophied hearts (137) and <1 mmHg/ml in failing dilated hearts (138). E_{es} measurements derived invasively differ from those derived non-invasively, by a mean of 0.1-1.3 mmHg/ml depending on the methods used (66,71). Chowdhury et al (126) studied children undergoing cardiac surgery and compared the different methods (66,67,71,139) of non-invasively estimated E_{es} with that derived from the gold standard of PV loop. When they used 2-dimensional echocardiography, the measurements differed by between 4.2 to 7 mmHg/ml (4.2 mmHg/ml (67), 5.7 mmHg/ml (66), 7 mmHg/ml (71)). 3-dimensional echocardiographic quantification reduced this difference to as little as 1.6 mmHg/ml (range 1.6-7.9 mmHg/ml) when they used the Tanoue method (67). They reported ICC (intra-class correlation) as a measure of their intra- and inter-observer variability. They reported good ICC for intra-observer (ICC 0.85-0.98) and inter-observer (ICC 0.82-0.92) measurements.: The authors (126)concluded that the

Tanoue (67) method was the simplest to use and produced E_{es} closest to the gold standard measurements.

With regards to my data, although applying the method of Kim et al produced significantly different values of E_{es} in the two study groups, the mean E_{es} of 4.3 ± 1.2 mmHg/ml in the blood donors would suggest the presence of left ventricular hypertrophy (137), which is inconsistent with their normal LVMI calculated using the established method (140). The Tanoue method was the quickest in producing a calculated E_{es} value, but the results in my study did not tell the two groups apart despite the marked difference in their cardiac structure and function (LVMI, LAVI, E/e', estimated LAP). The Chen method, in my study, produced E_{es} values consistent with previous published ranges (136–138) and it was able to distinguish the two groups of subjects. However, this method requires the estimation of a population-averaged elastance at onset of ejection, using a 7-degree polynomial function. This is cumbersome and not easily incorporated into routine clinical use.

4.7 Preload reduction and its effect on IVA

4.7.1 IVA following preload reduction

The following table (Table 4-12) shows the results of IVA following dialysis. As discussed in section 2.6.1 (page 69) and as illustrated by Figure 11 (page 71), IVA is the peak Isovolumetric acceleration (cm/s^2). This is calculated from the peak amplitude of colour processed TDI velocity (cm/s) divided by the time (s) to the peak velocity, during left ventricular isovolumetric contraction.

Table 4-12 IVA following preload reduction in dialysis and blood donor groups

IVA (cm/s^2)	**Number**	**Baseline**	**Post preload reduction**	**p value**
Dialysis subjects				
Septal	23	72 ± 35	70 ± 30	0.75
Lateral	22	51 ± 23	74 ± 55	0.06

4.7.2 Feasibility of IVA measurements

Out of the 45 subjects in both groups, 43 yielded a colour processed TDI graph suitable for IVA determination at baseline and 42 following load reduction. The measurements were not significantly different following load change: 64 ± 55 cm/s^2 and 69 ± 38 cm/s^2, paired t-test p=0.55.

The following figure (Figure 19) shows the linear correlation of the paired measurements. As IVA is calculated by dividing the peak isovolumic velocity by the time from zero crossing to peak isovolumic velocity, the repeatability of IVA measurement is therefore dependent on the repeatability of the TDI velocity. Figure 5 (page 62, chapter 2) and Table 2-3 (page 62, chapter 2) show significant linear correlation (Pearson's R=0.94, p<0.001) and coefficient of variation of 6.8% of repeated TDI measurements in my study. However, I did not perform a repeatability study of IVA measurements. The method is time consuming and a small error in the measurement of isovolumetric velocity and time to peak isovolumetric velocity is unavoidable due to the small magnitude of the measurements.

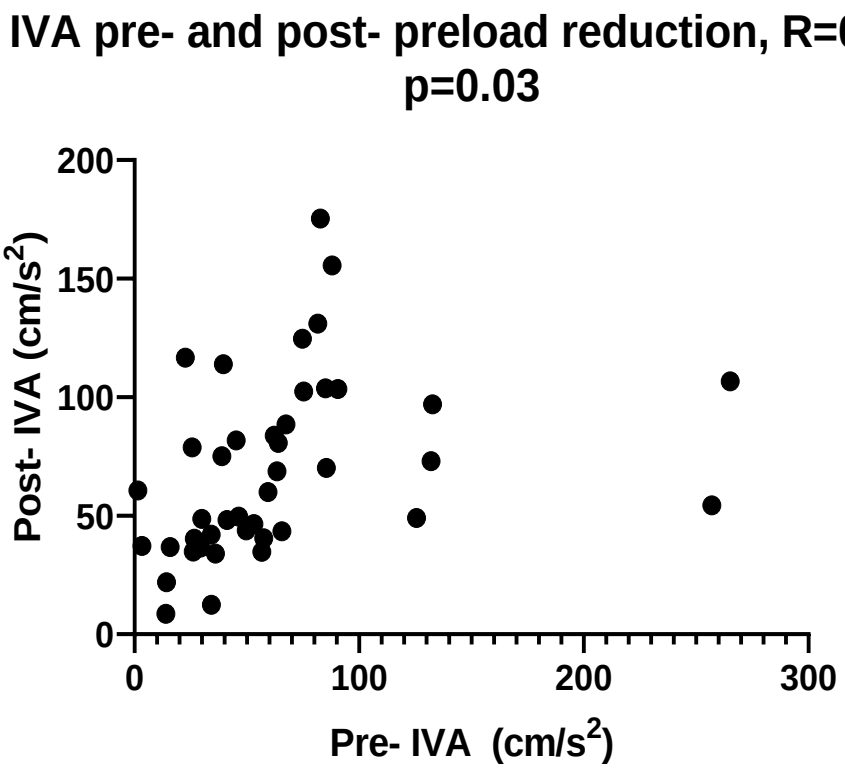

Figure 18 IVA before and after preload reduction, significant but moderate linear correlation.

4.8 Summary of effect of preload reduction following haemodialysis

Following a mean 1.6 ± 1.3 L preload reduction, the main findings were:

1. A significant reduction in cardiac dimensions (LVIDd, LVIDs, LAA) but unchanged wall thickness and mass (LVM, IVSd and PWd).
2. A shape change of left ventricle was apparent, driven by a reduction in LVIDd but unchanged LV length.
3. A significant reduction in diastolic blood flow filling velocities (E,A).
4. Estimated LAP decreased significantly although the values remained elevated.
5. Conventional indices of global and regional cardiac function (MAPSE, FS, EF, LV VTI) remained unchanged.
6. Novel indices of cardiac function showed differential load sensitivity. Longitudinal systolic tissue Doppler velocities (TDI), 2DSTE apex rotation and mid cavity circumferential strain (S_{circ}) were significantly different following dialysis. There was no change in radial tissue Doppler velocities (TDI), 2DSTE radial strain, basal rotation and longitudinal strain ($S_{systole}$) and $SR_{systole}$.
7. Non-invasive single beat estimation of E_{es} was feasible using all three methods (66,67,71).
8. E_{es}, estimated by the non-invasive methods, did not change.
9. Tanoue's method is the simplest, requiring only knowledge of ESV and systolic blood pressure. However using this method in my subjects did not characterise them as two distinct clinical groups. Chen's method is the most

complicated, requiring estimation of the normalised left ventricle elastance at onset of ejection, by a 7-degree polynomial equation. Kim's method is easier to use in comparison but assumes a constant EDP of 10 mmHg in the calculation.

10. Estimated E_{es} from the three methods were widely different but results of E_{es} using each method do correlate with each other well. Therefore, values of E_{es} derived from these three methods must not be used interchangeably.
11. IVA quantification is feasible in all my subjects but it is time consuming.
12. TDI derived IVA, as a marker of LV contractile state, is load insensitive within the range of preload reduction studied in my subjects.

Returning to the hypotheses at the beginning of this chapter, I conclude the following:

1. Conventional indices (EF, MAPSE, CO) of echocardiography are load resistant given a preload reduction of 1.6 litres.
2. Novel echocardiographic indices show differential load sensitivity to this amount of load change. Apical rotation, TDI longitudinal s' and mid LV S_{cir} are preload sensitive whilst mid LV S_{rad} and longitudinal $S_{systole}$ are preload resistant.
3. IVA and non-invasively estimated E_{es} are preload insensitive.

Chapter 6.

5 Effect of preload reduction on cardiac function following venesection

5.1 Aims of this chapter

In this chapter, I aim to investigate the effect of a modest preload reduction (500ml) on echocardiographic indices of cardiac function. I studied this in a group of healthy blood donors. I tested the hypothesis that most echocardiographic indices are preload sensitive. I also tested the hypothesis that non-invasively quantified E_{es} and IVA are insensitive to moderate preload reduction.

5.2 Subjects testing

15 subjects consented to take part in the study at the Welsh Blood Service. Each subject laid semi supine on a bed in the left lateral position and underwent echocardiography immediately before venesection. For the duration of blood donation, approximately ten minutes, each subject remained seated on the bed. Immediately after blood donation, each subject resumed the semi supine left lateral position whilst I performed echocardiography.

All images were stored digitally for offline analysis on a separate occasion. Each subject had a unique study identification number for anonymization purpose. I performed all the data analysis some time later.

Chapter 6.

5.3 General haemodynamic measurements

Blood pressure and heart rate were measured immediately before and after venesection. Compared to baseline, there was no change in arm cuff blood pressure, heart rate derived from arm cuff monitoring and heart rate at time of echocardiography. The following table (Table 5-1) shows the results.

5.4 Preload reduction and its effect on cardiac dimension and volume

As shown in the following table (Table 5-2), venesection significantly reduced left ventricular end diastolic (LVIDd) and end systolic (LVIDs) internal dimensions, left ventricular end diastolic volume (LVEDV), stroke volume (SV), and left atrial area (LAA) and volume (LAV). There was no change in left ventricular length. Sphericity index, calculated by dividing LV length with LVIDd, increased as the ventricle became less spherical following venesection.

5.5 Preload reduction and its effect on diastolic filling

Despite the relatively modest volume of blood loss (approximately 500ml), diastolic blood flow velocities were significantly reduced in early (E) and late (A) diastole. In addition, deceleration time (DT) and isovolumetric relaxation time (IVRT) were significantly longer and increased by 24% and 15% respectively. Table 5-3 shows the results. Estimated LAP was normal at baseline and remained so following venesection as shown in Table 5-4.

Table 5-1 Blood pressure and heart rate following venesection

	Pre venesection	**Post venesection**	**Paired t-test p value**
Systolic blood pressure (mmHg)	*127 ± 17*	*125 ± 19*	*0*.53
Diastolic blood pressure (mmHg)	*77 ± 19*	*76 ± 16*	*0*.84
Mean blood pressure (mmHg)	*94 ± 13*	*92 ± 17*	*0.49*
Pulse pressure (mmHg)	*50 ± 10*	*48 ± 10*	*0.73*
Heart rate (arm cuff) (bpm)	*64 ± 13*	*65 ± 11*	*0*.85

Table 5-2 Cardiac dimension following venesection

	Number	Pre venesection	Post venesection	Δ mean difference and 95% CI	P value
LVIDd (cm)	15	4.2 ± 0.6	3.7 ± 0.7	↓0.6 ± 0.1 14% *(0.3-0.8)*	0.001
LVIDs (cm)	15	2.9 ± 0.5	2.5 ± 0.5	↓0.5 ± 0.2 17% (0.0-0.9)	0.038
LV length (cm)	15	8.01 ± 0.51	7.92 ± 0.59	-	0.12
Sphericity Index_4c	15	1.9 ± 0.2	2.3 ± 0.4	↑0.3 ± 0.1 (-0.5 to 1.5)	0.001
LVEDV(ml)	15	86 ± 20	80 ± 20	↓6 ± 3 7% (0.1 to 12)	0.047
LVESV(ml)	15	31 ± 11	28 ± 9	↓2.8 (-1.8-7.4)	>0.05
SV by biplane method (ml)	15	55 ± 11	51 ± 15	↓3.4 (-2.8-9.6)	>0.05
LAA (cm^2)	14	15 ± 3	13 ± 4	↓1.9 (-0.1-4.0)	0.064
LAV (ml)	14	40 ± 12	34 ± 14	↓ 6 ± 2 15% (0.6-11)	0.031

Table 5-3 Blood pooled velocities following venesection

	Number	Pre	Post	Mean Δ and 95% CI	P value
E(m/s)	15	0.69 ± 0.12	0.55 ± 0.12	↓0.14 ± 0.11 13% (0.07 – 0.20)	0.000
A(m/s)	15	0.52 ± 0.12	0.46 ± 0.10	↓0.06 ± 0.09 3% (0.01- 0.12)	0.027
DT (ms)	15	218 ± 42	270 ± 72	↑52 ± 78 24% (9 – 96)	0.021
E/A	15	1.40 ± 0.39	1.27 ± 0.41	0.12 ± 0.28 9% (0.03-0.27)	0.122
IVRT (ms)	15	96 ± 13	110 ± 28	↑15 ± 23 16% (2-28)	0.030

Table 5-4 Estimated LAP following venesection

	Number	Pre venesection	Post venesection	Mean Δ and 95% CI	P value
Estimated LAP (130) **mmHg**	15	9.8 ± 1.6	8.7 ± 2.5	↓1.1 (-0.1-2.3)	0.076
E/e'	15	6.8 ± 1.4	6.3 ± 2.5	↓ 0.5 ± 2.3 (0.8 – 1.8)	0.423

5.6 Preload reduction and its effect on global and regional cardiac function

5.6.1 Global & regional cardiac function using conventional echo indices

The following table (Table 5-5) shows results using conventional echocardiography indices for regional and global cardiac function. Although there was a reduction in left ventricular (LV VTI) stroke distance, there was no change in overall global cardiac function following venesection. Fraction shortening (FS), biplane ejection fraction (EF), cardiac output (CO) and index (CI) remained unchanged.

5.6.2 Global and regional cardiac function using novel echo indices

5.6.2.1 Longitudinal cardiac function indices

5.6.2.1.1 Longitudinal tissue Doppler velocities

There was no change in the instantaneous tissue Doppler velocities. However, a change was apparent in the processed colour tissue Doppler velocities. Basal septal and average basal (septal and lateral) systolic velocities increased by 16%and 9% respectively. Basal lateral and average early diastolic velocities decreased by 13% and 10% respectively after venesection. Table 5-6 shows the results.

Table 5-5 regional and global cardiac indices following venesection.

	Number	Pre	Post	% change from baseline, 95% CI	P value
Fractional shortening (%)	15	30 ± 8	27 ± 7	3.33 (-1.6-8.3)	0.17
LV VTI(cm)	15	19 ± 3	18 ± 3	↓1.9 (0.14-3.61)	0.03
MAPSE(cm)	15	1.5 ± 0.4	1.4 ± 0.3	0.10 (-0.05-0.25)	0.18
Biplane EF (%)	15	64 ± 5	64 ± 7	-0.20 (-4.5-4.1)	0.92
CO biplane(l/min)	15	3.4 ± 0.7	3.1 ± 0.7	0.27 (-0.2-0.7)	0.22
CO by VTI (l/min)	15	3.8 ± 0.8	3.4 ± 0.9	0.5 (0.02-0.94)	0.04

Table 5-6 TDI velocities following venesection

	Number	Pre dialysis	Post dialysis	P value
Pulsed-wave TDI velocities (cm/s)				
Septal s’	14	8.8 ± 1.6	8.9 ± 1.6	0.869
Lateral s’	15	8.7 ± 2.2	9.3 ± 1.4	0.251
Septal e’	14	9.4 ± 2.9	8.0 ± 2.8	0.057
Lateral e’	15	11.1 ± 2.4	10.9 ± 2.7	0.666
Septal a’	15	8.4 ± 2.3	8.1 ± 2.4	0.598
Lateral a’	15	7.3 ± 2.9	7.5 ± 2.3	0.677
Septal e’/a’	14	1.3 ± 0.6	1.2 ± 0.8	0.46
Lateral e’/a’	15	1.6 ± 0.8	1.8 ± 1.1	0.47
Colour processed TDI velocities (cm/s)				
Septal s’	15	5.1 ± 0.7	5.9 ± .9	0.018
Lateral s’	14	5.9 ± 1.3	6.1 ± 1.1	0.638
Septal e’	15	6.4 ± 1.9	5.9 ± 2.5	0.215
Lateral e’	14	7.9 ± 2.0	6.9 ± 1.7	0.063
Septal a’	15	4.6 ± 1.7	4.7 ± 1.8	0.902
Lateral a’	14	4.2 ± 1.8	4.2 ± 1.8	0.906
Septal e’/a’	15	1.8 ± 1.3	2.3 ± 1.4	0.82
Lateral e’/a’	14	2.3 ± 1.4	2.1 ± 1.3	0.19

Chapter 6.

5.6.2.1.2 Two-dimensional longitudinal strain and strain rate

There was no change in peak longitudinal systolic strain ($S_{systole}$), or in the peak strain rate at systole ($SR_{systole}$). Table 5-7 shows these results.

5.6.2.2 Radial tissue Doppler velocities

When examining the radial plane tissue Doppler velocities in basal infero-lateral wall and basal infero-septum using colour processed TDI, I noted an increase in late diastolic velocities in the basal infero-lateral wall by 33% and average velocities by 22%. Only the infero-septum showed an insignificant decrease in early diastolic tissue velocity by 18% whilst the systolic velocities remained unchanged in both segments. Table 5-8 below shows the results.

5.6.2.3 Radial strain & circumferential strain at mid left ventricle

Not all the subjects had adequate images for 2DSTE analysis at the mid left ventricle. No significant difference was demonstrated in the 2-dimensional radial strain, and circumferential strain following venesection. Table 5-9 shows the results.

Table 5-7 Longitudinal strain and strain rate following venesection

	Number	**Pre venesection mean**	**Post venesection mean**	**P value**
Ssystole (%)	14	15.1 ± 1.2	15.1 ± 2.7	0.947
$SR_{systole}$ (/second)	14	0.8 ± 0.1	0.9 ± 0.2	0.553

Table 5-8 Radial TDI velocities following venesection

		number	Pre venesection	Post venesection	P value
Basal infero-lateral wall (cm/s)	s’	15	3.3 ± 1.1	3.4 ± 0.7	0.717
	e’	15	4.1 ± 1.1	3.7 ± 1.2	0.364
	a’	15	1.8 ± 1.2	2.4 ± 1.3	0.018
Basal infero-septum (cm/s)	s’	10	2.8 ± 0.6	3.1 ± 0.8	0.279
	e’	9	3.3 ± 0.9	2.7 ± 1.5	0.089
	a’	9	2.01.0	2.21.1	0.285

Table 5-9 Radial and circumferential strain following venesection

	Number	Pre venesection	Post venesection	P value
S_{rad} (%)	9	43 ± 16	36 ± 11	0.383
S_{circ} (%)	10	21 ± 3	21 ± 4	0.839

5.6.2.4 Left ventricular apex rotation, basal rotation & LV torsion

As shown in table below (Table 5-10), there was a 40% and 32% increase in apex rotation and untwisting following venesection but no change was noted in basal rotation, LV torsion and length. Apex time to peak to peak rotation, time to peak untwisting, early untwist, untwisting time and time to peak untwisting rate (UTR) were unchanged. There was a 32% increase in peak untwisting rate following venesection.

Table 5-10 LV rotation and torsion following venesection

	Number	Pre-venesection	Post-venesection	P value
Apex Rotation (^{0})	12	6.5 ± 2.2	9.1 ± 4.3	0.044
Basal Rotation (^{0})	13	5.6 ± 2.8	5.5 ± 2.6	0.897
LV length (cm)	11	8.0 ± 0.5	8.0 ± 0.5	0.123
Torsion (^{0}/cm)	11	1.9 ± 0.6	2.4 ± 0.9	0.140
Time to Peak Apex Rotation (% cycle length)	12	28 ± 12	32 ± 9	0.153
Peak UTR (/second)	12	59 ± 21	78 ± 28	0.033

Chapter 6.

5.7 Preload reduction and its effect on E_{es}

There was no change in the non-invasively estimated LV end-systolic elastance E_{es} following venesection. Figure 20 illustrates the pre and post load change measurements and correlation for each of the three methods (66,67,71). Table 5-11 shows the results of E_{es}, and its component measurements pre and post load change in the venesection group. ET, left ventricular ejection time was affected by preload reduction, which is expected and consistent with what was previously reported (104).

Table 5-11 E_{es} and its component measurements following venesection.

	Blood donors		
	pre	**post**	**P value**
E_{es} Chen (71) **mmHg/ml**	2.8 ± 0.9	2.9 ± 1.1	0.802
E_{es} Kim (66) **mmHg/ml**	4.3 ± 2.2	3.9 ± 2.0	0.410
E_{es} Tanoue (67) **mmHg/ml**	4.0 ± 1.3	4.3 ± 1.4	0.309
DBP mmHg	77 ± 12	76 ± 17	0.848
SBP mmHg	127 ± 17	125 ± 19	0.539
ET Milliseconds	293 ± 22	278 ± 23	0.013
PEP Milliseconds	59 ± 16	67 ± 20	0.105
SV ml	55 ± 11	51 ± 15	0.258
EF %	64 ± 5	64 ± 7	0.923
E_{NDavg}	0.2 ± 0.1	0.3 ± 0.1	0.039
ESV ml	31 ± 11	28 ± 9	0.209

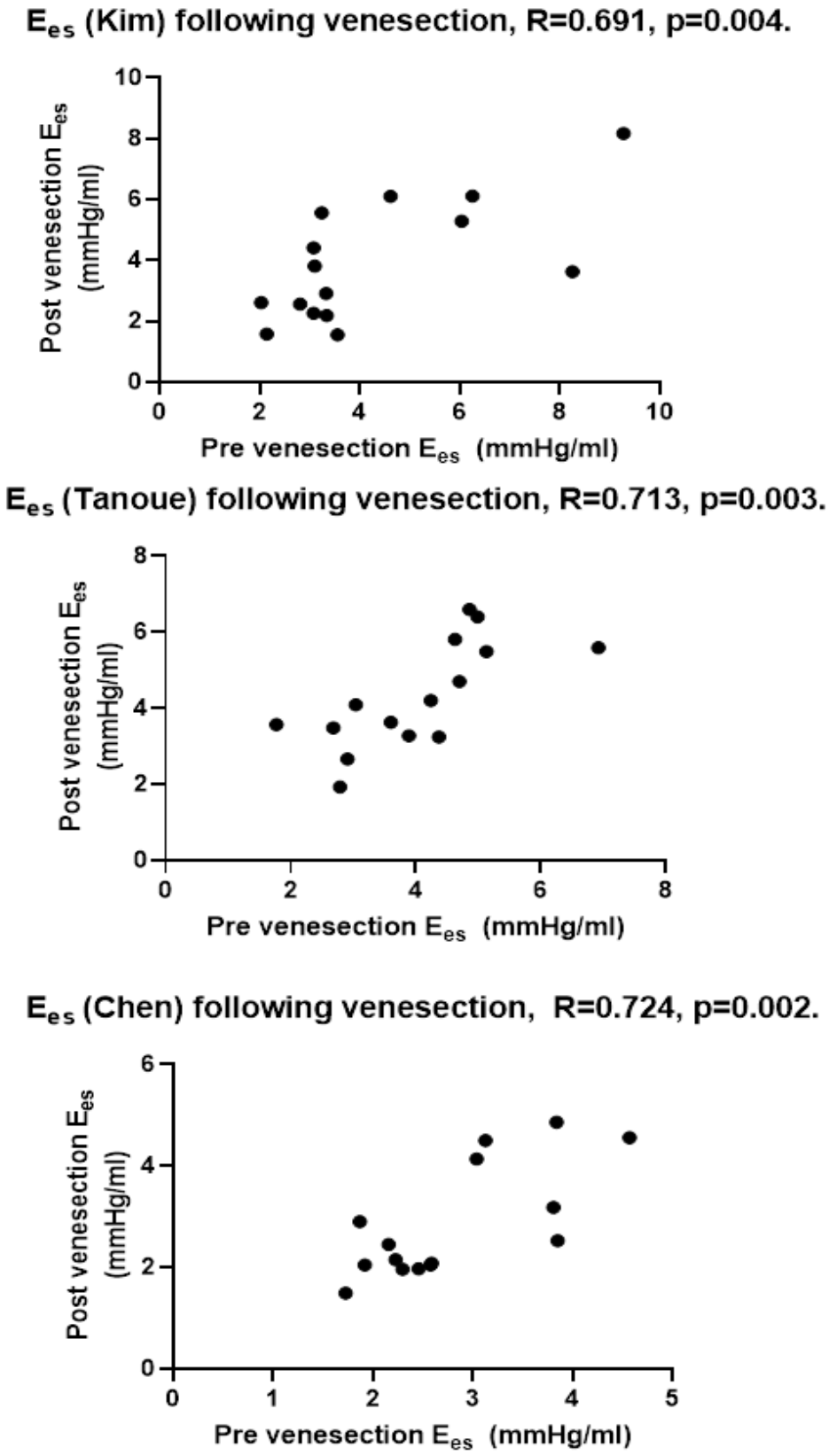

Figure 19 *E_{es} pre- and post-venesection, linear correlation graphs. Top panel Kim method, middle panel Tanoue method, and bottom panel Chen method.*

Chapter 6.

5.8 Preload reduction and its effect on IVA

The following table (Table 5-12) shows the results of IVA following venesection. As discussed in section 2.6.1 (page 69) and as illustrated by Figure 11 (page 71), IVA is the peak Isovolumetric acceleration (cm/s^2). This is calculated from the peak amplitude of colour processed TDI velocity (cm/s) divided by the time (s) to the peak velocity, during left ventricular isovolumetric contraction.

Table 5-12 IVA following preload reduction in dialysis and blood donor groups

IVA (cm/s^2)	**Number**	**Baseline**	**Post preload reduction**	**p value**
Blood donors				
Septal	15	60 ± 61	59 ± 41	0.956
Lateral	12	85 ± 111	71 ± 43	0.619

5.9 Summary of effect of preload reduction following venesection

The main findings following venesection in healthy blood donors are:

1) Peripheral haemodynamic indexes (systolic blood pressure, diastolic blood pressure, mean blood pressure, pulse pressure, heart rate) were unaffected by a modest volume of blood loss.
2) Despite the modest volume loss, there was reduction in cardiac chamber dimensions and volumes: 12% reduction in LVIDd, 14% reduction in LVIDs, 7% reduction in LVEDV, 13% reduction in SV, and 15% reduction in LAV.
3) A shape change of left ventricle resulted from unchanged LV length and reduced radial dimension: sphericity index increased by 16-21%. The left ventricle became less spherical following venesection.
4) Diastolic filling was affected by even a small volume loss: 29% reduction in E velocity, 20% reduction in A velocity, 24% increase in DT time, and 15% increase in IVRT time.
5) Conventional indices of cardiac function (FS, MAPSE, EF, CO, CI) were unaffected by this small volume change.
6) There was a differential preload sensitivity in regional tissue Doppler velocities. Systolic longitudinal tissue Doppler velocity (TDI) s' increased by 9-16% but radial tissue Doppler velocity (TDI) s' remained unchanged. Both longitudinal and radial e' decreased by 10-13% and 18% respectively. Radial a' increased by 22% whilst longitudinal a' was unchanged. Radial s' and longitudinal a' appear to be least load sensitive.

7) There was a differential preload sensitivity in 2-dimensional strain. Radial and circumferential strain, basal rotation and LV torsion did not change whilst there was a 40% increase in apex rotation. Apex rotation appears to be most load sensitive.
8) E_{es} and IVA did not change following venesection.

Returning to the hypotheses at the beginning of this chapter, I conclude the following:

1. Conventional indices (EF, MAPSE, CO) of echocardiography are not affected by a small change in preload.
2. Apical rotation and TDI longitudinal s' are sensitive to a small change in preload.
3. Scir, Srad and Ssystole are resistant to a small preload reduction.
4. Ees and IVA are preload resistant given a small preload reduction.

6 Effects of preload reduction on cardiac function

6.1 Aim of this chapter

Chapter 4 and Chapter 5 showed the results on cardiac function following a large (mean of 1.6 L) and moderate (500 ml) preload reduction in the two subject groups. As discussed in Chapter 3, there are significant difference in the baseline characteristics of the two groups in this study.

The aim of this chapter was to investigate if there was a different response to preload reduction, in the dialysis group compared to the blood donors, after adjusting for the confounding factors. The difference in response following preload reduction, if found, may be helpful in better characterisation of the dialysis group.

6.2 Baseline differences in the study groups

The dialysis subjects were older compared to the blood donors (mean age 59 ± 18 years and 45 ± 15 years, p=0.02). In addition, the magnitude of preload reduction was 1.6 ± 1.3 L in the dialysis group, compared to 0.5 ± 0.0 L in the blood donors, $p<0.001$. To detect a true difference in their response to preload reduction, I used ANCOVA (analysis of covariance) analysis to adjust for the confounding covariates of age and magnitude of preload change. The following sections show the results of this analysis.

Chapter 6.

6.3 Change in cardiac dimension and volume following preload reduction

As a combined group, following preload reduction, there is a significant reduction in left ventricular dimensions (LVIDd, LDIDs) and left atrial volume (LAV) whilst the LV length remained unchanged. The left ventricle became less spherical in both groups.

Before and after adjusting for the covariates of age and volume loss, there is no significant difference between the groups. Table 6-1 shows the unadjusted difference (independent t-test) and adjusted difference (ANCOVA analysis) for both the groups.

Table 6-1 Group comparison following preload reduction, adjusted using ANCOVA analysis

		Dialysis		**Venesection**		**p value for baseline comparison**	**p value for mean Δ comparison following preload reduction**
		Pre	**Δ post**	**Pre**	**Δ post**		
LVIDd (cm)	unadjusted	4.4 ± 0.7	0.6 ± 0.1	4.2 ± 0.6	0.6 ± 0.2	0.49	0.70
	adjusted	4.4 ± 0.1	0.6 ± 0.1	4.2 ± 0.2	0.6 ± 0.2	0.61	0.91
LVIDs (cm)	unadjusted	3.1 ± 0.7	0.4 ± 0.1	2.9 ± 0.4	0.5 ± 0.2	0.48	0.94
	adjusted	3.0 ± 0.1	0.4 ± 0.1	3.0 ± 0.2	0.6 ± 0.2	0.86	0.46
IVSd (cm)	unadjusted	1.2 ± 0.3	0.1 ± 0.5	0.9 ± 0.1	0.1 ± 0.2	0.00	0.98
	adjusted	1.2 ± 0.1	0.1 ± 0.1	1.0 ± 0.1	0.0 ± 0.2	0.01	0.67

Table 6-1 Group comparison following preload reduction, adjusted using ANCOVA analysis

		Dialysis		Venesection		p value for baseline comparison	p value for mean Δ comparison following preload reduction
		Pre	**Δ post**	**Pre**	**Δ post**		
PWd (cm)	unadjusted	1.2 ± 0.2	0.1 ± 0.2	1.0 ± 0.1	0.1 ± 0.1	0.00	0.56
	adjusted	1.2 ± 0.0	0.1 ± 0.1	1.0 ± 0.1	0.1 ± 0.1	0.00	0.73
LV length (cm)	unadjusted	7.8 ± 0.9	0.4 ± 0.1	8.0 ± 0.5	0.0 ± 0.1	0.36	0.78
	adjusted	8.3 ± 0.9	0.1 ± 0.1	8.0 ± 0.5	0.1 ± 0.2	0.14	0.48
Sphericity index	unadjusted	1.7 ± 0.2	0.3 ± 0.1	1.9 ± 0.2	0.3 ± 0.1	0.59	0.98
	adjusted	1.9 ± 0.1	0.3 ± 0.1	1.9 ± 0.1	0.4 ± 0.1	0.82	0.87

Table 6-1 Group comparison following preload reduction, adjusted using ANCOVA analysis

		Dialysis		**Venesection**		**p value for baseline comparison**	**p value for mean Δ comparison following preload reduction**
		Pre	**Δ post**	**Pre**	**Δ post**		
LAV (ml)	unadjusted	78 ± 33	15.5 ± 2.7	40 ± 12	6.0 ± 2.5	0.00	0.02
	adjusted	77 ± 6	15.1 ± 2.6	40 ± 7	6.6 ± 3.7	0.00	0.08
LVEDV (ml)	unadjusted	83 ± 23	4 ± 3	86 ± 20	6 ± 3	0.74	0.71
	adjusted	83 ± 5	11 ± 4	86 ± 6	2 ± 3	0.77	0.09
LVESV (ml)	unadjusted	35 ± 11	4 ± 2	31 ± 11	3 ± 2	0.33	0.58
	adjusted	35 ± 2	4 ± 2	31 ± 3	3 ± 2	0.36	0.78
SV (ml)	unadjusted	48 ± 15	0.2 ± 3	55 ± 11	3 ± 3	0.18	0.44

Table 6-1 Group comparison following preload reduction, adjusted using ANCOVA analysis

		Dialysis		**Venesection**		**p value for baseline comparison**	**p value for mean Δ comparison following preload reduction**
		Pre	**Δ post**	**Pre**	**Δ post**		
	adjusted	48 ± 3	6 ± 4	55 ± 4	2 ± 3	0.22	0.09
CO_sv (l)	unadjusted	3.5 ± 1.0	0.0 ± 0.2	3.4 ± 0.7	0.3 ± 0.2	0.66	0.46
	adjusted	3.6 ± 0.2	0.5 ± 0.3	3.3 ± 0.2	0.2 ± 0.1	0.41	0.11
CO_vti (l)	unadjusted	5.8 ± 1.3	0.7 ± 0.6	3.8 ± 0.9	0.5 ± 0.2	0.00	0.07
	adjusted	5.6 ± 0.3	0.4 ± 0.7	3.8 ± 0.4	0.7 ± 0.5	0.00	0.27
LVOTd (cm)	unadjusted	2.2 ± 0.3	0.0 ± 0.0	2.0 ± 0.2	0.0 ± 0.1	0.01	0.65
	adjusted	2.1 ± 0.1	0.0 ± 0.1	2.0 ± 0.1	0.0 ± 0.1	0.05	0.52

Table 6-1 Group comparison following preload reduction, adjusted using ANCOVA analysis

		Dialysis		Venesection		p value for baseline comparison	p value for mean Δ comparison following preload reduction
		Pre	**Δ post**	**Pre**	**Δ post**		
Heart rate (bpm)	unadjusted	74 ± 15	2 ± 2	63 ± 10	0.1 ± 1.5	0.02	0.36
	adjusted	73 ± 2	0.1 ± 2	61 ± 3	2 ± 2	0.00	0.42
LV VTI (cm)	unadjusted	21.5 ± 5.1	1.9 ± 2.1	19.4 ± 3.1	1.9 ± 0.8	0.15	0.19
	adjusted	21.2 ± 0.9	1 ± 3	19.5 ± 1.3	2 ± 3	0.29	0.44

6.4 Change in diastolic filling following preload reduction

At baseline, the dialysis group had high filling pressure (E/e', estimated LAP) and diastolic dysfunction (A, E/A) compared to the blood donor group. Following preload reduction, both groups demonstrated a reduction in diastolic blood pooled velocities E and A. E/A ratio and estimated LAP fell significantly after a large load change (1.6 L) but they were unaffected by venesection (volume loss of 500ml).

When adjusted for covariates of age and volume loss, there is no significant difference in the change of diastolic blood pooled velocities and filling pressure between the groups. Table 6-2 shows the results.

Table 6-2 Blood pooled diastolic velocities and filling pressure following preload reduction, group comparison.

		Baseline			**Δ from baseline following preload reduction**		
		dialysis	**venesection**	**P value**	**dialysis**	**venesection**	**P value**
E (m/s)	unadjusted	0.8 ± 0.3	0.7 ± 0.1	0.06	0.13 ± 0.22	0.14 ± 0.11	0.96
	adjusted	0.8 ± 0.1	0.7 ± 0.1	0.06	0.12 ± 0.04	0.18 ± 0.05	0.44
A(m/s)	unadjusted	0.8 ± 0.2	0.5 ± 0.1	0.00	0.06 ± 0.09	0.06 ± 0.09	0.93
	adjusted	0.8 ± 0.0	0.6 ± 0.1	0.01	0.07 ± 0.03	0.07 ± 0.03	0.97
DT(ms)	unadjusted	228 ± 58	218 ± 42	0.54	36 ± 65	52 ± 78	0.47
	adjusted	223 ± 10	227 ± 14	0.82	26 ± 16	70 ± 21	0.14
E/A	unadjusted	1.1 ± 0.4	1.4 ± 0.4	0.01	0.15 ± 0.28	0.12 ± 0.28	0.75
	adjusted	1.2 ± 0.1	1.3 ± 0.1	0.38	0.14 ± 0.06	0.15 ± 0.08	0.88

Table 6-2 Blood pooled diastolic velocities and filling pressure following preload reduction, group comparison.

		Baseline			**Δ from baseline following preload reduction**		
		dialysis	**venesection**	**P value**	**dialysis**	**venesection**	**P value**
IVRT(ms)	unadjusted	99 ± 21	96 ± 13	0.59	4.1 ± 22.6	14.7 ± 23.4	0.15
	adjusted	97 ± 4	98 ± 5	0.88	0.6 ± 4.5	21.2 ± 6.4	0.02
E/e'	unadjusted	13 ± 7	6.8 ± 1.4	0.00	2.03 ± 5.2	0.49 ± 2.31	0.29
	adjusted	7.9 ± 0.4	6.5 ± 0.5	0.03	1.6 ± 1.0	1.1 ± 1.3	0.76
Estimated LAP (130)	unadjusted	2.04 ± 0.09	1.98 ± 0.02	0.01	0.02 ± 0.06	0.01 ± 0.02	0.40
	adjusted	2.03 ± 0.01	1.98 ± 0.01	0.04	0.02 ± 0.01	0.02 ± 0.01	0.91

6.5 Change in cardiac function following preload reduction

6.5.1 Conventional indices of cardiac function

At baseline, there was no difference in the conventional indices of global and regional cardiac function between the groups. Following preload reduction, neither group exhibited a change in these indices. Table 6-3 shows the results.

6.5.2 Novel indices of cardiac function

6.5.2.1 Longitudinal TDI velocities

After adjusting for age as confounder, both groups had comparable longitudinal systolic and diastolic TDI velocities but the dialysis group has significantly higher filling pressure (E/e'). Table 6-4 (pulsed-wave TDI) & Table 6-5 (colour processed TDI) show the results of longitudinal mitral annular velocities following preload reduction. Following preload reduction, pulsed-waved septal s' and colour processed lateral s' increased significantly in the dialysis group. On the contrary, pulsed-wave septal s' and colour processed lateral s' decreased significantly in the blood donors. Colour processed septal e' fell significantly in the blood donors but remained unchanged in the dialysis group.

Table 6-3 Group comparison for conventional indices of global and regional cardiac function following preload reduction

		baseline			**Δ from baseline following preload reduction**		
		dialysis	**venesection**	**p value**	**dialysis**	**venesection**	**P value**
Fractional shortening (%)	**Unadjusted**	28 ± 9	30 ± 8	0.53	1.7 ± 0.4	3.3 ± 9.0	0.12
	Adjusted	29 ± 2	29 ± 2	0.93	1.4 ± 2.2	3.2 ± 2.9	0.26
LV VTI(cm)	**Unadjusted**	21 ± 5	19 ± 3	0.15	1.9 ± 10.8	1.9 ± 3.1	0.19
	Adjusted	21 ± 1	20 ± 1	0.30	1.8 ± 1.9	1.0 ± 2.6	0.44
MAPSE(cm)	**Unadjusted**	1.4 ± 0.4	1.5 ± 0.4	0.58	0.0 ± 0.3	0.1 ± 0.3	0.58
	Adjusted	1.4 ± 0.1	1.5 ± 0.1	0.62	0.0 ± 0.1	0.1 ± 0.1	0.37

Table 6-4 Mitral annular pulsed-wave TDI velocities following preload reduction, group comparison

Pulsed-wave TDI velocities (cm/s)		**Baseline**			**Change from baseline**		
		dialysis	**venesection**	**P value**	**dialysis**	**venesection**	**P value**
Septal s'	**Unadjusted**	7.2 ± 1.7	8.8 ± 1.6	0.02	1.3 ± 3.3	0.1 ± 1.6	0.21
	adjusted	7.5 ± 0.3	8.7 ± 0.5	0.06	↑1.7 ± 0.6	↓0.7 ± 0.8	0.03
Lateral s'	**Unadjusted**	7.6 ± 1.9	8.7 ± 2.2	0.19	1.3 ± 3.2	0.1 ± 1.6	0.21
	adjusted	7.7 ± 0.4	8.9 ± 0.6	0.10	1.0 ± 0.4	0.3 ± 0.5	0.30
Septal e'	**Unadjusted**	6.7 ± 2.3	9.4 ± 2.9	0.01	0.7 ± 2.4	1.4 ± 2.6	0.37
	adjusted	7.3 ± 0.4	8.7 ± 0.5	0.04	0.8 ± 0.6	1.2 ± 0.7	0.65
Lateral e'	**Unadjusted**	8.9 ± 2.8	11.1 ± 2.4	0.01	0.7 ± 2.4	1.4 ± 2.6	0.37
	adjusted	9.1 ± 0.5	10.7 ± 0.7	0.05	0.1 ± 0.5	-0.7 ± 0.7	0.34
Average E/e'	**Unadjusted**	13 ± 7	6.8 ± 1.4	0.00	2.0 ± 5.2	0.5 ± 2.3	0.29
	adjusted	7.9 ± 0.4	6.5 ± 0.5	0.03	1.6 ± 1.0	1.1 ± 1.3	0.76
Septal a'	**Unadjusted**	7.8 ± 2.7	8.4 ± 2.3	0.55	0.5 ± 1.5	0.3 ± 2.0	0.19
	adjusted	7.7 ± 0.5	8.7 ± 0.7	0.27	0.7 ± 0.4	-0.6 ± 0.5	0.10
Lateral a'	**Unadjusted**	8.6 ± 2.8	7.3 ± 2.9	0.20	0.5 ± 1.5	0.3 ± 2.0	0.19
	adjusted	8.5 ± 0.7	7.6 ± 0.8	0.42	-0.2 ± 0.5	0.0 ± 0.6	0.78

Table 6-5 Group comparison for colour processed mitral annular TDI velocities following preload reduction

Colour processed TDI velocities (cm/s)	**baseline**				**Δ from baseline**		
		dialysis	venesection	P value	dialysis	venesection	P value
Septal s'	**Unadjusted**	5.3 ± 1.9	5.9 ± .9	0.61	0.4 ± 1.1	0.8 ± 1.1	0.34
	adjusted	5.4 ± 0.3	5.0 ± 0.4	0.50	0.5 ± 0.2	0.6 ± 0.3	0.81
Lateral s'	**Unadjusted**	5.3 ± 1.4	6.1 ± 1.1	0.23	0.6 ± 1.6	0.2 ± 1.2	0.35
	adjusted	5.1 ± 0.3	6.0 ± 0.4	0.06	↑0.9 ± 0.3	↓0.3 ± 0.4	0.01
Septal e'	**Unadjusted**	4.8 ± 2.1	5.9 ± 2.5	0.03	0.4 ± 1.8	0.5 ± 1.5	0.87
	adjusted	5.3 ± 0.3	5.8 ± 0.4	0.34	0.0 ± 0.3	↓1.2 ± 0.4	0.05
Lateral e'	**Unadjusted**	5.8 ± 2.1	6.9 ± 1.7	0.01	0.3 ± 2.0	0.9 ± 1.7	0.37
	adjusted	6.2 ± 0.4	7.5 ± 0.5	0.06	-0.1 ± 0.5	-1.2 ± 0.6	0.19

6.5.2.2 Basal radial colour processed TDI velocities

Table 6-6 shows the results following preload reduction in both groups. Only a subset (6/30) of patients in the dialysis group has stored loops of radial colour processed TDI for analysis. There was an increase in infero-lateral e' following dialysis but a decrease in e' in the same segment was noted in the blood donors.

6.5.2.3 Global longitudinal strain and strain rate

There was no difference in the baseline longitudinal global strain ($S_{systole}$) and strain rate ($SR_{systole}$) between the groups. Following preload reduction, $S_{systole}$ and $SR_{systole}$ were both unchanged showing preload resistance to moderate-large load change. Table 6-7 shows the results following preload change in two groups.

Table 6-6 Group comparison for radial colour processed TDI following preload reduction

Unit, cm/s			**Baseline**			**Δ from baseline**		
			dialysis	**venesection**	**P value**	**dialysis**	**venesection**	**P value**
LV Infero-lateral wall	s’	Unadjusted	3.9 ± 1.2	3.3 ± 1.1	0.28	0.3 ± 0.9	0.1 ± 1.1	0.69
		adjusted	4.4 ± 0.5	3.1 ± 0.3	0.04	0.5 ± 0.8	-0.4 ± 0.4	0.40
	e’	Unadjusted	4.0 ± 1.7	4.1 ± 1.1	0.95	↑1.1 ± 1.3	↓0.4 ± 1.5	0.05
		adjusted	4.4 ± 0.6	3.9 ± 0.4	0.60	-0.5 ± 1.1	0.2 ± 0.5	0.64
	a’	Unadjusted	3.1 ± 1.1	1.8 ± 1.2	0.07	0.9 ± 0.4	0.6 ± 0.8	0.46
		adjusted	3.3 ± 0.7	1.8 ± 0.3	0.05	1.4 ± 0.9	0.4 ± 0.3	0.36
LV septum	s’	Unadjusted	2.4 ± 0.3	3.1 ± 1.1	0.21	0.0 ± 0.2	0.3 ± 0.7	0.66
		adjusted	2.9 ± 0.4	3.0 ± 0.2	0.81	0.0 ± 0.8	0.3 ± 0.3	0.80
	e’	Unadjusted	2.9 ± 0.5	3.6 ± 1.1	0.24	0.8 ± 0.1	0.6 ± 0.9	0.70
		adjusted	3.0 ± 0.6	3.6 ± 0.3	0.35	0.0 ± 0.7	0.8 ± 0.3	0.36
	a’	Unadjusted	1.4 ± 0.5	2.0 ± 0.9	0.33	0.2	0.3 ± 0.7	0.93
		adjusted	1.3 ± 0.5	2.0 ± 0.3	0.30	n/a	n/a	n/a
		adjusted	4.4 ± 0.6	3.9 ± 0.4	0.60	-0.6 ± 0.8	0.1 ± 0.6	0.57

Table 6-7 Group comparison for longitudinal strain and strain rate following preload reduction

		baseline			**Δ from baseline**		
		dialysis	**venesection**	**P value**	**dialysis**	**venesection**	**P value**
$S_{systole}$ (%)	unadjusted	-14.3 ± 3.4	-15.1 ± 1.2	0.73	-0.2 ± 0.5	0.1 ± 0.8	0.75
	adjusted	-14.4 ± 0.6	-14.7 ± 0.8	0.77	0.0 ± 0.6	0.3 ± 0.8	0.81
SR $_{systole}$ (/second)	unadjusted	0.79 ± 0.24	0.8 ± 0.1	0.64	0.0 ± 0.0	0.0 ± 0.0	0.69
	adjusted	0.8 ± 0.0	0.8 ± 0.1	0.89	0.1 ± 0.0	0.0 ± 0.0	0.10

6.5.2.4 Left ventricular rotation and torsion

There was no difference in LV rotation and torsion between the groups at baseline. Following preload reduction, apical rotation showed load sensitivity both with 500ml and at 1.6 L load change. LV torsion was however only sensitive to a larger preload reduction. Table 6-8 shows the results of apical rotation, basal rotation and LV torsion following preload change. Compared to the blood donor group, the dialysis group had delayed apical rotation and untwisting as shown in Table 6-9. These indices were load insensitive following preload change. The main difference between the groups was a significantly larger increase in apical peak untwisting rate (UTR) seen in the blood donors.

Table 6-8 Group comparison for LV rotation and torsion following preload reduction

	Baseline			Δ from baseline		
	dialysis	venesection	P value	dialysis	venesection	P value
Apex Rotation (^{0})	7.7 ± 4.2	6.5 ± 2.2	0.35	1.7 ± 0.8	2.6 ± 1.2	0.53
	7.6 ± 0.7	7.1 ± 1.0	0.70	1.1 ± 0.9	3.7 ± 1.4	0.15
Basal Rotation (^{0})	6.0 ± 2.5	5.6 ± 2.8	0.82	0.3 ± 0.7	0.1 ± 0.8	0.67
	5.8 ± 0.6	5.7 ± 0.7	0.95	0.2 ± 0.8	0.1 ± 0.9	0.99
Torsion	2.3 ± 1.1	1.9 ± 0.6	0.37	0.6 ± 0.2	0.5 ± 0.3	0.78
	2.2 ± 0.2	2.0 ± 0.2	0.57	0.3 ± 0.2	0.8 ± 0.3	0.27

Table 6-9 Group comparison for apical rotation and untwisting timing following preload change

		Baseline comparison			Δ from baseline following preload reduction		
		dialysis	venesection	P value	dialysis	venesection	P value
Time to Peak Apex Rotation (% cycle length)	unadjusted	40 ± 10	28 ± 12	0.00	1.5 ± 2.0	4.7 ± 3.1	0.38
	adjusted	40 ± 2	28 ± 3	0.00	0.2 ± 2	5.1 ± 3.1	0.22
Early Untwist (% completed)	unadjusted	35 ± 12	25 ± 7	0.08	1.8 ± 3.3	1.1 ± 3.4	0.90
	adjusted	35 ± 5	28 ± 3	0.06	2.2 ± 3.5	0.1 ± 5.4	0.74
Untwisting Time (% cycle length)	unadjusted	45 ± 11	38 ± 9	0.04	0.9 ± 2.4	5.4 ± 4.0	0.32
	adjusted	45 ± 2	39 ± 3	0.08	0.1 ± 2.8	7.8 ± 4.3	0.17
Time to Peak UTR (% Untwisting Time)	unadjusted	33 ± 19	45 ± 23	0.01	1.4 ± 4.9	2.2 ± 7.9	0.69
	adjusted	31 ± 4	47 ± 6	0.03	1.7 ± 4.8	2.7 ± 7.4	0.92
Peak UTR (/seconds)	unadjusted	73 ± 30	60 ± 21	0.15	2.8 ± 7.1	19.0 ± 7.8	0.18
	adjusted	72 ± 5	62 ± 8	0.26	4 ± 7	30 ± 11	0.02

6.5.2.5 Mid left ventricular radial strain & circumferential strain

There was no difference in the response of both groups, following preload reduction. At baseline, the dialysis group had impaired circumferential strain but similar radial strain compared to the blood donors. Table 6-10 shows the results of group comparison following preload reduction. Circumferential strain was preload resistant when the load change was small (500ml) but was ultimately load sensitive given a large load change (1.6 L). Radial strain was unaffected across this range of preload reduction.

Table 6-10 Group comparison for radial and circumferential strain following preload reduction

		Baseline			**Δ from baseline**		
		dialysis	**venesection**	**P value**	**dialysis**	**venesection**	**P value**
S_{rad} (%)	unadjusted	34.2 ± 16.3	33.4 ± 14.9	0.69	0.8 ± 2.2	6.4 ± 6.9	0.22
	adjusted	34 ± 4	42 ± 5	0.19	1.9 ± 3.6	4.3 ± 5.4	0.72
S_{circ} (%)	unadjusted	17.9 ± 3.9	18.6 ± 3.8	0.03	0.7 ± 0.3	0.3 ± 1.4	0.80
	adjusted	18.0 ± 0.1	21.0 ± 1.0	0.02	0.6 ± 0.7	0.5 ± 1.0	0.96

6.6 Differences in response to preload reduction in both groups

At baseline, the dialysis subjects were different from the blood donors. Although both groups had similar left ventricular dimensions (LVEDVI 44 ± 11 cm/m^2 and 46 ± 9 cm/m^2, p=0.51), the dialysis group had left ventricular hypertrophy (LVMI 114 ± 45 g/$m^2$and 69 ± 2 g/m^2, p<0.001). They also had abnormal diastolic filling (E/A 1.0 ± 0.3 and 1.4 ± 0.4, p<0.001), high filling pressure (E/e' 12 ± 7 and 7 ± 1, p<0.01) and dilated left atrium (LAVI 38 ± 17 ml/m^2 and 20 ± 6 ml.m^2, p<0.001). In addition, the dialysis group had preserved EF (60 ± 5 %) but they had lower TDI longitudinal velocities compared to the blood donors, although this difference became insignificant when adjusted for age as a confounder. Pulsed-wave TDI septal s' 7.2 ± 1.7 cm/s and 8.8 ± 1.6 cm/s, p=0.02. Pulsed-wave TDI septal e' 6.7 ± 2.3 cm/s and 9.42.9 cm/s, p<0.01. Pulsed-wave TDI lateral e' 8.9 ± 2.8 cm/s and 11.1 ± 2.4 cm/s, p=0.01. Processed colour TDI septal e' 4.8 ± 2.1 and 5.9 ± 2.5 cm/s, p-0.03. Processed colour TDI lateral e' 5.8 ± 2.1 cm/s and 6.9 ± 1.7 cm/s, p=0.02. Mid LV circumferential strain were lower in the dialysis group (17.9 ± 3.9, 18.6 ± 3.8, p=0.03) although mid LV radial strain, $S_{systole}$, apical rotation and LV torsion were similar in both groups.

Preload reduction had a differential effect on the various cardiac indices. Some indices are load sensitive after a moderate load change (500ml): E, A, E/e', processed colour TDI septal longitudinal s', processed colour TDI infero-lateral radial a' and apex rotation. Some indices were resistant to a moderate (500ml) load change but became load sensitive at a larger load change (1.6 L): E/A,

estimated LAP, pulsed-wave TDI lateral annular s', mid LV circumferential strain. Some indices are load insensitive: EF, MAPSE, pulsed-wave TDI septal longitudinal s', pulsed-wave TDI septal and lateral longitudinal e', global longitudinal 2-dimensional strain ($S_{systole}$) and systolic strain rate ($SR_{systole}$), and mid LV radial strain.

The main differences between the two groups in the response following preload reduction were:

1. Pulsed-wave septal s' increased in the dialysis group but decreased in the blood donors.
2. Colour processed lateral s' increased in the dialysis group but decreased in the blood donors.
3. Pulsed-wave septal e' was unchanged in the dialysis group but decreased in the blood donors.
4. Colour processed radial e' in the infero-lateral wall, increased in the dialysis group but decreased in the blood donors.
5. The blood donors showed a much larger increase in apical peak untwisting rate (UTR) compared to the dialysis group.

7 Results discussion and conclusion

7.1 Effect of changing preload on cardiac function

I have studied the effects of preload reduction in two groups of well-characterised subjects. Healthy blood donors underwent a moderate (480ml), and breathless dialysis patients underwent a large (1.6 ± 1.3 L) preload reduction. I aimed to draw a conclusion on the effect of differential preload reduction on many indices of cardiac function. In this section, I shall summarise (section 7.1.1) and compare (section 7.1.2) my findings to those reported by previous studies. I will discuss the limitations (section 7.2) of this current study and outline (section 7.3) findings that require confirmation and possible options for future studies.

7.1.1 Summary of results from my studies

To reiterate, amongst a group of asymptomatic healthy blood donors, a moderate (approximately 480ml) but rapid (over 10 minutes) reduction of preload resulted in a significant drop in cardiac chamber dimensions and volumes (LVIDd by 14%, LVIDs by 17%, LVEDV by 7%, LAV by 15%) and significant reduction in diastolic filling velocities (E by 13% and A by 3%). Though Diastolic filling ratio (E/A), E/e' and estimated LAP (130) remained unchanged, 2DSTE apical peak UTR increased by 32% suggesting its preload sensitivity. Subsequently stroke volume (biplane method), cardiac output, blood pressure, and heart rate remained unchanged. Although there was no apparent difference in 2DSTE peak systolic strain (longitudinal, radial, circumferential) and LVEF, a significant increase was noted in left ventricular apex

rotation (LV rotation increased by 40%), and colour processed TDI velocities (longitudinal septal s' increased by 8%, radial infero-lateral a' increased by 30%).

In contrast to the healthy blood donors who experienced relatively rapid change of preload, the dialysis group underwent a moderate rate of preload change (mean of 1.6 L) over a median duration of 4 hours. Preload reduction resulted in a significant decrease of diastolic filling velocities (E by 15%, A by 8%, and E/A by 14%), cardiac chamber dimensions (LVIDd by 14%, LVIDs by 13%) and volumes (LAA by 12%, LAV by 20%, LVEDV by 12%) to a similar extent that was seen in the blood donors. Diastolic filling profile (E/A and DT) was altered, from a pseudo-normalised (grade II diastolic dysfunction) pattern to a mildly impaired pattern (grade I diastolic dysfunction). This was evident in the observation of an unchanged IVRT, but reduced DT (16%) and E/A (14%) ratio. E/e' and estimated LAP (130) dropped by 15% but LV SV, CO, and BP were unchanged. An increase was apparent in some regional indices of systolic function suggesting their preload sensitivity: longitudinal tissue velocities (lateral s' increased by 11%), circumferential strain (S_{circ} increased by 4%), and apical rotation (apical Rot increased by 37%). Some regional indices (2DSTE longitudinal strain & strain rate, radial strain, basal rotation) were load insensitive despite this large preload reduction. This heterogeneity in regional response may be due to the shape change of the left ventricle following preload reduction. LV length remained unchanged whilst LV internal dimension reduced. Studies (141,142) have reported a gradient in LV layer-specific strain: there is a gradual decrease of longitudinal strain and circumferential strain values from endocardium to sub epicardium in health that is preserved with aging. As LV length was unaffected following preload reduction, Longitudinal strain remained constant

whilst circumferential strain increased in response to a reduction in wall stress (unchanged LVMI) and internal dimension.

Despite correcting the baseline difference in heart rate and amount of preload reduction using a statistical method (ANCOVA), notable differences in their response to preload reduction were apparent in the two groups. Firstly, preload reduction did not change longitudinal a' in both groups; but LAV decreased significantly more in the dialysis subjects compared to the blood donors. This may suggest LA reservoir and conduit function track preload reduction (preload dependent) but pump function (a') is unaffected. Secondly, both septal and lateral longitudinal s' increased in dialysis subjects but decreased in the blood donors. This difference, at first glance seemed contrary to the finding of E_{es}, which was significantly higher in the blood donors compared to the dialysis group. This might be explained by the Frank-Starling curve. The blood donors were euvolaemic and therefore their cardiac mechanics were operating at the linear part of the Frank Starling relationship. Hence a reduction in LVEDV expectedly produced a reduction in s'. In contrast, the dialysis group operated at the descending part of the Frank Starling curve, where further increase in LVEDV would cause a fall in contractile function. Reduced LVEDV following dialysis therefore moved the cardiac mechanics onto the plateau of the Frank-Starling curve, hence an increase in s' by comparison. Third and finally, preload reduction (at constant heart rate and blood pressure) increased apical peak UTR in the blood donors but remained unchanged in the dialysis subjects. This may indicate the donors' ability to increase diastolic untwisting and subsequent filling to maintain cardiac output through a largely

compliant LV. This response is diminished in the 'stiff hearts' of the HFpEF dialysis subjects.

From earlier discussion in Chapter one (section 1.2.2, page 5), we know that ESPVR/E_{es}, a marker of cardiac contractile state is unaffected within a physiological range of load change (13,31–33,73). As expected, both IVA and non-invasively estimated E_{es} (66,67,71) were unchanged in both subject groups following preload reduction. These markers are correlates of inotropic status which is unaffected by load (13,57,79,89,92). Therefore, any observed changes in regional and global echocardiographic indices greater than the variability of measurements reflect their preload sensitivity, at a constant contractile state.

7.1.2 Comparison with previous studies

A small change in an index with high measurement variability (35,36,143) such as MAPSE (18% inter- and 17% intra-observer variability) and 2DSTE radial strain (15% and 16% intra- and inter-observer variability) may not be apparent in this relative small sample. Similarly, an index with excellent measurement reproducibility may show a small change but it is of uncertain clinical relevance.

The coefficients of variation in my study for blood pool and TDI velocities were 4% and 7% respectively (Table 5, Chapter 2), comparable to reported intra-observer measurement variability by other studies (29,30,109,116). There was a significant drop in early diastolic filling velocity E, following dialysis and venesection. Estimated left ventricular filling pressure (130) dropped by 15% following dialysis and remained unchanged following venesection. These findings

were similar to earlier studies (105,107,112–114), though they did not report on intra- and inter-observer variability in their studies.

In the dialysis subjects, diastolic filling profile was altered following preload reduction. This changed from a pseudo-normalised (grade II diastolic dysfunction) pattern of E/A and DT towards mildly impaired relaxation pattern (grade I diastolic dysfunction). This was evident in the observation of an unchanged IVRT, but reduced DT (16%) and E/A (14%) ratio. The reverse is true, in a group of patients with abnormal diastolic function (144), defined as DT >240ms and E/A<1, following rapid infusion of 500-700ml normal saline. Preload expansion resulted in worsening of filling pattern from grade I to grade II diastolic dysfunction. Therefore, interpretation of transmitral filling pattern in clinical practice requires consideration of the loading status.

Septal s', e', a' and lateral e', a' remained preload resistant following dialysis and venesection. Lateral s' was preload resistant to a small change (480ml venesection) but it became preload sensitive and increased by 11% following dialysis. There could be several explanations for this discrepant observation of preload sensitivity in s', e' and a'. Firstly, the relative (1-18% for s', 2-15% for e', 2-6% for a',) and absolute (< 1cm/s for s', e' and a') change in these measurements, following venesection and dialysis were small. The relatively small sample size (30 in dialysis group and 15 in blood donor group) in my study made it prone to a type II error in accepting the null hypothesis. Secondly, the differential preload sensitivity of septal and lateral s' following dialysis could be explained by a higher burden of fibrosis in the septum compared to the lateral wall, as found in a previous study

(145). This study used cardiac MRI and late gadolinium enhancement (LGE) for detection of cardiac fibrosis in patients with hypertrophic cardiomyopathy. They found significantly more LGE in the septum compared to lateral wall in their subjects. Therefore, the lateral wall may be more responsive to a preload reduction compared to the septal wall, as marked by the increased in lateral s' but unchanged septal s'.

Vignon et al (109) studied the effect of differential load change following dialysis on cardiac function in two groups of subjects. The first group had acute renal failure and required urgent dialysis. These patients were intubated and received vasopressor (adrenaline or noradrenaline). The rate of filtration was adjusted and boluses of fluid were given to maintain adequate blood pressure during filtration. The second group of their subjects were stable patients on established maintenance dialysis. Echocardiography was performed before and at least one hour after dialysis. The critically ill patients underwent transoesophageal echocardiography (TOE) and had 1.9 L preload reduction whilst the stable patients underwent transthoracic echocardiography (TTE) and had 3 L preload reduction. They reported excellent intra- and inter- observer variability: 2% and 1% for E, 2% and 5% for e' respectively. Following a 1.9L preload reduction; there was no change in E, septal and lateral e' and the filling ratio E/e. A 3 L preload reduction significantly reduced E (24%), septal e' (17%) and E/e' but lateral e' remained unchanged. Their results, at first glance, seemed to be contradictory to my results. Firstly, E dropped significantly in my study following a moderate 480ml preload reduction, which was only apparent in their study with a much larger preload reduction of 3 L. Secondly, I showed an E/e' fall with 1.6 ± 1.3 L preload reduction.

This was not significant in their study after 1.9 L preload reduction. The differences in our two studies must be in part, attributable to the confounding effects of intra-dialytic inotropes and fluid administration (which they used) on cardiac function. In addition, I completed echocardiography within 30 minutes of preload reduction, whilst they completed their studies more than one hour afterwards. Therefore, they could have missed an opportunity to detect a small change in these indices immediately after preload reduction. Lastly, I used TTE and they used TOE echocardiography, in their critically ill patient group. Image alignment during TOE is notoriously difficult and this would have an impact on the absolute values obtained for Doppler and TDI velocities, which are of course angle-dependent.

Galetta et al (116) studied the effect of dialysis on cardiac function in a group of asymptomatic patients on established dialysis. The mean age of their patients were 51 ± 13 years and the mean preload reduction was 3 L. They performed repeat echocardiography within 30 minutes of the completion of dialysis. Their reported intra- and inter-observer variability (6% and 11% respectively) was much higher and perhaps more in keeping in daily clinical practice. Following dialysis, there were no significant changes in global EF, E (dropped by 0.1%), A (dropped by 2%) although LVIDd dropped by 10%. However, they reported a significant reduction in lateral and septal s' (25% and 22%), and lateral and septal e' (31% and 24%). Both our studies reported a similar reduction in preload as shown in similar reduction in LV dimension (drop of 10% and 14%) respectively. However, whilst I reported significant drop of 15% and 8% in E and A velocities, consistent with other observations (111–114) , it seemed peculiar that they did not detect a difference. This may be due to the relatively high variability of their measurements. In

addition, there was a significant rise in heart rate (increased by 8%, or 6 bpm) and a significant drop in systolic blood pressure (fell by 10% or 14 mmHg) in their study. Heart rate and blood pressure were unchanged in my study. Therefore, the interpretation of their reported significant drop in TDI s' and e' velocities, must take into account the effects of heart rate and afterload.

Patients with a previous history of myocardial infarction had significantly (37%) lower 2DSTE global longitudinal strain compared to healthy subjects (146). This large effect size is unlikely to be attributable to measurement variability although the authors did not report on this. Reported (30,36,120,147) measurement variability ranges are 2-11% for intra-observer and 3-13% for inter-observer respectively. The intra-observer variability of strain measurement in my study was 7% (Table 5, Chapter 2). My study did not show a difference in global longitudinal $S_{systole}$ following dialysis and venesection. This is in contrast to the results shown by Choi et al (118) in dialysis patients. They showed a small (5%) but significant decrease in longitudinal strain, $S_{systole}$ following dialysis. However, the reported intra-observer (ICC 0.96) and inter-observer (ICC 0.86) variability of their measurements suggest that this change could be a false positive (type I error). In addition, their subjects had an average $S_{systole}$ of -18%, in keeping with reported values amongst asymptomatic hypertensive subjects (148). My dialysis subjects, on the contrary, had values of $S_{systole}$ (-14%) consistent with $S_{systole}$ values reported in characterised patients with HFpEF (149). In addition, the difference in their results is confounded by a compensatory sympathetic response, evident in their subjects following dialysis. A significant increase in heart rate and decrease in blood pressure were present in their study but was absent in my study.

Chapter 7.

Reported (36,120) intra-observer variability and inter-observer variability are 3-6% and 5-10% for circumferential strain. In my studies, circumferential strain remained unchanged following venesection but showed a small (4%) significant increase following dialysis. This change is within the measurement variability (7% page 52) and therefore may not represent differential preload sensitivity of the index. In addition, reported (36,120) intra-observer variability and inter-observer variability for radial strain are relatively high: 6-15% and 8-16% respectively. There was no change in radial strain following preload reduction in my studies. It is possible that a small change went undetected, due to the small sample size in my study (page 45 Table 3, power calculation yielded >80% power of detecting of >30% change). Further studies with better measurement reproducibility are therefore required to conclude the effect of preload reduction on S_{circ} and S_{rad}.

Reported (36,143,150) intra-observer variability and inter-observer variability for apical rotation and LV torsion are 8-9% and 1-10% respectively. Apical rotation increased by 37% and 40% following dialysis and venesection, well above the reported measurement variability. This magnitude of change is likely a real difference and implies this index's preload sensitivity within a physiological range.

In summary, the present studies showed that:

1. A modest preload reduction (480 ml) in healthy subjects did not change estimated LAP (130), but reduced diastolic blood flow velocities (3-13%) and cardiac internal dimension (12-14%).
2. A large preload reduction (1.6 L) in dialysis patients with symptoms of HFpEF reduced estimated LAP (130), diastolic blood flow velocities (15 %) and

cardiac internal dimension (13-21%). Although there was significant reduction in estimated LAP using E/e', the performance of E/e' as a diagnostic test for detection of elevated filling pressure is poor (40).

3. Pulsed-wave TDI indices: septal and lateral e' and a', septal s' are resistant to modest and large preload reduction. Lateral s' is preload resistant at moderate preload reduction but becomes preload sensitive at large preload reduction (12% change).
4. Radial TDI a' velocities are more sensitive to preload reduction compared to longitudinal TDI a' velocities. Coloured processed radial a' increased by 29-30% whilst longitudinal a' remained unchanged.
5. 2DSTE indices of longitudinal strain & radial strain are load resistant at moderate and large preload reduction. Circumferential strain is load insensitive at moderate preload reduction but is sensitive (4% change) to large preload reduction. Due to its high measurement variability, further studies with improved measurement reproducibility are needed to conclude the effect of preload reduction on these markers (S_{circ} and S_{rad}).
6. 2DSTE apical rotation is preload sensitive (37-40 % increase) with moderate and large preload reduction.
7. Non-invasive estimation of E_{es} is feasible in clinical practice and this measurement is preload resistant.
8. IVA is preload resistant at moderate and large preload reduction.

In addition, cardiac response following preload reduction are different in the dialysis group and blood donors. Longitudinal TDI s' increased from baseline in

the dialysis group but decreased in the blood donors, suggesting the two groups were operating at two different parts of the Frank-Starling curve. The blood donors have a compliant LV and increased their peak apical UTR after preload reduction. Both groups have unchanged radial TDI a' but a reduced LAV following preload reduction. This suggests atrial pump function is resistant to preload change whilst reservoir and conduit function are sensitive to preload change.

7.2 Limitations of the study

7.2.1 Sample size, effect size and measurements reproducibility

Bearing in mind the sample size and power calculation (page 43-45 Chapter 2), the current studies has >80% power in detecting a >30% difference in measurements following preload reduction. Although all blood donors had adequate images for analysis of all indices, not all dialysis subjects had images of sufficient quality for analysis. A small to medium size difference in an index with high measurement variability may not become apparent in this small sample. Similarly, an index with good measurement reproducibility may show a small change but is of uncertain clinical relevance.

7.2.2 Cardiovascular medications

Another limitation in the dialysis study is the existing usage of cardiovascular medication. To reiterate the findings (Table 6, page 76, Chapter 3), 23% of dialysis subjects were on a beta-blocker, 23% were on a diuretic, 16% were on an

angiotensin receptor blocker, and 1% were on a calcium channel blocker. Therefore, the interpretation of these results must take into account the effect of these medications on indices of cardiac function following preload reduction. As my sample size is small, it cannot support subgroup analysis to delineate the impact these medications may have on indices of cardiac function. Hence, in the following paragraphs I will discuss briefly results of other studies.

Tohmo et al (151) studied the effect of intravenous enalaprilat on cardiac function, with preload manipulation, in patients presenting with acute heart failure following myocardial infarction. Pulmonary artery wedge pressure and arterial blood pressure fell significantly, but cardiac index and stroke volume index did not change.

Nemoto et al (152) used a experimental canine model and mitral regurgitation to investigate the effects of an angiotensin-converting enzyme inhibitor and beta-blocker on cardiac function. Significant mitral regurgitation was defined as a regurgitant fraction of > 50%. After 3 months of continuous exposure to mitral regurgitation, LV end-diastolic pressure rose significantly indicating increasing preload. The animals then received Lisinopril for 3 months followed by a combination of Lisinopril and atenolol for another 3 months. They found that either Lisinopril alone or the combination therapy did not significantly reduce LVEDP. However, E_{es} improved significantly following Lisinopril therapy and returned to almost normal values following combination therapy with a beta-blocker.

Chapter 7.

Another study used a porcine model (153) and found the use of a carvedilol-enriched cold oxygenated-blood during cardiac bypass and cardioplegia did not result in a change in ESPVR, 2DSTE radial, longitudinal and circumferential strain following preload reduction. However, indices such as Tau, maximum -dp/dt, maximum +dp/dt were significantly reduced following preload reduction.

To summarise, intravenous infusion of an angiotensin-enzyme inhibitor lowered LV filling pressure significantly following preload reduction but this did not change indices of cardiac function (151). Medium term use of an angiotensin-enzyme inhibitor led to preload reduction and improved E_{es} (152). Beta-blocker did not alter the preload sensitivity of many indices (ESPVR, 2DSTE $S_{systole}$, S_{circ} and S_{rad}) of cardiac function. This knowledge aids relevant clinical interpretation of echocardiographic indices, and may be applicable in scenarios such as chronic mitral regurgitation and aortic regurgitation.

7.2.3 Gender difference in response to preload reduction

I did not recruit an equal ratio of female and male participants in my study (68% men in the dialysis group, 80% women in the blood donor groups). Although it was not my objective to evaluate the gender difference in cardiac response following preload reduction, I shall discuss briefly the gender difference, firstly in cardiac structure, followed by their cardiac response following preload reduction in this section.

Women have lower cardiac mass (154,155), smaller cardiac dimension (154,155) and higher baseline heart rate (154,156) compared to men, though there is no difference in indexed cardiac output (157) . In addition, young women (<45

years) have lower sympathetic activity (MSNA) and central arterial stiffness (carotid artery intima thickness to internal lumen ratio) (158).

Following progressive lower body negative pressure, females have a greater HR increase (157,159), SV reduction (157), apical rotation and UTR augmentation (154) compared to males; despite a similar increase in systemic vascular resistance and serum norepinephrine level (157). Following head up tilt, young females exhibits a larger HR increase despite similar SV reduction and increase in BP, total peripheral resistance and MSNA in comparison with males (160). These observations suggest females have a more pronounced cardiac mechanics response following preload alteration, mediated through the baroreceptor (heart rate) reflex.

7.2.4 Influence of the autonomic system

Previous studies (157,159,160) showed preload and SV reduction resulted in an increase in HR and sympathetic activity (MSNA and norepinephrine). Whilst one study showed (154) augmented apical rotation and UTR, with increased HR following preload reduction; their findings were not reproduced following blood extraction when heart rate was unchanged (161). These studies confirmed the autonomic nervous system plays a role in cardiac response following load reduction. The current study is limited in this regard, as I did not examine the level of MSNA/epinephrine following preload reduction.

7.2.5 Mode of dialysis, dialysate composition, haematocrit and their effects on cardiac function

I studied only stable patients on established dialysis (median duration 26 months). A previous study showed that the correction of uraemia without loss of volume improves LV contractile state, whilst ultrafiltration (volume loss) has the effect expected according to the Frank-Starling relationship (162). In addition, a high dialysate concentration of calcium, potassium and bicarbonate is associated with worsened global longitudinal strain and cardiac index following dialysis (163,164). Blood donation (165,166) produces an average 9% haematocrit reduction and SV reduction but does not alter heart rate and maximal oxygen uptake during exercise.

The current study cannot separate the effect of correcting uraemia from that of pure preload reduction in the dialysis group. Similarly, I cannot separate the effect of haematocrit reduction from that of preload reduction in the blood donors. The current study therefore cannot exclude this confounding effect when comparing cardiac response in the two groups following preload reduction.

In summary, the small sample size, use of cardiovascular medications in some participants, unequal gender ratio in recruitment, limit the applicability of my results to a wider population. I cannot separate the effects of preload reduction from that of haematocrit reduction, uraemia correction, and electrolytes redistribution on cardiac function. In addition, I cannot isolate the effect of the autonomic nervous system on cardiac response following preload reduction, as I did not study this specifically.

7.3 Study results and implication in clinical practice

The results from my study are relevant to clinical practice. Firstly, the findings support that the proposed European criteria (38) for identification of diastolic dysfunction are robust and unaffected by a physiological reduction of preload (1.6 L during dialysis). The European Society of Cardiology proposed a finding of LAVI >34 ml/m^2 or LVMI >115 g/m^2 for men and LVMI >95 g/m^2 for women, E/e' >13, averaged septal and lateral e' < 9 cm/s (167–172) for detection of diastolic dysfunction amongst patients with symptoms of heart failure and preserved EF. Applying the above echocardiographic criteria, all of my study subjects in the dialysis group have LVMI (mean LVMI 120 ± 46 g/m^2 for men and 118 ± 44 g/m^2 for women) and LAVI (mean LAVI 43 ± 19 ml/m^2) above this threshold and the results were unaffected by preload reduction. The mean E/e' was 12 ± 7 and dropped significantly to 10 ± 4 following dialysis. Mean e' did not change following dialysis and remained < 9 cm/s.

Secondly, my results confirmed previous findings (94,101–103,107,110,116) that some indices of systolic function are sensitive to changes in preload. Apical rotation derived from 2DSTE is sensitive to a moderate preload reduction of 500 ml. 2DSTE derived circumferential strain (mid LV S_{circ}) and pulsed-wave TDI lateral s' are unaffected following a 500ml preload reduction. Pulsed-wave TDI septal and lateral e', septal s' and 2DSTE derived longitudinal strain ($S_{systole}$) and radial strain (mid LV S_{rad}) are preload insensitive following a 1.6 L preload reduction. This knowledge is applicable to clinical practice. Many indices of cardiac function such as TDI

velocities (173) either in isolation or in combination (174) with 2DSTE (E/SR_E), and $S_{systole}$ (175) are independent predictors of median term mortality and adverse outcome in a general population. Additional prognostic information is also offered by knowledge of $S_{systole}$ in diseased population including patients with hypertrophic cardiomyopathy (176,177), aortic stenosis (178–180), mitral regurgitation (179,181), chronic kidney disease (182,183) and diabetes mellitus (184). Therefore, the knowledge of either their preload insensitivity or dependency is crucial in the long-term disease surveillance and therapeutic response monitoring.

Finally, I showed that non-invasive estimation of E_{es} and colour processed TDI derived IVA are resistant to a reduction of LV diastolic volume caused by a reduction of 1.6 L in circulating volume. However, IVA has large measurement variability (117) and it did not distinguish the two clinical groups in this study. Nonetheless, the results may have been useful in differentiating the two groups if the sample size was larger. Estimated E_{es} using the Chen method (71), compared to other methods (66,67) produced the most clinically consistent results. However, the many calculations involved make this method prone to error, which limit its wider clinical application. Nonetheless, non-invasive E_{es} estimation, and its insensitivity to preload change, have a role in patient selection for complex high-risk cardiac surgery, and it can aid fluid resuscitation in patients undergoing laparotomy (185–188).

7.4 Options for further work

Non-invasively estimated E_{es} and colour-processed and TDI-derived IVA, are preload insensitive across a physiological range in my study. Routine clinical use is currently limited due to the complexity (E_{es}) and poorly reproducible (IVA) methods (71,117). Recently, the longitudinal TDI velocity profile throughout the cardiac cycle was successfully used in an unsupervised multiple kernel learning method (189) to better characterise patients with HFpEF compared to healthy controls. Machine learning (ML) (190,191) accurately classified subject groups comparable to current clinical diagnostic criteria (38); either by using TDI velocity graph(191) or 2DSTE longitudinal strain graph (190). IVA is derived from a TDI velocity graph, whilst non-invasive estimation of E_{es} requires polynomial estimation of normalised elastance from the LVOT Doppler velocity trace. Hence, it would seem feasible that ML can eradicate observer's error for these indices and may overcome current limitation for its clinical use. This may be the subject of future studies.

Whilst my study showed E/e' dropped following preload reduction, other studies have shown E/e' increased during exercise (33,192–194) in patients with HFpEF(33,169–171). These results are expectedly consistent. Recently, two Japanese studies (195,196) showed that following lower body positive pressure (preload increase) , a disproportionate rise in E/e' when corrected to SV increment, is associated with higher rate of adverse cardiac events amongst symptomatic patients awaiting aortic stenosis surgery and in patients with HFrEF. If this finding is confirmed on subsequent studies, the change of E/e' following preload increase, may have a place in clinical prioritisation of patients awaiting surgical intervention.

Following preload reduction, my study showed a significant reduction in LAVI whilst longitudinal TDI a' remained constant. Although LA dilatation is associated with increased LV mass (197,198), diastolic dysfunction (197), extra cellular volume/fibrosis (ECV) (198) and increased all-cause mortality (199); LAVI is preload dependent that can impact on the diagnostic sensitivity of the current proposed criteria for HFpEF (38). A low TDI a' amongst HFpEF patients was associated with reduced cardiac event-free survival (200). Therefore, it would be reasonable to propose that a' (not LAVI) is used in the diagnostic algorithm for HFpEF; provided this finding can be confirmed in further studies.

8 References

1. Mosterd A, Hoes AW. Clinical epidemiology of heart failure. Heart. 2007 Sep;93(9):1137–46. doi: 10.1136/hrt.2003.025270

2. Owan TE, Hodge DO, Herges RM, Jacobsen SJ, Roger VL, Redfield MM. Trends in prevalence and outcome of heart failure with preserved ejection fraction. N Engl J Med. 2006 Jul 20;355(3):251–9. doi: 10.1056/NEJMoa052256

3. Curtis LH, Whellan DJ, Hammill BG, Hernandez AF, Anstrom KJ, Shea AM, et al. Incidence and prevalence of heart failure in elderly persons, 1994-2003. Arch Intern Med. 2008 Feb 25;168(4):418–24. doi: 10.1001/archinternmed.2007.80

4. Redfield MM, Borlaug BA. Sildenafil and exercise capacity in heart failure--in reply. JAMA. 2013 Jul 24;310(4):432–3. doi: 10.1001/jama.2013.7440

5. Krumholz HM, Merrill AR, Schone EM, Schreiner GC, Chen J, Bradley EH, et al. Patterns of hospital performance in acute myocardial infarction and heart failure 30-day mortality and readmission. Circ Cardiovasc Qual Outcomes. 2009 Sep;2(5):407–13. doi: 10.1161/CIRCOUTCOMES.109.883256

6. Stewart S, Horowitz JD. Home-based intervention in congestive heart failure: long-term implications on readmission and survival. Circulation. 2002 Jun 18;105(24):2861–6.

7. Dougherty AH, Naccarelli GV, Gray EL, Hicks CH, Goldstein RA. Congestive heart failure with normal systolic function. Am J Cardiol. 1984 Oct 1;54(7):778–82.

8. McAlister FA, Teo KK, Taher M, Montague TJ, Humen D, Cheung L, et al. Insights into the contemporary epidemiology and outpatient management of congestive heart failure. Am Heart J. 1999 Jul;138(1 Pt 1):87–94.

9. Owan TE, Redfield MM. Epidemiology of diastolic heart failure. Prog Cardiovasc Dis. 2005 Mar;47(5):320–32.

10. Chinali M, Joffe SW, Aurigemma GP, Makam R, Meyer TE, Goldberg RJ. Risk factors and comorbidities in a community-wide sample of patients hospitalized with acute systolic or diastolic heart failure: the Worcester Heart Failure Study. Coron Artery Dis. May;21(3):137–43. doi: 10.1097/MCA.0b013e328334eb46

11. Tribouilloy C, Rusinaru D, Mahjoub H, Souliere V, Levy F, Peltier M, et al. Prognosis of heart failure with preserved ejection fraction: a 5 year prospective population-based study. Eur Heart J. 2008 Feb;29(3):339–47. doi: 10.1093/eurheartj/ehm554

12. Nussbacher A, Gerstenblith G, O'Connor FC, Becker LC, Kass DA, Schulman SP, et al. Hemodynamic effects of unloading the old heart. Am J Physiol. 1999 Nov;277(5 Pt 2):H1863-71.

13. Penicka M, Bartunek J, Trakalova H, Hrabakova H, Maruskova M, Karasek J, et al. Heart failure with preserved ejection fraction in outpatients with unexplained dyspnea: a pressure-volume loop analysis. J Am Coll Cardiol. 2010 Apr 20;55(16):1701–10. doi: 10.1016/j.jacc.2009.11.076

14. Bursi F, Weston SA, Redfield MM, Jacobsen SJ, Pakhomov S, Nkomo VT, et al. Systolic and diastolic heart failure in the community. JAMA. 2006 Nov 8;296(18):2209–16. doi: 10.1001/jama.296.18.2209

15. Bhatia RS, Tu JV, Lee DS, Austin PC, Fang J, Haouzi A, et al. Outcome of heart failure with preserved ejection fraction in a population-based study. N Engl J Med. 2006 Jul 20;355(3):260–9. doi: 10.1056/NEJMoa051530

16. Uchino K, Ishigami T, Ohshige K, Sugano T, Ishikawa T, Kimura K, et al. Left ventricular geometry, risk factors, and outcomes of hospitalized patients with diastolic heart failure in Japan. J Cardiol. 2009 Aug;54(1):101–7. doi: 10.1016/j.jjcc.2009.04.015

17. Klapholz M, Maurer M, Lowe AM, Messineo F, Meisner JS, Mitchell J, et al. Hospitalization for heart failure in the presence of a normal left ventricular ejection fraction: results of the New York Heart Failure Registry. J Am Coll Cardiol. 2004 Apr 21;43(8):1432–8. doi: 10.1016/j.jacc.2003.11.040

18. Adabag S, Smith LG, Anand IS, Berger AK, Luepker RV. Sudden cardiac death in heart failure patients with preserved ejection fraction. J Card Fail. 2012 Oct;18(10):749–54. doi: 10.1016/j.cardfail.2012.08.357

19. Perez de Isla L, Canadas V, Contreras L, Almeria C, Rodrigo JL, Aubele AL, et al. Diastolic heart failure in the elderly: in-hospital and long-term outcome after the first episode. Int J Cardiol. 2009 May 15;134(2):265–70. doi: 10.1016/j.ijcard.2007.12.059

20. Lewis BS, Shotan A, Gottlieb S, Behar S, Halon DA, Boyko V, et al. Late mortality and determinants in patients with heart failure and preserved systolic left ventricular function: the Israel Nationwide Heart Failure Survey. Isr Med Assoc J. 2007 Apr;9(4):234–8.

21. Tsuchihashi-Makaya M, Hamaguchi S, Kinugawa S, Yokota T, Goto D, Yokoshiki H, et al. Characteristics and outcomes of hospitalized patients with heart failure and reduced vs preserved ejection fraction. Report from the Japanese Cardiac Registry of Heart Failure in Cardiology (JCARE-CARD). Circ J. 2009 Oct;73(10):1893–900.

22. Cleland JG, Tendera M, Adamus J, Freemantle N, Polonski L, Taylor J. The perindopril in elderly people with chronic heart failure (PEP-CHF) study. Eur Heart J. 2006 Oct;27(19):2338–45. doi: 10.1093/eurheartj/ehl250

23. Massie BM, Carson PE, McMurray JJ, Komajda M, McKelvie R, Zile MR, et al. Irbesartan in patients with heart failure and preserved ejection fraction. N Engl J Med. 2008 Dec 4;359(23):2456–67. doi: 10.1056/NEJMoa0805450

24. Ahmed A, Rich MW, Fleg JL, Zile MR, Young JB, Kitzman DW, et al. Effects of digoxin on morbidity and mortality in diastolic heart failure: the ancillary digitalis investigation group trial. Circulation. 2006 Aug 1;114(5):397–403. doi: 10.1161/CIRCULATIONAHA.106.628347

25. Yusuf S, Pfeffer MA, Swedberg K, Granger CB, Held P, McMurray JJ, et al. Effects of candesartan in patients with chronic heart failure and preserved left-ventricular ejection fraction: the CHARM-Preserved Trial. Lancet. 2003 Sep 6;362(9386):777–81. doi: 10.1016/S0140-6736(03)14285-7

26. Rickenbacher P, Pfisterer M, Burkard T, Kiowski W, Follath F, Burckhardt D, et al. Why and how do elderly patients with heart failure die? Insights from the TIME-CHF study. Eur J Heart Fail. 2012 Nov;14(11):1218–29. doi: 10.1093/eurjhf/hfs113

27. Zile MR, Gaasch WH, Carroll JD, Feldman MD, Aurigemma GP, Schaer GL, et al. Heart failure with a normal ejection fraction: is measurement of diastolic function necessary to make the diagnosis of diastolic heart failure? Circulation. 2001 Aug 14;104(7):779–82.

28. Zile MR, Baicu CF, Gaasch WH. Diastolic heart failure--abnormalities in active relaxation and passive stiffness of the left ventricle. N Engl J Med. 2004 May 6;350(19):1953–9. doi: 10.1056/NEJMoa032566

29. Yu C-M, Lin H, Yang H, Kong S-L, Zhang Q, Lee SW-L. Progression of systolic abnormalities in patients with 'isolated' diastolic heart failure and diastolic dysfunction. Circulation. 2002 Mar 12;105(10):1195–201.

30. Carluccio E, Biagioli P, Alunni G, Murrone A, Leonelli V, Pantano P, et al. Advantages of deformation indices over systolic velocities in assessment of longitudinal systolic function in patients with heart failure and normal ejection fraction. Eur J Heart Fail. 2011 Mar;13(3):292–302. doi: 10.1093/eurjhf/hfq203

31. Lam CSP, Roger VL, Rodeheffer RJ, Bursi F, Borlaug BA, Ommen SR, et al. Cardiac structure and ventricular-vascular function in persons with heart failure and preserved ejection fraction from Olmsted County, Minnesota. Circulation. 2007 Apr 17;115(15):1982–90. doi: 10.1161/CIRCULATIONAHA.106.659763

32. Lee AP-W, Song J-K, Yip GW-K, Zhang Q, Zhu T-G, Li C, et al. Importance of dynamic dyssynchrony in the occurrence of hypertensive heart failure with

normal ejection fraction. Eur Heart J. 2010 Nov;31(21):2642–9. doi: 10.1093/eurheartj/ehq248

33. Tan YT, Wenzelburger F, Lee E, Heatlie G, Leyva F, Patel K, et al. The pathophysiology of heart failure with normal ejection fraction: exercise echocardiography reveals complex abnormalities of both systolic and diastolic ventricular function involving torsion, untwist, and longitudinal motion. J Am Coll Cardiol. 2009 Jun 30;54(1):36–46. doi: 10.1016/j.jacc.2009.03.037

34. Chattopadhyay S, Alamgir MF, Nikitin NP, Rigby AS, Clark AL, Cleland JGF. Lack of diastolic reserve in patients with heart failure and normal ejection fraction. Circ Heart Fail. 2010 Jan;3(1):35–43. doi: 10.1161/CIRCHEARTFAILURE.108.824888

35. Wenzelburger FWG, Tan YT, Choudhary FJ, Lee ESP, Leyva F, Sanderson JE. Mitral annular plane systolic excursion on exercise: a simple diagnostic tool for heart failure with preserved ejection fraction. Eur J Heart Fail. 2011 Sep;13(9):953–60. doi: 10.1093/eurjhf/hfr081

36. Yip GW-K, Zhang Q, Xie J-M, Liang Y-J, Liu Y-M, Yan B, et al. Resting global and regional left ventricular contractility in patients with heart failure and normal ejection fraction: insights from speckle-tracking echocardiography. Heart Br Card Soc. 2011 Feb;97(4):287–94. doi: 10.1136/hrt.2010.205815

37. Tan YT, Wenzelburger F, Lee E, Nightingale P, Heatlie G, Leyva F, et al. Reduced left atrial function on exercise in patients with heart failure and normal ejection fraction. Heart Br Card Soc. 2010 Jul;96(13):1017–23. doi: 10.1136/hrt.2009.189118

38. Ponikowski P, Voors AA, Anker SD, Bueno H, Cleland JGF, Coats AJS, et al. 2016 ESC Guidelines for the diagnosis and treatment of acute and chronic heart failure: The Task Force for the diagnosis and treatment of acute and chronic heart failure of the European Society of Cardiology (ESC)Developed with the special contribution of the Heart Failure Association (HFA) of the ESC. Eur Heart J. 2016 Jul 14;37(27):2129–200. doi: 10.1093/eurheartj/ehw128

39. Nagueh SF, Smiseth OA, Appleton CP, Byrd BF 3rd, Dokainish H, Edvardsen T, et al. Recommendations for the Evaluation of Left Ventricular Diastolic Function by Echocardiography: An Update from the American Society of Echocardiography and the European Association of Cardiovascular Imaging. Eur Heart J Cardiovasc Imaging. 2016 Dec;17(12):1321–60. doi: 10.1093/ehjci/jew082

40. Sharifov OF, Schiros CG, Aban I, Denney TS, Gupta H. Diagnostic Accuracy of Tissue Doppler Index E/e' for Evaluating Left Ventricular Filling Pressure and Diastolic Dysfunction/Heart Failure With Preserved Ejection Fraction: A Systematic Review and Meta-Analysis. J Am Heart Assoc. 2016 Jan 25;5(1). doi: 10.1161/JAHA.115.002530

41. Nauta JF, Hummel YM, van der Meer P, Lam CSP, Voors AA, van Melle JP. Correlation with invasive left ventricular filling pressures and prognostic relevance of the echocardiographic diastolic parameters used in the 2016 ESC heart failure guidelines and in the 2016 ASE/EACVI recommendations: a systematic review in patients with heart failure with preserved ejection fraction. Eur J Heart Fail. 2018 Sep;20(9):1303–11. doi: 10.1002/ejhf.1220

42. Lancellotti P, Galderisi M, Edvardsen T, Donal E, Goliasch G, Cardim N, et al. Echo-Doppler estimation of left ventricular filling pressure: results of the multicentre EACVI Euro-Filling study. Eur Heart J Cardiovasc Imaging. 2017 Sep;18(9):961–8. doi: 10.1093/ehjci/jex067

43. Borlaug BA, Olson TP, Lam CSP, Flood KS, Lerman A, Johnson BD, et al. Global cardiovascular reserve dysfunction in heart failure with preserved ejection fraction. J Am Coll Cardiol. 2010 Sep 7;56(11):845–54. doi: 10.1016/j.jacc.2010.03.077

44. Tan YT, Wenzelburger FW, Sanderson JE, Leyva F. Exercise-induced torsional dyssynchrony relates to impaired functional capacity in patients with heart failure and normal ejection fraction. Heart Br Card Soc. 2013 Feb;99(4):259–66. doi: 10.1136/heartjnl-2012-302489

45. Patterson SW, Starling EH. On the mechanical factors which determine the output of the ventricles. J Physiol. 1914 Sep 8;48(5):357–79. doi: 10.1113/jphysiol.1914.sp001669

46. O Frank. On the dynamics of cardiac muscle. American Heart Journal. Volume 58, Issue 2, August 1959, Pages 282-317.

47. de Tombe PP. Cardiac myofilaments: mechanics and regulation. J Biomech. 2003 May;36(5):721–30.

48. Indraratna K. Cardiovascular assessment following vasoplegia in cardiac surgery. Anesth Pain Res. 2018;2(2):1–4.

49. van Daele ME, Trouwborst A, van Woerkens LC, Tenbrinck R, Fraser AG, Roelandt JR. Transesophageal echocardiographic monitoring of preoperative acute hypervolemic hemodilution. Anesthesiology. 1994 Sep;81(3):602–9.

50. Muller FU, Lewin G, Matus M, Neumann J, Riemann B, Wistuba J, et al. Impaired cardiac contraction and relaxation and decreased expression of sarcoplasmic Ca2+-ATPase in mice lacking the CREM gene. FASEB J Off Publ Fed Am Soc Exp Biol. 2003 Jan;17(1):103–5. doi: 10.1096/fj.02-0486fje

51. Baan J, van der Velde ET, de Bruin HG, Smeenk GJ, Koops J, van Dijk AD, et al. Continuous measurement of left ventricular volume in animals and humans by conductance catheter. Circulation. 1984 Nov;70(5):812–23.

52. Parmley WW, Sonnenblick EH. Relation between mechanics of contraction and relaxation in mammalian cardiac muscle. Am J Physiol. 1969 May;216(5):1084–91.

53. Jewell BR, Wilkie DR. The mechanical properties of relaxing muscle. J Physiol. 1960 Jun;152:30–47.

54. Ashley CC, Ridgway EB. On the relationships between membrane potential, calcium transient and tension in single barnacle muscle fibres. J Physiol. 1970 Jul;209(1):105–30.

55. Weiss JL, Frederiksen JW, Weisfeldt ML. Hemodynamic determinants of the time-course of fall in canine left ventricular pressure. J Clin Invest. 1976 Sep;58(3):751–60. doi: 10.1172/JCI108522

56. Spinale FG. Assessment of Cardiac Function--Basic Principles and Approaches. Compr Physiol. 2015 Sep 20;5(4):1911–46. doi: 10.1002/cphy.c140054

57. Kass DA, Maughan WL, Guo ZM, Kono A, Sunagawa K, Sagawa K. Comparative influence of load versus inotropic states on indexes of ventricular contractility: experimental and theoretical analysis based on pressure-volume relationships. Circulation. 1987 Dec;76(6):1422–36.

58. Quinones MA, Gaasch WH, Alexander JK. Influence of acute changes in preload, afterload, contractile state and heart rate on ejection and isovolumic indices of myocardial contractility in man. Circulation. 1976 Feb;53(2):293–302.

59. Suga H, Sagawa K, Shoukas AA. Load independence of the instantaneous pressure-volume ratio of the canine left ventricle and effects of epinephrine and heart rate on the ratio. Circ Res. 1973 Mar;32(3):314–22.

60. Suga H, Sagawa K. Instantaneous pressure-volume relationships and their ratio in the excised, supported canine left ventricle. Circ Res. 1974 Jul;35(1):117–26.

61. Sunagawa K, Yamada A, Senda Y, Kikuchi Y, Nakamura M, Shibahara T, et al. Estimation of the hydromotive source pressure from ejecting beats of the left ventricle. IEEE Trans Biomed Eng. 1980 Jun;27(6):299–305. doi: 10.1109/TBME.1980.326737

62. Igarashi Y, Suga H. Assessment of slope of end-systolic pressure-volume line of in situ dog heart. Am J Physiol. 1986 Apr;250(4 Pt 2):H685-692. doi: 10.1152/ajpheart.1986.250.4.H685

63. Takeuchi M, Igarashi Y, Tomimoto S, Odake M, Hayashi T, Tsukamoto T, et al. Single-beat estimation of the slope of the end-systolic pressure-volume relation in the human left ventricle. Circulation. 1991 Jan;83(1):202–12.

64. Senzaki H, Chen CH, Kass DA. Single-beat estimation of end-systolic pressure-volume relation in humans. A new method with the potential for noninvasive application. Circulation. 1996 Nov 15;94(10):2497–506.

65. Shishido T, Hayashi K, Shigemi K, Sato T, Sugimachi M, Sunagawa K. Single-beat estimation of end-systolic elastance using bilinearly approximated time-varying elastance curve. Circulation. 2000 Oct 17;102(16):1983–9.

66. Kim YJ, Jones M, Greenberg NL, Popovic ZB, Sitges M, Bauer F, et al. Evaluation of left ventricular contractile function using noninvasively determined single-beat end-systolic elastance in mitral regurgitation: experimental validation and clinical application. J Am Soc Echocardiogr Off Publ Am Soc Echocardiogr. 2007 Sep;20(9):1086–92. doi: 10.1016/j.echo.2007.02.009

67. Tanoue Y, Sese A, Ueno Y, Joh K, Hijii T. Bidirectional Glenn procedure improves the mechanical efficiency of a total cavopulmonary connection in high-risk fontan candidates. Circulation. 2001 May 1;103(17):2176–80.

68. Tanoue Y, Morita S, Ochiai Y, Hisahara M, Masuda M, Kawachi Y, et al. Inhibition of lipid peroxidation with the lazaroid U74500A attenuates ischemia-reperfusion injury in a canine orthotopic heart transplantation model. J Thorac Cardiovasc Surg. 1996 Oct;112(4):1017–26. doi: 10.1016/S0022-5223(96)70103-4

69. Tanoue Y, Morita S, Hisahara M, Tominaga R, Kawachi Y, Yasui H. Arresting donor hearts with extracellular-type cardioplegia prevents vasoconstriction induced by UW solution. Cardiovasc Surg Lond Engl. 1998 Dec;6(6):622–8.

70. Tanoue Y, Morita S, Ochiai Y, Haraguchi N, Tominaga R, Kawachi Y, et al. Nitroglycerin as a nitric oxide donor accelerates lipid peroxidation but preserves ventricular function in a canine model of orthotopic heart transplantation. J Thorac Cardiovasc Surg. 1999 Sep;118(3):547–56. doi: 10.1016/S0022-5223(99)70195-9

71. Chen CH, Fetics B, Nevo E, Rochitte CE, Chiou KR, Ding PA, et al. Noninvasive single-beat determination of left ventricular end-systolic elastance in humans. J Am Coll Cardiol. 2001 Dec;38(7):2028–34.

72. Redfield MM, Jacobsen SJ, Borlaug BA, Rodeheffer RJ, Kass DA. Age- and gender-related ventricular-vascular stiffening: a community-based study. Circulation. 2005 Oct 11;112(15):2254–62. doi: 10.1161/CIRCULATIONAHA.105.541078

73. Sasso L, Capuano A, Minco M, Paglia A, Pirozzi F, Memoli B, et al. Hemodialysis does not affect ventricular-arterial coupling beyond the reduction of blood pressure and preload. Int J Cardiol. 2013 Sep 30;168(2):1553–4. doi: 10.1016/j.ijcard.2012.12.024

74. Herberg U, Gatzweiler E, Breuer T, Breuer J. Ventricular pressure-volume loops obtained by 3D real-time echocardiography and mini pressure wire-a feasibility study. Clin Res Cardiol Off J Ger Card Soc. 2013 Jun;102(6):427–38. doi: 10.1007/s00392-013-0548-3

75. Scali MC, Basso M, Gandolfo A, Bombardini T, Bellotti P, Sicari R. Real time 3D echocardiography (RT3D) for assessment of ventricular and vascular function in hypertensive and heart failure patients. Cardiovasc Ultrasound. 2012 Jun 28;10:27. doi: 10.1186/1476-7120-10-27

76. Gayat E, Mor-Avi V, Weinert L, Yodwut C, Lang RM. Noninvasive quantification of left ventricular elastance and ventricular-arterial coupling using three-dimensional echocardiography and arterial tonometry. Am J Physiol Heart Circ Physiol. 2011 Nov;301(5):H1916-1923. doi: 10.1152/ajpheart.00760.2011

77. Greenberg NL, Firstenberg MS, Castro PL, Main M, Travaglini A, Odabashian JA, et al. Doppler-derived myocardial systolic strain rate is a strong index of left ventricular contractility. Circulation. 2002 Jan 1;105(1):99–105.

78. Gorcsan J 3rd, Abraham T, Agler DA, Bax JJ, Derumeaux G, Grimm RA, et al. Echocardiography for cardiac resynchronization therapy: recommendations for performance and reporting--a report from the American Society of Echocardiography Dyssynchrony Writing Group endorsed by the Heart Rhythm Society. J Am Soc Echocardiogr Off Publ Am Soc Echocardiogr. 2008 Mar;21(3):191–213. doi: 10.1016/j.echo.2008.01.003

79. Urheim S, Edvardsen T, Torp H, Angelsen B, Smiseth OA. Myocardial strain by Doppler echocardiography. Validation of a new method to quantify regional myocardial function. Circulation. 2000 Sep;102(10):1158–64.

80. Amundsen BH, Helle-Valle T, Edvardsen T, Torp H, Crosby J, Lyseggen E, et al. Noninvasive myocardial strain measurement by speckle tracking echocardiography: validation against sonomicrometry and tagged magnetic resonance imaging. J Am Coll Cardiol. 2006 Feb 21;47(4):789–93. doi: 10.1016/j.jacc.2005.10.040

81. Edvardsen T, Gerber BL, Garot J, Bluemke DA, Lima JA, Smiseth OA. Quantitative assessment of intrinsic regional myocardial deformation by Doppler strain rate echocardiography in humans: validation against three-dimensional tagged magnetic resonance imaging. Circulation. 2002 Jul;106(1):50–6.

82. Langeland S, D'hooge J, Wouters PF, Leather HA, Claus P, Bijnens B, et al. Experimental validation of a new ultrasound method for the simultaneous assessment of radial and longitudinal myocardial deformation independent of insonation angle. Circulation. 2005 Oct 4;112(14):2157–62. doi: 10.1161/CIRCULATIONAHA.105.554006

83. Torrent Guasp F. [Macroscopic structure of the ventricular myocardium]. Rev Esp Cardiol. 1980;33(3):265–87.

84. Streeter DD Jr, Spotnitz HM, Patel DP, Ross J Jr, Sonnenblick EH. Fiber orientation in the canine left ventricle during diastole and systole. Circ Res. 1969 Mar;24(3):339–47.

85. Greenbaum RA, Ho SY, Gibson DG, Becker AE, Anderson RH. Left ventricular fibre architecture in man. Br Heart J. 1981 Mar;45(3):248–63.

86. Helle-Valle T, Crosby J, Edvardsen T, Lyseggen E, Amundsen BH, Smith HJ, et al. New noninvasive method for assessment of left ventricular rotation: speckle tracking echocardiography. Circulation. 2005 Nov 15;112(20):3149–56. doi: 10.1161/CIRCULATIONAHA.104.531558

87. Kasner M, Westermann D, Steendijk P, Gaub R, Wilkenshoff U, Weitmann K, et al. Utility of Doppler echocardiography and tissue Doppler imaging in the estimation of diastolic function in heart failure with normal ejection fraction: a comparative Doppler-conductance catheterization study. Circulation. 2007 Aug;116(6):637–47. doi: 10.1161/CIRCULATIONAHA.106.661983

88. Kasner M, Gaub R, Sinning D, Westermann D, Steendijk P, Hoffmann W, et al. Global strain rate imaging for the estimation of diastolic function in HFNEF compared with pressure-volume loop analysis. Eur J Echocardiogr J Work Group Echocardiogr Eur Soc Cardiol. 2010 Oct;11(9):743–51. doi: 10.1093/ejechocard/jeq060

89. Vogel M, Cheung MM, Li J, Kristiansen SB, Schmidt MR, White PA, et al. Noninvasive assessment of left ventricular force-frequency relationships using tissue Doppler-derived isovolumic acceleration: validation in an animal model. Circulation. 2003 Apr;107(12):1647–52. doi: 10.1161/01.CIR.0000058171.62847.90

90. A'Roch R, Gustafsson U, Johansson G, Poelaert J, Haney M. Left ventricular strain and peak systolic velocity: responses to controlled changes in load and contractility, explored in a porcine model. Cardiovasc Ultrasound. 2012 May 28;10:22. doi: 10.1186/1476-7120-10-22

91. Dong SJ, Hees PS, Huang WM, Buffer SA Jr, Weiss JL, Shapiro EP. Independent effects of preload, afterload, and contractility on left ventricular torsion. Am J Physiol. 1999 Sep;277(3 Pt 2):H1053-60.

92. Dalsgaard M, Snyder EM, Kjaergaard J, Johnson BD, Hassager C, Oh JK. Isovolumic acceleration measured by tissue Doppler echocardiography is preload independent in healthy subjects. Echocardiography. 2007 Jul;24(6):572–9. doi: 10.1111/j.1540-8175.2007.00454.x

93. Kumar A, Anel R, Bunnell E, Habet K, Neumann A, Wolff D, et al. Effect of large volume infusion on left ventricular volumes, performance and contractility

parameters in normal volunteers. Intensive Care Med. 2004 Jul;30(7):1361–9. doi: 10.1007/s00134-004-2191-y

94. Abali G, Tokgozoglu L, Ozcebe OI, Aytemir K, Nazli N. Which Doppler parameters are load independent? A study in normal volunteers after blood donation. J Am Soc Echocardiogr Off Publ Am Soc Echocardiogr. 2005 Dec;18(12):1260–5. doi: 10.1016/j.echo.2005.06.012

95. Velasquez MT, Menitove JE, Skelton MM, Cowley AW Jr. Hormonal responses and blood pressure maintenance in normal and hypertensive subjects during acute blood loss. Hypertension. 1987 May;9(5):423–8.

96. Thomas SH, Smith SW, Slater NG, Pearson TC, Treacher DF. The haemodynamic responses to venesection and the effects of cardiovascular disease. Clin Lab Haematol. 1992;14(3):201–8.

97. Casiglia E, Mazza A, Ginocchio G, Onesto C, Pessina AC, Rossi A, et al. Hemodynamics following real and hypnosis-simulated phlebotomy. Am J Clin Hypn. 1997 Jul;40(1):368–75.

98. Bergenwald L, Freyschuss U, Melcher A, Sjostrand T. Circulatory and respiratory adaptation in man to acute withdrawal and reinfusion of blood. Pflugers Arch. 1975 Apr 2;355(4):307–18.

99. Bellitti P, Valeriano R, Gasperi M, Sodini L, Barletta D. Cortisol and heart rate changes in first- and fourth-time donors. Vox Sang. 1994;67(1):42–5.

100. Kumar A, Anel R, Bunnell E, Zanotti S, Habet K, Haery C, et al. Preload-independent mechanisms contribute to increased stroke volume following large volume saline infusion in normal volunteers: a prospective interventional study. Crit Care. 2004 Jun;8(3):R128-36. doi: 10.1186/cc2844

101. Park SJ, Nishimura RA, Borlaug BA, Sorajja P, Oh JK. The effect of loading alterations on left ventricular torsion: a simultaneous catheterization and two-dimensional speckle tracking echocardiographic study. Eur J Echocardiogr J Work Group Echocardiogr Eur Soc Cardiol. 2010 Oct;11(9):770–7. doi: 10.1093/ejechocard/jeq064

102. Burns AT, La Gerche A, Prior DL, Macisaac AI. Left ventricular torsion parameters are affected by acute changes in load. Echocardiography. 2010 Apr;27(4):407–14. doi: 10.1111/j.1540-8175.2009.01037.x

103. Burns AT, La Gerche A, D'Hooge J, MacIsaac AI, Prior DL. Left ventricular strain and strain rate: characterization of the effect of load in human subjects. Eur J Echocardiogr J Work Group Echocardiogr Eur Soc Cardiol. 2010 Apr;11(3):283–9. doi: 10.1093/ejechocard/jep214

104. Bornstein A, Gaasch WH, Harrington J. Assessment of the cardiac effects of hemodialysis with systolic time intervals and echocardiography. Am J Cardiol. 1983 Jan 15;51(2):332–5.

105. Hung KC, Huang HL, Chu CM, Chen CC, Hsieh IC, Chang ST, et al. Evaluating preload dependence of a novel Doppler application in assessment of left ventricular diastolic function during hemodialysis. Am J Kidney Dis Off J Natl Kidney Found. 2004 Jun;43(6):1040–6.

106. Assa S, Hummel YM, Voors AA, Kuipers J, Groen H, de Jong PE, et al. Changes in left ventricular diastolic function during hemodialysis sessions. Am J Kidney Dis Off J Natl Kidney Found. 2013 Sep;62(3):549–56. doi: 10.1053/j.ajkd.2013.02.356

107. Drighil A, Madias JE, Mathewson JW, El Mosalami H, El Badaoui N, Ramdani B, et al. Haemodialysis: effects of acute decrease in preload on tissue Doppler imaging indices of systolic and diastolic function of the left and right ventricles. Eur J Echocardiogr J Work Group Echocardiogr Eur Soc Cardiol. 2008 Jul;9(4):530–5. doi: 10.1093/ejechocard/jen125

108. Park CS, Kim YK, Song HC, Choi EJ, Ihm SH, Kim HY, et al. Effect of preload on left atrial function: evaluated by tissue Doppler and strain imaging. Eur Heart J Cardiovasc Imaging. 2012 Nov;13(11):938–47. doi: 10.1093/ehjci/jes069

109. Vignon P, Allot V, Lesage J, Martaille JF, Aldigier JC, Francois B, et al. Diagnosis of left ventricular diastolic dysfunction in the setting of acute changes in loading conditions. Crit Care. 2007;11(2):R43. doi: 10.1186/cc5736

110. Gerede DM, Turhan S, Kaya CT, Ozcan OU, Goksuluk H, Vurgun VK, et al. Effects of Hemodialysis on Tei Index: Comparison between Flow Doppler and Tissue Doppler Imaging. Echocardiography. 2015 Oct;32(10):1520–6. doi: 10.1111/echo.12895

111. Hayashi SY, Brodin LA, Alvestrand A, Lind B, Stenvinkel P, Mazza do Nascimento M, et al. Improvement of cardiac function after haemodialysis. Quantitative evaluation by colour tissue velocity imaging. Nephrol Dial Transplant Off Publ Eur Dial Transpl Assoc - Eur Ren Assoc. 2004 Jun;19(6):1497–506. doi: 10.1093/ndt/gfh205

112. Sztajzel J, Ruedin P, Monin C, Stoermann C, Leski M, Rutishauser W, et al. Effect of altered loading conditions during haemodialysis on left ventricular filling pattern. Eur Heart J. 1993 May;14(5):655–61.

113. Chakko S, Girgis I, Contreras G, Perez G, Kessler KM, Myerburg RJ. Effects of hemodialysis on left ventricular diastolic filling. Am J Cardiol. 1997 Jan 1;79(1):106–8.

114. Fijalkowski M, Koprowski A, Gruchala M, Galaska R, Debska-Slizien A, Rogowski J, et al. Effect of preload reduction by hemodialysis on myocardial ultrasonic

characterization, left atrial volume, and Doppler tissue imaging in patients with end-stage renal disease. J Am Soc Echocardiogr Off Publ Am Soc Echocardiogr. 2006 Nov;19(11):1359–64. doi: 10.1016/j.echo.2006.05.020

115. Govind SC, Roumina S, Brodin LA, Nowak J, Ramesh SS, Saha SK. Differing myocardial response to a single session of hemodialysis in end-stage renal disease with and without type 2 diabetes mellitus and coronary artery disease. Cardiovasc Ultrasound. 2006;4:9. doi: 10.1186/1476-7120-4-9

116. Galetta F, Cupisti A, Franzoni F, Carpi A, Barsotti G, Santoro G. Acute effects of hemodialysis on left ventricular function evaluated by tissue Doppler imaging. Biomed Pharmacother Biomedecine Pharmacother. 2006 Feb;60(2):66–70. doi: 10.1016/j.biopha.2005.10.008

117. Margulescu AD, Thomas DE, Ingram TE, Vintila VD, Egan MA, Vinereanu D, et al. Can isovolumic acceleration be used in clinical practice to estimate ventricular contractile function? Reproducibility and regional variation of a new noninvasive index. J Am Soc Echocardiogr Off Publ Am Soc Echocardiogr. 2010 Apr;23(4):423–31, 431 e1-6. doi: 10.1016/j.echo.2010.01.008

118. Choi J-O, Shin D-H, Cho SW, Song YB, Kim JH, Kim YG, et al. Effect of preload on left ventricular longitudinal strain by 2D speckle tracking. Echocardiogr Mt Kisco N. 2008 Sep;25(8):873–9. doi: 10.1111/j.1540-8175.2008.00707.x

119. Chen C-H, Lin Y-P, Yu W-C, Yang W-C, Ding Y-A. Volume status and blood pressure during long-term hemodialysis: role of ventricular stiffness. Hypertens Dallas Tex 1979. 2003 Sep;42(3):257–62. doi: 10.1161/01.HYP.0000085857.95253.79

120. Wang H, Liu J, Yao X, Li J, Yang Y, Cao T, et al. Multidirectional myocardial systolic function in hemodialysis patients with preserved left ventricular ejection fraction and different left ventricular geometry. Nephrol Dial Transplant Off Publ Eur Dial Transpl Assoc - Eur Ren Assoc. 2012 Dec;27(12):4422–9. doi: 10.1093/ndt/gfs090

121. Ross RM. ATS/ACCP statement on cardiopulmonary exercise testing. Am J Respir Crit Care Med. 2003 May 15;167(10):1451; author reply 1451. doi: 10.1164/ajrccm.167.10.950

122. ATS statement: guidelines for the six-minute walk test. Am J Respir Crit Care Med. 2002 Jul 1;166(1):111–7. doi: 10.1164/ajrccm.166.1.at1102

123. Bland JM, Altman DG. Statistical methods for assessing agreement between two methods of clinical measurement. Lancet Lond Engl. 1986 Feb 8;1(8476):307–10.

124. Lang RM, Bierig M, Devereux RB, Flachskampf FA, Foster E, Pellikka PA, et al. Recommendations for chamber quantification: a report from the American Society of Echocardiography's Guidelines and Standards Committee and the

Chamber Quantification Writing Group, developed in conjunction with the European Association of Echocardiography, a branch of the European Society of Cardiology. J Am Soc Echocardiogr Off Publ Am Soc Echocardiogr. 2005 Dec;18(12):1440–63. doi: 10.1016/j.echo.2005.10.005

125. Abozguia K, Nallur-Shivu G, Phan TT, Ahmed I, Kalra R, Weaver RA, et al. Left ventricular strain and untwist in hypertrophic cardiomyopathy: relation to exercise capacity. Am Heart J. 2010 May;159(5):825–32. doi: 10.1016/j.ahj.2010.02.002

126. Chowdhury SM, Butts RJ, Taylor CL, Bandisode VM, Chessa KS, Hlavacek AM, et al. Validation of Noninvasive Measures of Left Ventricular Mechanics in Children: A Simultaneous Echocardiographic and Conductance Catheterization Study. J Am Soc Echocardiogr Off Publ Am Soc Echocardiogr. 2016 Jul;29(7):640–7. doi: 10.1016/j.echo.2016.02.016

127. Temporelli PL, Scapellato F, Corra U, Eleuteri E, Imparato A, Giannuzzi P. Estimation of pulmonary wedge pressure by transmitral Doppler in patients with chronic heart failure and atrial fibrillation. Am J Cardiol. 1999 Mar 1;83(5):724–7.

128. Sohn DW, Song JM, Zo JH, Chai IH, Kim HS, Chun HG, et al. Mitral annulus velocity in the evaluation of left ventricular diastolic function in atrial fibrillation. J Am Soc Echocardiogr Off Publ Am Soc Echocardiogr. 1999 Nov;12(11):927–31.

129. Garcia MJ, Ares MA, Asher C, Rodriguez L, Vandervoort P, Thomas JD. An index of early left ventricular filling that combined with pulsed Doppler peak E velocity may estimate capillary wedge pressure. J Am Coll Cardiol. 1997 Feb;29(2):448–54.

130. Nagueh SF, Middleton KJ, Kopelen HA, Zoghbi WA, Quinones MA. Doppler tissue imaging: a noninvasive technique for evaluation of left ventricular relaxation and estimation of filling pressures. J Am Coll Cardiol. 1997 Nov 15;30(6):1527–33.

131. Reinders A, Reggiori F, Shennan AH. Validation of the DINAMAP ProCare blood pressure device according to the international protocol in an adult population. Blood Press Monit. 2006 Oct;11(5):293–6. doi: 10.1097/01.mbp.0000217998.96967.fb

132. Hildebrandt P, Collinson PO, Doughty RN, Fuat A, Gaze DC, Gustafsson F, et al. Age-dependent values of N-terminal pro-B-type natriuretic peptide are superior to a single cut-point for ruling out suspected systolic dysfunction in primary care. Eur Heart J. 2010 Aug;31(15):1881–9. doi: 10.1093/eurheartj/ehq163

133. Shvartz E, Reibold RC. Aerobic fitness norms for males and females aged 6 to 75 years: a review. Aviat Space Environ Med. 1990 Jan;61(1):3–11.

134. Enright PL, Sherrill DL. Reference equations for the six-minute walk in healthy adults. Am J Respir Crit Care Med. 1998 Nov;158(5 Pt 1):1384–7. doi: 10.1164/ajrccm.158.5.9710086

135. Nagueh SF, Appleton CP, Gillebert TC, Marino PN, Oh JK, Smiseth OA, et al. Recommendations for the evaluation of left ventricular diastolic function by echocardiography. Eur J Echocardiogr J Work Group Echocardiogr Eur Soc Cardiol. 2009 Mar;10(2):165–93. doi: 10.1093/ejechocard/jep007

136. Chen CH, Nakayama M, Nevo E, Fetics BJ, Maughan WL, Kass DA. Coupled systolic-ventricular and vascular stiffening with age: implications for pressure regulation and cardiac reserve in the elderly. J Am Coll Cardiol. 1998 Nov;32(5):1221–7.

137. Pak PH, Maughan WL, Baughman KL, Kieval RS, Kass DA. Mechanism of acute mechanical benefit from VDD pacing in hypertrophied heart: similarity of responses in hypertrophic cardiomyopathy and hypertensive heart disease. Circulation. 1998 Jul 21;98(3):242–8.

138. Feldman MD, Pak PH, Wu CC, Haber HL, Heesch CM, Bergin JD, et al. Acute cardiovascular effects of OPC-18790 in patients with congestive heart failure. Time- and dose-dependence analysis based on pressure-volume relations. Circulation. 1996 Feb 1;93(3):474–83.

139. Shishido T, Hayashi K, Shigemi K, Sato T, Sugimachi M, Sunagawa K. Single-Beat Estimation of End-Systolic Elastance Using Bilinearly Approximated Time-Varying Elastance Curve. Circulation. 2000 Oct 17;102(16):1983–9. doi: 10.1161/01.CIR.102.16.1983

140. Devereux RB, Reichek N. Echocardiographic determination of left ventricular mass in man. Anatomic validation of the method. Circulation. 1977 Apr;55(4):613–8.

141. Alcidi GM, Esposito R, Evola V, Santoro C, Lembo M, Sorrentino R, et al. Normal reference values of multilayer longitudinal strain according to age decades in a healthy population: A single-centre experience. Eur Heart J Cardiovasc Imaging. 2018 Dec 1;19(12):1390–6. doi: 10.1093/ehjci/jex306

142. Nagata Y, Wu VC-C, Otsuji Y, Takeuchi M. Normal range of myocardial layer-specific strain using two-dimensional speckle tracking echocardiography. PloS One. 2017;12(6):e0180584. doi: 10.1371/journal.pone.0180584

143. Wang J, Khoury DS, Yue Y, Torre-Amione G, Nagueh SF. Left ventricular untwisting rate by speckle tracking echocardiography. Circulation. 2007 Nov 27;116(22):2580–6. doi: 10.1161/CIRCULATIONAHA.107.706770

144. Sohn DW, Chai IH, Lee DJ, Kim HC, Kim HS, Oh BH, et al. Assessment of mitral annulus velocity by Doppler tissue imaging in the evaluation of left ventricular diastolic function. J Am Coll Cardiol. 1997 Aug;30(2):474–80.

145. Doesch C, Sperb A, Sudarski S, Lossnitzer D, Rudic B, Tulumen E, et al. Mitral annular plane systolic excursion is an easy tool for fibrosis detection by late gadolinium enhancement cardiovascular magnetic resonance imaging in patients with hypertrophic cardiomyopathy. Arch Cardiovasc Dis. 2015 Jul;108(6–7):356–66. doi: 10.1016/j.acvd.2015.01.010

146. Reisner SA, Lysyansky P, Agmon Y, Mutlak D, Lessick J, Friedman Z. Global longitudinal strain: a novel index of left ventricular systolic function. J Am Soc Echocardiogr Off Publ Am Soc Echocardiogr. 2004 Jun;17(6):630–3. doi: 10.1016/j.echo.2004.02.011

147. Zhao Y, Henein MY, Morner S, Gustavsson S, Holmgren A, Lindqvist P. Residual compromised myocardial contractile reserve after valve replacement for aortic stenosis. Eur Heart J Cardiovasc Imaging. 2012 Apr;13(4):353–60. doi: 10.1093/ejechocard/jer246

148. Uzieblo-Zyczkowska B, Krzesinski P, Gielerak G, Skrobowski A. Speckle tracking echocardiography and tissue Doppler imaging reveal beneficial effect of pharmacotherapy in hypertensives with asymptomatic left ventricular dysfunction. J Am Soc Hypertens JASH. 2017 Jun;11(6):334–42. doi: 10.1016/j.jash.2017.03.009

149. DeVore AD, McNulty S, Alenezi F, Ersboll M, Vader JM, Oh JK, et al. Impaired left ventricular global longitudinal strain in patients with heart failure with preserved ejection fraction: insights from the RELAX trial. Eur J Heart Fail. 2017 Jul;19(7):893–900. doi: 10.1002/ejhf.754

150. Phan TT, Shivu GN, Abozguia K, Gnanadevan M, Ahmed I, Frenneaux M. Left ventricular torsion and strain patterns in heart failure with normal ejection fraction are similar to age-related changes. Eur J Echocardiogr J Work Group Echocardiogr Eur Soc Cardiol. 2009 Aug;10(6):793–800. doi: 10.1093/ejechocard/jep072

151. Tohmo H, Karanko M, Korpilahti K. Haemodynamic effects of enalaprilat and preload in acute severe heart failure complicating myocardial infarction. Eur Heart J. 1994 Apr;15(4):523–7.

152. Nemoto S, Hamawaki M, De Freitas G, Carabello BA. Differential effects of the angiotensin-converting enzyme inhibitor lisinopril versus the beta-adrenergic receptor blocker atenolol on hemodynamics and left ventricular contractile function in experimental mitral regurgitation. J Am Coll Cardiol. 2002 Jul 3;40(1):149–54.

153. Dahle GO, Salminen P-R, Moen CA, Eliassen F, Nygreen E, Kyto V, et al. Carvedilol-Enriched Cold Oxygenated Blood Cardioplegia Improves Left Ventricular Diastolic Function After Weaning From Cardiopulmonary Bypass. J Cardiothorac Vasc Anesth. 2016 Aug;30(4):859–68. doi: 10.1053/j.jvca.2016.03.152

154. Williams AM, Shave RE, Stembridge M, Eves ND. Females have greater left ventricular twist mechanics than males during acute reductions to preload. Am J Physiol Heart Circ Physiol. 2016 Jul 1;311(1):H76-84. doi: 10.1152/ajpheart.00057.2016

155. Kitzman DW, Edwards WD. Age-related changes in the anatomy of the normal human heart. J Gerontol. 1990 Mar;45(2):M33-39.

156. Legato MJ. Gender and the heart: sex-specific differences in normal anatomy and physiology. J Gend-Specif Med JGSM Off J Partnersh Womens Health Columbia. 2000 Oct;3(7):15–8.

157. Fu Q, Arbab-Zadeh A, Perhonen MA, Zhang R, Zuckerman JH, Levine BD. Hemodynamics of orthostatic intolerance: implications for gender differences. Am J Physiol Heart Circ Physiol. 2004 Jan;286(1):H449-457. doi: 10.1152/ajpheart.00735.2002

158. Holwerda SW, Luehrs RE, DuBose LE, Majee R, Pierce GL. Sex and age differences in the association between sympathetic outflow and central elastic artery wall thickness in humans. Am J Physiol Heart Circ Physiol. 2019 Jul 5; doi: 10.1152/ajpheart.00275.2019

159. White DD, Gotshall RW, Tucker A. Women have lower tolerance to lower body negative pressure than men. J Appl Physiol Bethesda Md 1985. 1996 Apr;80(4):1138–43. doi: 10.1152/jappl.1996.80.4.1138

160. Shoemaker JK, Hogeman CS, Khan M, Kimmerly DS, Sinoway LI. Gender affects sympathetic and hemodynamic response to postural stress. Am J Physiol Heart Circ Physiol. 2001 Nov;281(5):H2028-2035. doi: 10.1152/ajpheart.2001.281.5.H2028

161. Lord R, MacLeod D, George K, Oxborough D, Shave R, Stembridge M. Reduced left ventricular filling following blood volume extraction does not result in compensatory augmentation of cardiac mechanics. Exp Physiol. 2018 Apr 1;103(4):495–501. doi: 10.1113/EP086761

162. Nixon JV, Mitchell JH, McPhaul JJJ, Henrich WL. Effect of hemodialysis on left ventricular function. Dissociation of changes in filling volume and in contractile state. J Clin Invest. 1983 Feb;71(2):377–84. doi: 10.1172/jci110779

163. Silva VB, Macedo TA, Braga TMS, Silva BC, Graciolli FG, Dominguez WV, et al. High Dialysate Calcium Concentration is Associated with Worsening Left Ventricular Function. Sci Rep. 2019 Feb 20;9(1):2386. doi: 10.1038/s41598-019-38887-y

164. Silva BC, Freitas GRR, Silva VB, Abensur H, Luders C, Pereira BJ, et al. Hemodynamic behavior during hemodialysis: effects of dialysate concentrations of bicarbonate and potassium. Kidney Blood Press Res. 2014;39(5):490–6. doi: 10.1159/000368459

165. Johnson DM, Roberts J, Gordon D. The acute effects of whole blood donation on cardiorespiratory and haematological factors in exercise: A systematic review. PloS One. 2019;14(4):e0215346. doi: 10.1371/journal.pone.0215346

166. Leonetti P, Audat F, Girard A, Laude D, Lefrere F, Elghozi JL. Stroke volume monitored by modeling flow from finger arterial pressure waves mirrors blood volume withdrawn by phlebotomy. Clin Auton Res Off J Clin Auton Res Soc. 2004 Jun;14(3):176–81. doi: 10.1007/s10286-004-0191-1

167. Paulus WJ, Tschope C, Sanderson JE, Rusconi C, Flachskampf FA, Rademakers FE, et al. How to diagnose diastolic heart failure: a consensus statement on the diagnosis of heart failure with normal left ventricular ejection fraction by the Heart Failure and Echocardiography Associations of the European Society of Cardiology. Eur Heart J. 2007 Oct;28(20):2539–50. doi: 10.1093/eurheartj/ehm037

168. Dokainish H, Nguyen JS, Bobek J, Goswami R, Lakkis NM. Assessment of the American Society of Echocardiography-European Association of Echocardiography guidelines for diastolic function in patients with depressed ejection fraction: an echocardiographic and invasive haemodynamic study. Eur J Echocardiogr J Work Group Echocardiogr Eur Soc Cardiol. 2011 Nov;12(11):857–64. doi: 10.1093/ejechocard/jer157

169. Caballero L, Kou S, Dulgheru R, Gonjilashvili N, Athanassopoulos GD, Barone D, et al. Echocardiographic reference ranges for normal cardiac Doppler data: results from the NORRE Study. Eur Heart J Cardiovasc Imaging. 2015 Sep;16(9):1031–41. doi: 10.1093/ehjci/jev083

170. Cohen GI, Pietrolungo JF, Thomas JD, Klein AL. A practical guide to assessment of ventricular diastolic function using Doppler echocardiography. J Am Coll Cardiol. 1996 Jun;27(7):1753–60.

171. Ommen SR, Nishimura RA, Appleton CP, Miller FA, Oh JK, Redfield MM, et al. Clinical utility of Doppler echocardiography and tissue Doppler imaging in the estimation of left ventricular filling pressures: A comparative simultaneous Doppler-catheterization study. Circulation. 2000 Oct 10;102(15):1788–94.

172. Lang RM, Badano LP, Mor-Avi V, Afilalo J, Armstrong A, Ernande L, et al. Recommendations for cardiac chamber quantification by echocardiography in adults: an update from the American Society of Echocardiography and the European Association of Cardiovascular Imaging. J Am Soc Echocardiogr Off Publ Am Soc Echocardiogr. 2015 Jan;28(1):1-39.e14. doi: 10.1016/j.echo.2014.10.003

173. Mogelvang R, Sogaard P, Pedersen SA, Olsen NT, Marott JL, Schnohr P, et al. Cardiac dysfunction assessed by echocardiographic tissue Doppler imaging is an independent predictor of mortality in the general population. Circulation. 2009 May 26;119(20):2679–85. doi: 10.1161/CIRCULATIONAHA.108.793471

174. Lassen MCH, Biering-Sorensen SR, Olsen FJ, Skaarup KG, Tolstrup K, Qasim AN, et al. Ratio of transmitral early filling velocity to early diastolic strain rate predicts long-term risk of cardiovascular morbidity and mortality in the general population. Eur Heart J. 2018 Apr 5; doi: 10.1093/eurheartj/ehy164

175. Biering-Sorensen T, Biering-Sorensen SR, Olsen FJ, Sengelov M, Jorgensen PG, Mogelvang R, et al. Global Longitudinal Strain by Echocardiography Predicts Long-Term Risk of Cardiovascular Morbidity and Mortality in a Low-Risk General Population: The Copenhagen City Heart Study. Circ Cardiovasc Imaging. 2017 Mar;10(3). doi: 10.1161/CIRCIMAGING.116.005521

176. Ozawa K, Funabashi N, Takaoka H, Kobayashi Y. Successful MACE risk stratification in hypertrophic cardiomyopathy patients using different 2D speckle-tracking TTE approaches. Int J Cardiol. 2017 Feb 1;228:1015–21. doi: 10.1016/j.ijcard.2016.11.141

177. Hartlage GR, Kim JH, Strickland PT, Cheng AC, Ghasemzadeh N, Pernetz MA, et al. The prognostic value of standardized reference values for speckle-tracking global longitudinal strain in hypertrophic cardiomyopathy. Int J Cardiovasc Imaging. 2015 Mar;31(3):557–65. doi: 10.1007/s10554-015-0590-5

178. Dahl JS, Videbaek L, Poulsen MK, Rudbaek TR, Pellikka PA, Moller JE. Global strain in severe aortic valve stenosis: relation to clinical outcome after aortic valve replacement. Circ Cardiovasc Imaging. 2012 Sep 1;5(5):613–20. doi: 10.1161/CIRCIMAGING.112.973834

179. Ternacle J, Berry M, Alonso E, Kloeckner M, Couetil J-P, Rande J-LD, et al. Incremental value of global longitudinal strain for predicting early outcome after cardiac surgery. Eur Heart J Cardiovasc Imaging. 2013 Jan;14(1):77–84. doi: 10.1093/ehjci/jes156

180. Kearney LG, Lu K, Ord M, Patel SK, Profitis K, Matalanis G, et al. Global longitudinal strain is a strong independent predictor of all-cause mortality in patients with aortic stenosis. Eur Heart J Cardiovasc Imaging. 2012 Oct;13(10):827–33. doi: 10.1093/ehjci/jes115

181. Marciniak A, Sutherland GR, Marciniak M, Kourliouros A, Bijnens B, Jahangiri M. Prediction of postoperative left ventricular systolic function in patients with chronic mitral regurgitation undergoing valve surgery--the role of deformation imaging. Eur J Cardio-Thorac Surg Off J Eur Assoc Cardio-Thorac Surg. 2011 Nov;40(5):1131–7. doi: 10.1016/j.ejcts.2011.02.049

182. Valocikova I, Vachalcova M, Valocik G, Kurecko M, Dvoroznakova M, Mitro P, et al. Incremental value of global longitudinal strain in prediction of all-cause mortality in predialysis and dialysis chronic kidney disease patients. Wien Klin Wochenschr. 2016 Jul;128(13–14):495–503. doi: 10.1007/s00508-016-0978-9

183. Krishnasamy R, Isbel NM, Hawley CM, Pascoe EM, Burrage M, Leano R, et al. Left Ventricular Global Longitudinal Strain (GLS) Is a Superior Predictor of All-

Cause and Cardiovascular Mortality When Compared to Ejection Fraction in Advanced Chronic Kidney Disease. PloS One. 2015;10(5):e0127044. doi: 10.1371/journal.pone.0127044

184. Jorgensen PG, Biering-Sorensen T, Mogelvang R, Fritz-Hansen T, Vilsboll T, Rossing P, et al. Predictive value of echocardiography in Type 2 diabetes. Eur Heart J Cardiovasc Imaging. 2018 Nov 13; doi: 10.1093/ehjci/jey164

185. Lavall D, Reil J-C, Segura Schmitz L, Mehrer M, Schirmer SH, Bohm M, et al. Early Hemodynamic Improvement after Percutaneous Mitral Valve Repair Evaluated by Noninvasive Pressure-Volume Analysis. J Am Soc Echocardiogr Off Publ Am Soc Echocardiogr. 2016 Sep;29(9):888–98. doi: 10.1016/j.echo.2016.05.012

186. Guinot P-G, Abou-Arab O, Guilbart M, Bar S, Zogheib E, Daher M, et al. Monitoring dynamic arterial elastance as a means of decreasing the duration of norepinephrine treatment in vasoplegic syndrome following cardiac surgery: a prospective, randomized trial. Intensive Care Med. 2017 May;43(5):643–51. doi: 10.1007/s00134-016-4666-z

187. Lavall D, Mehrer M, Schirmer SH, Reil J-C, Wagenpfeil S, Bohm M, et al. Long-Term Hemodynamic Improvement after Transcatheter Mitral Valve Repair. J Am Soc Echocardiogr Off Publ Am Soc Echocardiogr. 2018 Sep;31(9):1013–20. doi: 10.1016/j.echo.2018.05.010

188. Messina A, Romano SM, Bonicolini E, Colombo D, Cammarota G, Chiostri M, et al. Cardiac cycle efficiency and dicrotic pressure variations: new parameters for fluid therapy: An observational study. Eur J Anaesthesiol. 2017 Nov;34(11):755–63. doi: 10.1097/EJA.0000000000000661

189. Sanchez-Martinez S, Duchateau N, Erdei T, Fraser AG, Bijnens BH, Piella G. Characterization of myocardial motion patterns by unsupervised multiple kernel learning. Med Image Anal. 2017 Jan;35:70–82. doi: 10.1016/j.media.2016.06.007

190. Tabassian M, Sunderji I, Erdei T, Sanchez-Martinez S, Degiovanni A, Marino P, et al. Diagnosis of Heart Failure With Preserved Ejection Fraction: Machine Learning of Spatiotemporal Variations in Left Ventricular Deformation. J Am Soc Echocardiogr Off Publ Am Soc Echocardiogr. 2018 Dec;31(12):1272-1284.e9. doi: 10.1016/j.echo.2018.07.013

191. Sanchez-Martinez S, Duchateau N, Erdei T, Kunszt G, Aakhus S, Degiovanni A, et al. Machine Learning Analysis of Left Ventricular Function to Characterize Heart Failure With Preserved Ejection Fraction. Circ Cardiovasc Imaging. 2018 Apr;11(4):e007138. doi: 10.1161/CIRCIMAGING.117.007138

192. Pugliese NR, Fabiani I, Santini C, Rovai I, Pedrinelli R, Natali A, et al. Value of combined cardiopulmonary and echocardiography stress test to characterize the haemodynamic and metabolic responses of patients with heart failure and

mid-range ejection fraction. Eur Heart J Cardiovasc Imaging. 2019 Jul 1;20(7):828–36. doi: 10.1093/ehjci/jez014

193. Belyavskiy E, Morris DA, Url-Michitsch M, Verheyen N, Meinitzer A, Radhakrishnan A-K, et al. Diastolic stress test echocardiography in patients with suspected heart failure with preserved ejection fraction: a pilot study. ESC Heart Fail. 2019 Feb;6(1):146–53. doi: 10.1002/ehf2.12375

194. Obokata M, Kane GC, Reddy YNV, Olson TP, Melenovsky V, Borlaug BA. Role of Diastolic Stress Testing in the Evaluation for Heart Failure With Preserved Ejection Fraction: A Simultaneous Invasive-Echocardiographic Study. Circulation. 2017 Feb 28;135(9):825–38. doi: 10.1161/CIRCULATIONAHA.116.024822

195. Matsuzoe H, Matsumoto K, Tanaka H, Hatani Y, Hatazawa K, Shimoura H, et al. Significant Prognostic Value of Acute Preload Stress Echocardiography Using Leg-Positive Pressure Maneuver for Patients With Symptomatic Severe Aortic Stenosis Awaiting Aortic Valve Intervention. Circ J Off J Jpn Circ Soc. 2017 Nov 24;81(12):1927–35. doi: 10.1253/circj.CJ-17-0143

196. Matsumoto K, Onishi A, Yamada H, Kusunose K, Suto M, Hatani Y, et al. Noninvasive Assessment of Preload Reserve Enhances Risk Stratification of Patients With Heart Failure With Reduced Ejection Fraction. Circ Cardiovasc Imaging. 2018 May;11(5):e007160. doi: 10.1161/CIRCIMAGING.117.007160

197. Pritchett AM, Mahoney DW, Jacobsen SJ, Rodeheffer RJ, Karon BL, Redfield MM. Diastolic dysfunction and left atrial volume: a population-based study. J Am Coll Cardiol. 2005 Jan 4;45(1):87–92. doi: 10.1016/j.jacc.2004.09.054

198. Rodrigues JCL, Erdei T, Dastidar AG, Szantho G, Burchell AE, Ratcliffe LEK, et al. Left ventricular extracellular volume fraction and atrioventricular interaction in hypertension. Eur Radiol. 2019 Mar;29(3):1574–85. doi: 10.1007/s00330-018-5700-z

199. Khan MA, Yang EY, Zhan Y, Judd RM, Chan W, Nabi F, et al. Association of left atrial volume index and all-cause mortality in patients referred for routine cardiovascular magnetic resonance: a multicenter study. J Cardiovasc Magn Reson Off J Soc Cardiovasc Magn Reson. 2019 Jan 7;21(1):4. doi: 10.1186/s12968-018-0517-0

200. Okura H, Kataoka T, Yoshida K. Comparison of Left Ventricular Relaxation and Left Atrial Function in Patients With Heart Failure and Preserved Ejection Fraction Versus Patients With Systemic Hypertension and Healthy Subjects. Am J Cardiol. 2016 Oct 1;118(7):1019–23. doi: 10.1016/j.amjcard.2016.07.013